UNIVERSITY OF NAPLES
FEDERICO II

DEPARTMENT OF MATHEMATICS AND APPLICATIONS
"RENATO CACCIOPPOLI"

Ph.D. THESIS IN
"MATHEMATICS AND APPLICATIONS"
CYCLE XXXIII

Mathematical Modeling of Dry Anaerobic Digestion in Plug-Flow Reactors

Daniele Bernardo Panaro

"Everything is relative. Take a centenarian that breaks a mirror. He will be happy to know he still has seven years of misfortune."
Albert Einstein

Thesis Committee

Thesis Promoter

Prof. F. Capone
Full Professor
Department of Mathematics and Applications "Renato Caccioppoli"
University of Naples "Federico II", Naples, Italy

Thesis Supervisor

Dr. L. Frunzo
Assistant Professor
Department of Mathematics and Applications "Renato Caccioppoli"
University of Naples "Federico II", Naples, Italy

Thesis co-Supervisors

Dr. M.R. Mattei
Research fellow
Department of Mathematics and Applications "Renato Caccioppoli"
University of Naples "Federico II", Naples, Italy

Prof. G. Esposito
Associate Professor
Department of Civil, Architectural and Environmental Engineering
University of Naples "Federico II", Naples, Italy

Dr. J.P. Steyer
Director of Research
Laboratoire de Biotechnologie de l'Environnement
Institut national de recherche pour l'agriculture, l'alimentation et l'environnement (INRAE) Narbonne, France.

Dr. R. Escudie
Director of Research
Laboratoire de Biotechnologie de l'Environnement
Institut national de recherche pour l'agriculture, l'alimentation et l'environnement (INRAE) Narbonne, France.

Table of Contents

List of Figures

List of Tables

Acknowledgements

I would like to thank the italian Ministry of University Education and Research that gave me the opportunity to take part to this innovative formation program of the *Industrial Ph.D in Mathematics and Applications*, through the *Programma Operativo Nazionale FSE-FESR "Ricerca e Innovazione 2014-2020"* .
In this context I would like to sincerely thank the Partners of this program: the University of Naples *Federico II*, the foreign partner "*INRAE-LBE*" and the Italian company *Corradi e Ghisolfi Srl*. I would like to thank also the *Gruppo Nazionale per la Fisica Matematica (GNFM)*.
Moreover, I would like to thank all the people who had an important role during these years of Ph.D.
First of all I would like to thank my promoters Florinda Capone and Luigi Frunzo for giving me the opportunity to work as a Ph.D student in the fantastic world of mathematical modeling and mathematical physics. Thank you for helping me with important scientific discussions and suggestions, allowing me to develop a critical view on several topics.
Dr. Luigi Frunzo in particular, has been a crucial figure for my personal and professional growth. Thank you for treating me as a younger brother, when needed, and teaching me how to make research, how to overcome obstacles, the most important secrets of doing a fruitful research and for teaching me so many things about mathematical modeling.
Many thanks to the Coordinator of the Ph.D. Programme professor Gioconda Moscariello, for her important activity of super visioning my Ph.D. progresses.
Thank you to my thesis co-supervisor Dr. Maria Rosaria Mattei, for the fundamental scientific (and not) support activity, the discussions and all the efforts that she made to help me to obtain fantastic results in terms of scientific growth.
Many thanks also to Professor Giovanni Esposito for helping me to understand the process dynamics from an engineering point of view, thanks for all the comments, suggestions and discussions.
I would like to thank also Dr. Vincenzo Luongo and Dr. Andrea Trucchia for always giving me great suggestions for my problems and for helping me in many situations.
Thank you to the supervisors during my research activities in Narbonne, Jean-Philippe Steyer and Renaud Escudie. Working in your lab was a great opportunity and your contribution in broaden my knowledge about modeling and interpretation of results from an engineering point of view has revealed very important for my scientific growth.
To all the fantastic colleagues who shared with me this formation program: Alberto Tenore, Grazia Guer-

riero and Fabiana Russo, thank you. Days went by so quickly and less heavily with you by my side. Who has the fortune to share the Ph.D. experience with so amazing people? Thank you!
To all the members of my family, many thanks. My mother Teresa, ever proud of me, whatever step and choice I made. My father Raffaele and my sister Alessandra, silent but important figures, accepting and supporting me during my studies.
Lastly, I would like to thank my fantastic girlfriend Simona Pignata for being my anchor, my guide and my precious advisor. If I overcame psychologically many situations I owe it to you, to your support. Please do not stop to love me and to make me feel so fortunate to be by your side.

Summary

In the framework of the project *"XXXIII ciclo di dottorato, borsa di dottorato aggiuntiva del programma operativo nazionale Ricerca e Innovazione 2014-2020, fondo sociale europeo, azione I.1 dottorati innovativi con caratterizzazione industriale"* the objective of this work of thesis is to present the main scientific results achieved during this Ph.D course in applied mathematics. The project was aimed to develop a mathematical model describing the dry anaerobic digestion process in plug-flow reactors. Anaerobic digestion is one of the most used technologies for the treatment of organic compounds contained in a great variety of waste through which the production of a renewable energy is obtained, the biogas. Mathematical modeling plays a key role in providing tools supporting the design and management of this kind of plants performing this kind of process. The vast majority of mathematical models describing the anaerobic digestion process focus their attention on systems in wet conditions and are formulated as non-linear systems of Ordinary Differential Equations. Due to the reactor configuration and phenomena involved, dry anaerobic digestion modeling requires the use of Partial Differential Equations to describe properly the dynamics of the process.

The lack of scientific literature on this topic and the desire to provide a contribute to the development of sustainable technologies drove the interests and the efforts of these research activities, whose results are summarized in the chapters of this work of thesis.

The development of the model required the study of the physical and bio-chemical processes governing the considered system dynamics and made use of mathematical techniques typical of continuum mechanics. The study of the bio-chemical transformations taking place in anaerobic digestion systems was performed in a first work of calibration and validation of a mathematical model describing the anaerobic co-digestion of the organic fraction of municipal solid waste and sewage sludge using a surface-based disintegration kinetic, taking into account the influence of particle size on the disintegration process. A mathematical model describing the dry anaerobic digestion in plug-flow reactors was derived from mass balance considerations in the framework of continuum mechanics. The main assumptions, variables, boundary conditions and equations have been described for a one-dimensional domain. A Global Sensitivity Analysis joint with Uncertainty Quantification were performed to identify the main model parameters influencing the quantity of interest represented by the main output of the model, the methane production. Model calibration and validation, aimed to assess the capability of the model to describe and emulate real cases of dry anaerobic digestion, were performed successfully, leading the way to a future application of the model to real scale plants. A general discussion with suggestions for future developments close the work.

Chapter 1

Introduction

Anaerobic digestion is a widely used technology for the treatment of the organic fraction of solid waste and wastewater. Biogas, the main product of the anaerobic digestion, is generated through the conversion processes of the organic compounds catalized by the activity, in an oxygen-free environment, of two families of microorganisms: bacteria and archaea [141]. Biogas is mainly composed of methane (between 50% and 75% [130]), which contributes to define the biogas calorific power (the lower calorific power is between 15 and 30 $\mathrm{MJ/Nm^3}$ [118]), and carbon dioxide. A by-product of the whole process is the digestate that is used as fertilizer in agriculture, due to its nutritional potential (it is very rich in ammonium and other nutrients [111]). One of the environmental advantages coming from the utilization of anaerobic digestion is represented by the fact that it contributes to the reduction of pollution trough a sustainable way of treating the waste. Moreover, it contributes to the reduction of the greenhouse gases, due to the utilization of the biogas as a bio-fuel for the vehicles and its utilization into natural gas grids [2]. Biogas is also burned into co-generation units to produce heat and electricity used for improving the digestion process itself or, in the case of those plants with a high biogas production efficiency, for its introduction in heating and electricity lines.

Anaerobic digestion is realized by means of a chain of five main mechanisms which lead to the production of biogas: disintegration, hydrolysis, acidogenesis, acetogenesis and methanogenesis. Disintegration includes different steps such as lysis, non-enzymatic decay, phase separation and physical breakdown, which are phenomena occurring when the substrate to be treated presents complex composite particulate components. Through the disintegration those components are converted in simpler particulate substrates such as carbohydrates, proteins and lipids. These less complex substances are decomposed through the hydrolysis step into soluble monomers that are used as substrate for the subsequent phase of acidogenesis, which produces fundamental intermediate products, such as volatile fatty acids. These acids consist in short chain carboxylic acids having from 2 to 5 carbon atoms in the molecule and are among the essential intermediates of the anaerobic digestion process. In the fourth step of acetogenesis, volatile fatty acids are metabolized by hydrogen-producing microorganisms called acetogens to acetic acid with a yield of hydrogen and carbon dioxide. Moreover, in this phase, a small number of so called homo-acetogenic bacteria utilize carbon dioxyde CO_2 and hydrogen H_2 as substrates to produce an additional amount of acetic acid. Finally, these products are converted into methane by means of the strictly anaerobic activity of methanogenic archaea [72, 81]. The produced methane and the other components in soluble form (mainly carbon dioxide, hydrogen, nitrogen, carbon monoxide and hydrogen sulphide) are in equilibrium with their gas-phase. Moreover, association/dissociation of ionic species that are present in the environment where these bio-processes occur determines the pH value of the system.

The various microbial groups taking part to the conversion process of particulate organic compounds into methane, have different nutritional needs, sensitivity to the environment (pH, temperature etc.) and life cycle that sometimes make difficult to keep the right conditions for allowing the growth of all of them during a process of anaerobic digestion.

Anaerobic digestion classification is based on several operating conditions and reactor designs: total solids

content, temperature regime, feeding conditions and number of stage [97].

The total solids content is a measure of all the suspended, colloidal and dissolved solids in a medium and when the total solids content of the treated substrate is less or equal to 10% the anaerobic digestion is classified as *wet* otherwise, if it is greater or equal to 20%, it is denoted as *dry*. Lastly, the anaerobic digestion is denoted as *semi-dry* when the total solids content is between 10% and 20% [1]. Drawbacks and advantages characterize both wet and dry systems. Generally, in wet systems the contact between the dissolved substrates and microorganisms is facilitated thanks to the presence of a greater amount of water, but this implies higher reactors sizes with respect to dry systems. Moreover, despite the fact that complete mixing is not possible in dry systems due to the high viscosity of the medium, very high organic loading rates can be used and higher volatile solids conversion efficiency with respect to wet systems are realized. The organic loading rate indicates a measure of the amount of volatile solids per unit reactor volume fed into an anaerobic digestion system in a given unit time period while volatile solids represents the portion of the total solids content that is volatilized at $550\,^{\circ}\mathrm{C}$ and gives an idea on the amount of the readily vaporizing matter present in the solid fraction of a substrate. The degree of reduction of the volatile solids content is an important parameter used for evaluating the efficiency of a biological treatment process [64, 90].

Based on temperature regime the anaerobic digestion is classified as *psychrophilic* ($< 20\,^{\circ}\mathrm{C}$), *mesophilic* (20-40 $^{\circ}\mathrm{C}$) and *thermophilic* (50-65 $^{\circ}\mathrm{C}$). Process performances are improved at higher level of temperature but the operating costs increase as it is necessary to heat-up the environment where the process is performed.

Concerning the feeding conditions there is the main differentiation in batch and continuous systems. In the former the time that elapses between one feeding and another depends on the needed time for the complete degradation of the fed substrate while in the latter the input compounds are fed continuously, allowing to maintain a constant methane production during the whole process. This improves methane yield and the treatment capacity of reactors using this kind of configuration.

Lastly, in single-stage systems all the degrading processes are performed in a unique environment while in multi-stage systems it is realized a physical separation between methanogenesis and the other conversion processes. This allow to improve the performances of the methanogenesis process because it is not influenced by the environmental conditions that are established when there is the coexistence with the other processes. Indeed, the activity of the acidogenic microorganisms is faster with respect to the activity of the microorganisms involved in the production of methane and this implies a faster development of environmental conditions where an acidic pH value is determined, disturbing and inhibiting the activity of the methanogenic microorganisms.

Basically, the reactor configuration depends on the wet or dry conditions established for the process development. Wet anaerobic digestion is mainly performed in complete mixed systems while dry anaerobic digestion are is usually carried out in plug-flow reactors [79]. Complete mixed systems are mainly represented by Continuous Stirred Tank Reactors (CSTRs). In a CSTR, the intermittent or continuous mixing allow to maximize the contact between dissolved compounds and microorganisms with slight mass

transfer resistance [84]. On the contrary, the Plug-Flow Reactor (PFR) is characterized by a tubular or parallelepiped shape in which the digester content is not completely mixed, but moves as a plug through the reactor from the inlet to the outlet section [71], determining a profile in the concentration of the compounds along the reactor. A portion of the effluent is typically recirculated to improve the process efficiency [73]. Several commercial solutions are available for PFRs, with some differences in the hydrodynamic configuration adopted. For example in Dranco systems the vertical down-flow characterizes the movement of the treated substrate, while an horizontal-flow is used in the Kompogas configuration. Lastly, the horizontal plug-flow is circular in the Valorga configuration.

Mathematical modeling of the dynamics of CSTR and PFR configurations is based on mass balances on the state variables represented by the concentration of the bio-components inside the reactor. It usually consists of a system of non-linear Ordinary Differential Equations (ODE) and non-linear parabolic Partial Differential Equations (PDE), respectively. Indeed, due to the complete mixing, the concentrations of the compounds in a CSTR are considered homogeneous inside the reactor. For this reason the dynamics, in this case, depends only on time. On the contrary, both time and space must be considered in the description of the process development in PFR systems, due to the spatial variability of the state variables.

The process dynamics in completely mixed systems has been extensively studied for decades. The first mathematical models focused only on the limiting-step of the whole process (e.g [56] and [40]) due to the high number of processes and components to be considered. With the growth of the knowledge on the kinetics involved in the anaerobic digestion process, scientific experts tried to incorporate different aspects and species in their models. With the aim to create a generic model of anaerobic digestion, the IWA Task Group for Mathematical Modeling of Anaerobic Digestion Processes developed the Anaerobic Digestion Model No.1 (ADM1) [10]. ADM1 consists of a system of non-linear ODEs summarizing bio-chemical and physico-chemical phenomena occurring during an anaerobic digestion process. It includes disintegration, hydrolysis, acidogenesis, acetogenesis and methanogenesis as bio-chemical processes of transformation of the organic compounds, acid-base equilibria and gas-transfer as physico-chemical phenomenon. The model incorporate the co-existence of particulate, soluble and gaseous components and the main equations describing substrates and bacterial groups dynamics can be written in general form as follows:

$$\begin{aligned}\frac{dV_{liq}S_i}{dt} &= V_{liq}(\gamma_i\rho_{A,i}(t,\mathbf{S}) - \rho_{T,i}(t,\mathbf{S},\mathbf{S_{gas}}))+ \\ &+V_{liq}\sum_{j=1}^{m}\alpha_{i,j}\rho_j(t,\mathbf{S},\mathbf{X}),\end{aligned}$$

$$i = 1,...,n_1, \quad t > 0 \tag{1.1}$$

$$\frac{dV_{liq}X_i}{dt} = V_{liq}\sum_{j=1}^{m}\alpha_{i,j}\rho_j(t,\mathbf{S},\mathbf{X}),$$

$$i = n_1+1,...,n_2, \quad t>0 \tag{1.2}$$

$$\frac{dV_{gas}S_{gas,i}}{dt} = -q_{gas}S_{gas,i} + V_{liq}\rho_{T,i}(t,\mathbf{S},\mathbf{S_{gas}}),$$

$$i = 1,...,n_1, \quad t>0 \tag{1.3}$$

where:

n_1 denotes the number of soluble components,

$n_2 - n_1$ denotes the number of particulate components,

m denotes the number of biochemical processes taken into account,

$\alpha_{i,j}$ is the stoichiometric coefficient of species i on biochemical process j,

γ_i is the stoichiometric coefficient for the acid base reaction involving the i^{th} soluble component,

S_i denotes the i^{th} soluble component,

X_i denotes the i^{th} particulate component,

$S_{gas,i}$ denotes the i^{th} gaseous component,

$\rho_j(t,\mathbf{S},\mathbf{X})$ represents the rate of the j^{th} biochemical process,

$\rho_{A,i}(t,\mathbf{S})$ represents the acid base kinetic rate equation for the i^{th} soluble component,

$\rho_{T,i}(t,\mathbf{S},\mathbf{S_{gas}})$ represents the gas transfer rate for the i^{th} soluble component;

V_{liq} is the volume of the environment where reactions occur;

V_{gas} is the volume of the head-space where the biogas is stored;

q_{gas} is the volumetric gas-flow tapped from the head-space.

A charge balance consisting in an algebraic equation accounting for the ionic species concentrations is needed to evaluate pH and initial conditions are prescribed to set a closed mathematical problem. ADM1 has been widely used in scientific works describing anaerobic digestion processes. Despite this, ADM1 neglects some processes as reduction of sulphate and nitrates, precipitation of solids, inhibitor phenomena

and other aspects as the influence of particle size on the disintegration phenomenon. Various authors proposed some modifications of it to take into account these aspects. For instance, Esposito et al. [44] presented an ADM1-based model to analyse the effect of particle size on methane production during an anaerobic digestion process. They used a surface-based kinetics for the disintegration process, depending on both the type of substrate and the particle size.

Despite the high number of models for wet anaerobic digestion processes, there is a very limited formal literature on dry anaerobic digestion in PFRs [11]. Some existing models apply simplifications to avoid the resolution of a PDE system, such as the CSTR-in-series approximation [76]. The higher is the number of CSTR considered to approximate the plug-flow the closer to the PFR behavior is the system development. Examples of works adopting this approach are those of A. Donoso-Bravo et al. in [39], who solved the ADM1 for each CSTR used to approximate an anaerobic PFR, and H. Benbelkacem et al. in [16] who proposed a CSTR in series configuration to model the macro-mixing behavior of the liquid phase of laboratory scale digester based on Valorga technology. However, this kind of approach fails when, to properly describe the process dynamics in a PFR, is needed the knowledge of the concentration profiles of the compounds along the reactor. Other existing models solve the PDE system describing the PFR dynamics [125, 127] neglecting the mass variation along the reactor that takes place due to the conversion of solids in gaseous compounds. This is a valid hypothesis in wet systems, where the mass and consequently the volume variation of the treated substrate can be neglected due to the small amount of solids involved. When the total solids content increases, as in the case of dry anaerobic digestion in PFRs, the solids removal and the consequent mass/volume reduction of the reactor content must be accounted. Moreover, since in these kind of systems the process is performed maximizing the working reactor volume keeping constant the level of the treated substrate along the reactor, a variation in the convective velocity of the system should balance the loss in mass due to the conversion of solids along the reactor.

Another aspect of this topic that need deeper studies is the definition of an equation describing the gas-transfer phenomenon characterized by point-wise equilibria at the liquid-gas interface.

During the modeling of processes carried out in PFRs involving convective-diffusive-reactive phenomena, a critical aspect concerns also the boundary conditions to be prescribed. Several authors proposed different kind of boundary conditions and different studies focused on the debate about mathematical and physical justification to their application. For example, P.V. Danckwerts [34] proposed boundary conditions (1.4)-(1.5) for flow reactors in steady state conditions, considering the diffusion phenomenon in the first section of the PFR domain.

$$vC_{IN} = vC(0) - D\frac{dC(0)}{dz} \tag{1.4}$$

$$\frac{dC(L)}{dz} = 0 \tag{1.5}$$

On the contrary HM Hulburt [59] neglected any decomposition of the feed before it enters the reactor

imposing equation (1.6) and agreed with Danckwerts that no concentration gradient due to diffusion can be present in the outlet section.

$$C_{IN} = C(0) \tag{1.6}$$

According to DJ Batstone [9] anaerobic digestion modeling is facing three main challenges that are limiting its application in developing control systems: input substrate characterisation, physico-chemical modeling and modeling of systems whose dynamics depends on space as well as on time. Solid phase and semi-solid plug-flow systems can be strongly optimized with the aid of mathematical modeling, but there is the need of efforts in developing models capable to describe these kinds of systems.

In this perspective is inserted this work of thesis. Particularly, research activities were aimed to the development of a mathematical model describing the dynamics of the main compounds involved in a dry anaerobic digestion process in plug-flow reactors. The thesis is divided in 6 chapters. In the present section the main topic has been introduced. Chapter 2 presents the calibration and validation of the mentioned ADM1-based model of Esposito et al. [44], based on the results of experimental campaigns using potato waste whose particle size varied in a wide range as main substrate. The study of the original ADM1 and ADM1-based models has revealed fundamental to understand all the bio-chemical aspects of the anaerobic digestion process and it has been used as a training step for the following modeling activity. Chapter 3 describe the derived mathematical model of anaerobic digestion in plug-flow reactors: model equations and hypothesis are presented and model consistency with experimental observations is shown through numerical simulations. The model considers the variation of compounds concentrations in both space and time and takes into account the mass/volume variation of the treated matrix along the reactor. Moreover, a new equation describing the gas-transfer phenomenon is presented in this Chapter. A global sensitivity analysis and uncertainty quantification for the model of dry anaerobic digestion in plug-flow reactors is performed in Chapter 4. These activities revealed the most important model parameters influencing the methane production, the main output of the model. In Chapter 5, based on the global sensitivity analysis and uncertainty quantification results, model parameters have been calibrated and validated. Results of two experimental campaigns of dry anaerobic digestion in a plug-flow reactor have been used to this purpose. Lastly, in Chapter 6 a general discussion for future research developments is given.

Chapter 2

Calibration, Validation and Sensitivity Analysis of an anaerobic digestion Modified Surface-Based Model*

*The results of this chapter will be submitted in the form of a manuscript entitled: *Calibration, Validation and Sensitivity Analysis of an anaerobic digestion Modified Surface-Based Model.*

2.1 Abstract

In this work a modified surface-based mathematical model for the anaerobic digestion of potato waste was proposed. The model was calibrated and validated and a local sensitivity analysis to investigate the most sensitive parameters was performed. The model consisted of a modified version of the Anaerobic Digestion Model n.1, where the disintegration process was defined through a surface-based approach able to account for the influence of the particle size on the process development. Ad-hoc experimental activities were carried out to calibrate and validate the model with real data obtained at a laboratory scale. The calibration and validation procedures accounted for the net methane production and organic acids concentration, obtained with different sets of biochemical methane potential tests. The quality of fitting with lab scale data was evaluated by the Modeling Efficiency method, the Index of Agreement method and the Root Mean Square Error method, including its normalized form. The results confirmed the high accuracy of the model in describing the bio-methane and organic by-products evolution during the anaerobic conversion of potato waste.

2.2 Introduction

During the last decades, the Anaerobic Digestion (AD) process has been widely used for the stabilization and the treatment of organic waste biomasses. Notable examples of AD application are the treatment of the organic fraction of municipal solid wastes and the stabilization of the sewage sludge from municipal wastewater treatment plants [35, 114, 54]. Due to the ability of specific microbial species involved in the process, AD allows the simultaneous stabilization of wastes and production of a renewable energy source in form of biogas [58, 30, 66]. The latter is characterized by a high methane content (40-75$\%$) and can be effectively used for clean heat and electricity generation.

The mathematical modeling of AD process has been a challenging topic for the scientific community for about half a century. Indeed, the development of predictive mathematical models plays a key role for the definition of management strategies and the designing of full scale bio-reactors. According to [133], mathematical models of AD processes can be divided into four different categories: i) kinetic, ii) statistical, iii) computational fluid dynamics (CFD) and iv) ADM1 based models. Kinetic models are able to account for microbial growth and substrate consumption rates to describe the system evolution. Among them, some models describe the AD process based on its limiting steps: these are usually simplified models describing the slower kinetics related to substrates and/or species involved in the process [4, 3, 67, 5]. Other kinetic models are more complex and entirely describe the AD process without establishing a limiting step [126, 6]. Statistical models are mainly focused on the link between some key parameters and the model outputs. These models give information about the optimum set of initial conditions able to maximize the specific process target. For instance, some of them try to find the best substrate composition by using a polynomial regression which describes the relationship between the output and the substrate components

[129]. CFD models numerically simulate physics phenomena occurring into bio-reactors. Given a specific reactor configuration, they are able to predict many abiotic conditions, such as the velocity field, the turbulence, the temperature distribution and the residence time. The main aim is to study the effect of mixing conditions on the microbial population performing the AD process. Indeed, these information might be very useful at a real scale to determine the contact time between the substrate and the microbial biomass [139]. It is important to notice that CFD based models completely neglect the aspects related to the biological reactions occurring in AD. To predict the evolution of the process, a separate biological compartment constituted by a different system of equations is required. However, CFD models are computationally more demanding than all the other models. In 2002, the International Water Association (IWA) Task Group for Mathematical Modeling of Anaerobic Digestion Processes developed a comprehensive mathematical model known as Anaerobic Digestion Model no.1 [10], which was based on experiences acquired over the previous years in modeling and simulating the anaerobic digestion process.

Although some processes involved in the AD are neglected, ADM1 was the first real attempt to create a common framework in the AD modeling field. From its publication in 2002, almost 2000 works have been inspired on ADM1 structure. The model considers different biochemical (e.g. substrate decomposition, biomass growth etc.) and physico-chemical (e.g. gas-transfer, acid-base equilibrium etc.) processes taking place in an AD reactor. It is based on mass balance equations for different state variables (particulate, soluble and gaseous substance concentrations) and it reproduces the conversion of complex organic matter in a methane rich biogas. The ADM1 considers a continuous stirred tank reactor (CSTR) where a perfect mixing is implemented. Hence, the derived mass balance equation represent a system of nonlinear ordinary differential equations (ODE) where the state variables only depend on time and the non-linearity is due to the source terms. The model schematizes the process in five main phases: disintegration, hydrolysis, acidogenesis, acetogenesis and methanogenesis. In its first edition in 2002, ADM1 neglected crucial processes involved in AD: reduction of sulphate and nitrates, oxidation of acetate, homoacetogenesis, precipitation of solids, inhibition due to sulfide, nitrates, long chain fatty acids (LCFAs) and weak acids and bases. Over the years, many modifications have been proposed to the original ADM1 to take into account some of these processes overlooked by the model. For instance, in 2008 *Esposito et al.*[44] proposed a modified ADM1 model to study the effect of the solid particles size on the production of methane. The authors modeled the disintegration process with a surface-based kinetic approach (SBK) and they introduced a kinetic constant as a function of two terms: the specific disintegration rate (K_{sbk}), which is affected by the nature of the substrate, and the overall surface area of the treated complex organic particles per unit mass (a^*), which is affected by the characteristic dimension of the particles. In particular they considered spherical shape particles fed to the bio-reactor. In another work [43], the same authors calibrated and validated the model, considering a small particle size range ($0.5-2.5$ mm) of the fed particles, and the calibration was performed based on real AD experimental data.

In the present study, a modified version of ADM1 has been calibrated and validated for a wider range of particle size. A local sensitivity analysis was performed to obtain information about the influence of all

model parameters on the numerical output of the mathematical model. Moreover, the understanding of the most sensitive parameters for the model output can give useful information for the correct management of real scale AD plants. The calibration was based on experimental data of the cumulative methane production and acidic byproducts concentrations achieved with lab scale bio-reactors. The experimental tests were carried out by using potato waste as substrate with characteristic dimension of fed particles lower than one millimeter (Figure 2.1 d). Finally, the validation of the model was carried out with other experimental data-sets related to the anaerobic digestion of potato waste with characteristic dimension of 4 and 20 mm respectively (Figure 2.1,b and c).

2.3 Mathematical modeling

The mathematical model analyzed in the present work is based on a modified version of ADM1 proposed by *Esposito et al.* [44, 43]. The model accounts for the effect of particle size distribution during the disintegration process by using a surface based kinetic. In addition, it removes the ADM1 discrepancies in both carbon and nitrogen balances according to [21]. In particular, the use of a surface based kinetic approach for the disintegration kinetic allows to contextually account for the mechanical and granulometric characteristics of substrates. The equation governing the disintegration is defined as

$$\frac{dC}{dt} = -K_{sbk} a^* C, \tag{2.1}$$

where K_{sbk} is the surface based kinetic constant and $a^* = a^*(r_0)$ is the specific surface area of the disintegrating substrate, which directly depends on the particle geometry (e.g. radius r_0, height h_0,.. etc). Notably, K_{sbk} is independent from the granulometry of the waste, as it is a function of the mechanical characteristics of the substrate (i.e. the physical resistance of the waste to disintegration). On the other hand, the specific area a^* only depends on the geometry of waste particles involved in the process. In particular, K_{sbk} is experimentally determined based on the quality of the organic material, while a^* can be derived from the geometry of the waste.

Assuming cylindrical particles with radius r_0 and height $h = 2r_0$, a^* can be calculated as

$$a^* = \frac{3}{\delta r_0}, \tag{2.2}$$

where δ is the mass density of the waste material.

The model is based on mass conservation principles and it is formulated as a set of ordinary differential equations for soluble and particulate components. Based on the difference of the state variables, the system of equations is organized in three different groups: i) soluble components in liquid phase S_i, including the compounds deriving from the hydrolysis of the complex organic matter; ii) particulate components X_i, representing the concentration of the microbial groups involved in the biochemical reactions,

the complex organic matter fed to the AD system, and the macromolecules deriving from the disintegration step; iii) gas components $S_{gas,i}$ (i.e. hydrogen, carbon dioxide, methane), which are in equilibrium with the corresponding components in the liquid phase.

The differential equations governing soluble, particulate, and gas components involved in the AD processes are defined as:

$$\frac{dV_{liq}S_i}{dt} = V_{liq}(\gamma_i \rho_{A,i}(t,\mathbf{S}) - \rho_{T,i}(t,\mathbf{S},\mathbf{S_{gas}}) + V_{liq}\sum_{j=1}^{m}\alpha_{i,j}\rho_j(t,\mathbf{S},\mathbf{X}), \;\; i = 1,...,n_1, \;\; t > 0, \tag{2.3}$$

$$\frac{dV_{liq}X_i}{dt} = V_{liq}\sum_{j=1}^{m}\alpha_{i,j}\rho_j(t,\mathbf{S},\mathbf{X}), \;\; i = n_1+1,...,n_2, \;\; t > 0, \tag{2.4}$$

$$\frac{dV_{gas}S_{gas,i}}{dt} = -q_{gas}S_{gas,i} + V_{liq}\rho_{T,i}(t,\mathbf{S},\mathbf{S_{gas}}), \;\; i = 1,...,n_1, \;\; t > 0, \tag{2.5}$$

where n_1 denotes the number of soluble components, $n_2 - n_1$ denotes the number of particulate components, m_1 denotes the number of biochemical processes taken into account, $\alpha_{i,j}$ is the stoichiometric coefficient of the species i referred to the biochemical process j, γ_i is the stoichiometric coefficient for the acid base reaction involving the i^{th} soluble component, S_i denotes the i^{th} soluble component, X_i denotes the i^{th} particulate component, $S_{gas,i}$ denotes the i^{th} component in gas form, $\rho_j(t,\mathbf{S},\mathbf{X})$ represents the rate of the j^{th} biochemical process, $\rho_{A,i}(t,\mathbf{S})$ represents the acid base kinetic rate equation for the i^{th} soluble component, and $\rho_{T,i}(t,\mathbf{S},\mathbf{S_{gas}})$ represents the gas transfer rate for the i^{th} soluble component.

One of the main issues of AD bio-reactors is the accumulation of inhibiting byproducts, such as organic acids, in the bio-reactor environment. This phenomenon typically leads to undesired pH levels, which negatively affect the biological production of methane and the stabilization of the organic waste fed to the AD units. To account for pH variations and control the AD process, a charge balance equation accounting for all the dissolved ionic species has been considered:

$$\sum_{i=1}^{p}\mathbf{Q_i^+} - \sum_{i=1}^{q}\mathbf{Q_i^-} = 0, \;\; p+q < n_1, \tag{2.6}$$

where:

p defines the number of cationic components, q defines the number of anionic components, $\mathbf{Q_i^+}$ represents the cationic equivalent concentration of species i^{th}, $\mathbf{Q_i^-}$ represents the anionic equivalent concentration of species i^{th}.

To solve the differential-algebraic equations system [2.3-2.6], suitable initial conditions have been prescribed:

$$S_i(0) = S_i^0, \;\; i = 1,...,n_1, \tag{2.7}$$

$$X_i(0) = X_i^0, \;\; i = n_1 + 1, ..., n_2, \tag{2.8}$$

$$S_{gas,i}(0) = S_{gas,i}^0, \;\; i = 1, ..., n_1. \tag{2.9}$$

The detailed biochemical ($\rho_j(t, \mathbf{S}, \mathbf{X})$), acid/base ($\rho_{A,i}(t, \mathbf{S})$) and gas transfer ($\rho_{T,i}(t, \mathbf{S}, \mathbf{S_{gas}})$) reaction rates adopted in the model are reported in the following sections. In Section (2.8) the model equations are shown in the Petersen matrix form.

2.3.1 Biochemical reaction rates

During the anaerobic bio-conversion, many biological processes are contextually performed by different microbial species, which can grow, proliferate, and decay at specific kinetic rates depending on the availability of substrates over time. According to the ADM1, the process can be considered as five main sub-processes or degradation steps: i) the *disintegration* of complex organic matter X_C in readily and slowly degradable particulate organic macromolecules (X_{ch}, X_{pr}, X_{li}, X_I), with the contextual release of inorganic carbon (X_{IC}) and inorganic nitrogen (X_{IN}); ii) the *hydrolysis* of the particulate macromolecules in soluble monomers (S_{su}, S_{aa}, S_{fa}); iii) the degradation of soluble monomers in organic volatile acids (S_{va}, S_{pr}, S_{bu}), this step is usually named *acidogenesis*; iv) the formation of the acetic acid (S_{ac}) and hydrogen gas (S_{h2}) from the degradation of volatile acids and partially from the hydrolysis of soluble monomers (i.e *acetogenesis*); v) the formation of methane gas (S_{ch4}) through acetoclastic and hydrogenotrophic *methanogenesis*.

In ADM1, these sub-processes are performed by seven microbial groups: sugar degraders (X_{su}), amino acid degraders (X_{aa}), LCFA degraders (X_{fa}), valerate and buryrate degraders (X_{c4}), propionate degraders (X_{pro}), acetate degraders (X_{ac}), hydrogen degraders (X_{h2}), whose kinetics are usually described as conversion rates equations defined as $\rho_j(t, \mathbf{S}, \mathbf{X})$. The rates describe all biological processes occurring in AD, based on the availability of the required substrates. In the present work the kinetics rates have been formulated as:

$$\rho_1 = K_{sbk} a^* X_C, \tag{2.10}$$

$$\rho_2 = k_{hyd,ch} X_{ch}, \tag{2.11}$$

$$\rho_3 = k_{hyd,pr} X_{pr}, \tag{2.12}$$

$$\rho_4 = k_{hyd,li} X_{li}, \tag{2.13}$$

$$\rho_5 = k_{m,su}\frac{S_{su}}{K_{s,su}+S_{su}}X_{su}I_1, \tag{2.14}$$

$$\rho_6 = k_{m,aa}\frac{S_{aa}}{K_{s,aa}+S_{aa}}X_{aa}I_1, \tag{2.15}$$

$$\rho_7 = k_{m,fa}\frac{S_{fa}}{K_{s,fa}+S_{fa}}X_{fa}I_{2,fa}, \tag{2.16}$$

$$\rho_8 = k_{m,c4}\frac{S_{va}}{K_{s,c4}+S_{va}}\frac{1}{1+S_{bu}/S_{va}}X_{c4}I_{2,va}, \tag{2.17}$$

$$\rho_9 = k_{m,c4}\frac{S_{bu}}{K_{s,c4}+S_{bu}}\frac{1}{1+S_{va}/S_{bu}}X_{c4}I_{2,bu}, \tag{2.18}$$

$$\rho_{10} = k_{m,pro}\frac{S_{pro}}{K_{s,pro}+S_{pro}}X_{pro}I_{2,pro}, \tag{2.19}$$

$$\rho_{11} = k_{m,ac}\frac{S_{ac}}{K_{s,ac}+S_{ac}}X_{ac}I_3, \tag{2.20}$$

$$\rho_{12} = k_{m,h2}\frac{S_{h2}}{K_{s,h2}+S_{h2}}X_{h2}I_1, \tag{2.21}$$

$$\rho_{13} = k_{dec,all}X_{su}, \tag{2.22}$$

$$\rho_{14} = k_{dec,all}X_{aa}, \tag{2.23}$$

$$\rho_{15} = k_{dec,all}X_{fa}, \tag{2.24}$$

$$\rho_{16} = k_{dec,c4}X_{c4}, \tag{2.25}$$

$$\rho_{17} = k_{dec,pro}X_{pro}, \tag{2.26}$$

$$\rho_{18} = k_{dec,ac}X_{ac}, \tag{2.27}$$

$$\rho_{19} = k_{dec,all}X_{h2}. \tag{2.28}$$

where k_{hyd} is the first order constant for the hydrolysis, k_m is the Monod maximum specific uptake rate ($k_m = \mu_{max}/Y$), K_s is the half-saturation constant, I is the inhibition function, k_{dec} is the first order decay rate, μ_{max} is the Monod maximum specific growth rate and Y is the yield of biomass on substrate.

According to the ADM1, the inhibition terms in eqs.(2.14-2.21) allow for the inclusion of additional environmental aspects influencing specific bacterial species during the anaerobic bio-conversion. The inhibition factors included in the model are pH level, inorganic nitrogen concentration, hydrogen concentration, and ammonia nitrogen concentration. Based on experimental evidences, specific microbial species involved in AD process are strongly affected by these inhibiting factors, and the inclusion of inhibition functions is required to properly describe the related kinetic rates. These functions assume the form:

$$I_1 = I_{pH} I_{IN,lim}, \tag{2.29}$$

$$I_{2,i} = I_{pH} I_{IN,lim} I_{H2,i},\ i = (fa, va, bu, pro), \tag{2.30}$$

$$I_3 = I_{pH} I_{IN,lim} I_{NH3}, \tag{2.31}$$

where:

$$I_{pH} = \begin{cases} exp\left(-3\left(\frac{pH-pH_{UL}}{pH-pH_{LL}}\right)^2\right), & pH < pH_{UL}, \\ 0, & pH > pH_{UL}, \end{cases} \tag{2.32}$$

$$I_{IN,lim} = \frac{1}{1 + K_{S,IN}/S_{IN}}, \tag{2.33}$$

$$I_{H2,i} = \frac{1}{1 + S_{H2}/K_{I,H2,i}},\ i = (fa, va, bu, pro), \tag{2.34}$$

$$I_{NH3} = \frac{1}{1 + S_{NH3}/K_{I,NH3}}. \tag{2.35}$$

For mass balance conservation, it is important to notice that all decayed microbial species partially constitute new composite materials, in terms of biodegradable substrates. Contextually, they can be differently converted in inert materials depending on the considered species. In particular, for the microorganisms involved in the degradation of butyric and valeric acids, propionic acid, and acetic acid a percentage of 20% of the dead biomass has been supposed to constitute new substrates in the present model. For all other microbial species, the same percentage was fixed at 25%. Moreover, specific decay kinetic constants were used for the bacterial groups acting the uptake of butyric, valeric, propionic and acetic acid ($k_{dec,c4}$, $k_{dec,pro}$, $k_{dec,ac}$), while the constant decay term ($k_{dec,all}$) was used for all the other bacterial groups. This is in contrast with the ADM1, where the decay kinetic constant assumes the same value for all the bacterial

groups involved in the process. The present approach allows to consider the different nature of microbial species involved in the process avoiding under/over estimation errors due to biomass decay quantification.

2.3.2 Acid-base process rate

To account for all different cationic and anionic species influencing the pH evolution (Eq.(2.6)), the model includes acid-base equilibrium equations of all soluble compounds involved in the AD process. Soluble compounds, such as organic acids, inorganic carbon and inorganic nitrogen, can be found in different ionic forms depending on the specific pH level of the anaerobic environment. Kinetic rate equations regulate the form of soluble compounds in AD bio-reactors. They can be expressed as:

$$\rho_{A,va^-} = K_{A/B,va}(S_{va^-}(S_{H^+}K_{a,va}) - K_{a,va}S_{va}), \tag{2.36}$$

$$\rho_{A,bu^-} = K_{A/B,bu}(S_{bu^-}(S_{H^+}K_{a,bu}) - K_{a,bu}S_{bu}), \tag{2.37}$$

$$\rho_{A,pro^-} = K_{A/B,pro}(S_{pro^-}(S_{H^+}K_{a,pro}) - K_{a,pro}S_{pro}), \tag{2.38}$$

$$\rho_{A,ac^-} = K_{A/B,ac}(S_{ac^-}(S_{H^+}K_{a,ac}) - K_{a,ac}S_{ac}), \tag{2.39}$$

$$\rho_{A,hco3^-} = K_{A/B,co2}(S_{hco3^-}(S_{H^+}K_{a,co2}) - K_{a,co2}S_{IC}), \tag{2.40}$$

$$\rho_{A,nh3} = K_{A/B,IN}(S_{nh3}(S_{H^+}K_{a,IN}) - K_{a,IN}S_{IN}). \tag{2.41}$$

where $K_{A/B,i}$ and $K_{a,i}$ are the acid-base kinetic parameter and the acid-base equilibrium coefficient for the i^{th} species, $i = (va, bu, pro, ac, co2, IN)$, respectively.

The coefficient γ_i of equation (2.3) is equal to 1 when $i = (va^-, bu^-, pro^-, ac^-, hco3^-, nh3)$. It assumes the value of zero in all other cases.

2.3.3 Gas-transfer process rate

According to the ADM1, the liquid-gas transfer processes regulating the concentrations of hydrogen S_{H2}, methane S_{CH4}, and inorganic carbon S_{IC} in the liquid and gaseous phases have been considered. Based on thermodynamic principles, these compounds can be found in two different forms due to concentration gradients, which are generated between the liquid and gaseous phases of the AD reactors. The mass-transfer

kinetic rates included in the present work are described as:

$$\rho_{T,h2} = kLa(S_{h2} - 16K_{H,h2}p_{gas,h2}), \tag{2.42}$$

$$\rho_{T,ch4} = kLa(S_{ch4} - 64K_{H,ch4}p_{gas,ch4}), \tag{2.43}$$

$$\rho_{T,IC} = kLa(S_{co2} - K_{H,co2}p_{gas,co2}). \tag{2.44}$$

where kLa is the gas-liquid transfer coefficient, K_H is the Henry's law coefficient and $p_{gas,i}$, $i = (h2, ch4, co2)$, is the steady-state gas-phase partial pressure of the i^{th} component.

2.4 Experimental activities

2.4.1 AD bio-reactors

Ad-hoc AD experiments in semi-batch conditions were set-up to achieve the required data for model calibration and validation. The reactors were constituted by a airtight $2000\ mL$ transparent borosilicate glass bottle (Simax, Czech Republic) with caps equipped with thin tubing on the top for sampling and gas extraction. The produced biogas was forced to pass into a volumetric gas measurement system (Figure 2.1,a) constituted by two different overturned bottles: the first was filled with a $NaOH$ solution to trap the produced carbon dioxide before methane evaluation; the second bottle, filled with distilled water, allowed for the determination of the produced methane volume from the AD process. The reactors were immersed in a thermostatic bath at 33 ± 1 °C to ensure mesophilic conditions. The initial substrate to inoculum ratio F/M (Food/Microorganisms) was set at 0.5 to promote catabolic reactions. The substrate used during the experiments (F) was constituted by potato waste: it was pre-treated prior its feeding to reach different desired sizes (Figure 2.1,b-d). However, it was possible to study the effect of the initial particles size distribution on the disintegration process. Indeed, the same amount of potato waste of 10 $kg_{COD}\ m^{-3}$ was fed twice during 2 different experimental sets, named A, B, where the substrate particle size was fixed to $\leqslant 1$, and 4 mm, respectively. An additional experimental set, bio-reactor C, was carried out by using a substrate particle size of $20\ mm$, fed twice with 8.5 and $11\ kg_{COD}\ m^{-3}$, respectively. For each bio-reactor, the second organic load was applied when the cumulative biological methane production reached constant value, after 16, 16 and 17 days respectively. Noteworthy, each reactor was fed twice to allow the microbial community to acclimate to the specific substrate and to avoid lag phases and undesired byproducts accumulation. The inoculum for AD tests (M) was obtained from a full-scale AD reactor operating the bio-conversion of buffalo manure to biogas. All the tests were carried out in triplicate.

The organic substrate and the anaerobic digestate were characterized in terms of Total Solids (TS) and Volatile Solids (VS) to estimate their organic content prior to start the experiments. The results are shown

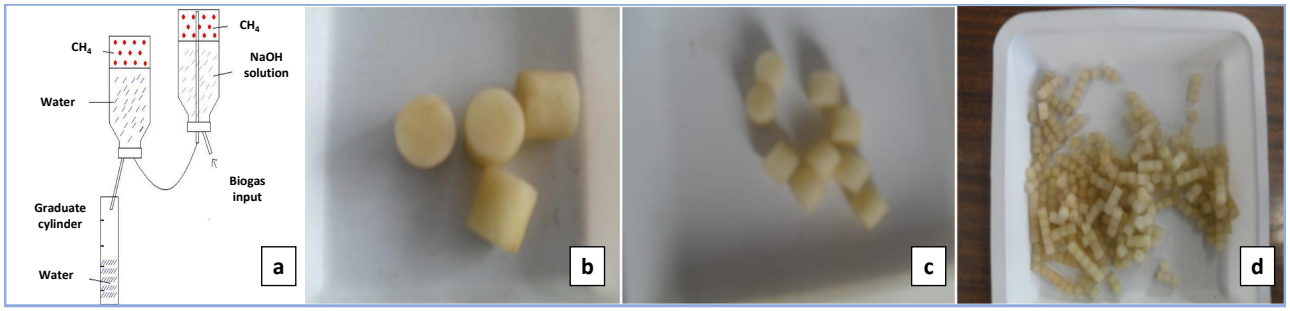

Figure 2.1: a) Biogas measurement system adopted. Characteristic dimension of the particles: b) 20 mm, c) 4 mm and d) < 1 mm.

Organic biomass	Total Solids %	Volatile Solids %
Potato waste	20.87	19.51
Inoculum	2.76	1.84

Table 2.1: Substrate and inoculum characterization.

in Table (2.1). In addition, potato waste was characterized in terms of carbohydrates, proteins, lipids and inert material (Table (2.2)) to achieve information on the organic composition of the waste. These analysis were required to set the ADM1 based mathematical model. All the reactors were operated at the same working volume of $1500\ mL$ by adding the same amount of substrate, digestate, water and a buffer solution to avoid inhibition effects due to acids accumulation.

2.4.2 Analytical methods

Total Solids (TS) and Volatile Solids (VS) were determined according to Standard Methods [7]. Carbohydrates, proteins and lipids, were quantified according to the Handbook of Food Analysis [91]. The daily methane production was measured using the volumetric method described above. To control the efficiency of the system in removing carbon dioxide, some gaseous samples were checked with a Varian Star 3400 gas chromatograph equipped with ShinCarbon ST $80/100$ column and a thermal conductivity detector. Only methane was detected in the outflow biogas. Temperature and pH were monitored for at least once a day with a WTW pH meter (WTW, Germany). The extracted liquid samples were characterized in terms of organic content: chemical oxygen demand (COD) concentration was obtained using a conversion factor from

Carbohydrates %	Proteins %	Lipids %	Inert %
75	10	0.1	14.9

Table 2.2: Potato waste composition in terms of carbohydrates, proteins, lipids and inert material.

the VS content ($\approx 1.5\ g_{COD} g_{VS}^{-1}$); volatile fatty acid (VFA) concentrations were obtained by a solid phase micro-extraction of the head space (HS-SPME) technique followed by a gas chromatographic coupled to mass spectrometry (GC-MS) analysis with a Nukol (SUPELCO, USA) fused silica capillary column [93]. Total VFAs (TVFAs) were also evaluated by direct titration of the samples. Total nitrogen and ammonia nitrogen were obtained with the total Kjeldahl nitrogen (TKN) technique according to the Standard Methods [7]. Total organic carbon (TOC) and total inorganic carbon (TIC) measurements were performed using a Shimadzu $5000A$ TOC analyzer (Kyoto, Japan).

2.5 Model application

2.5.1 Initial conditions

A crucial step to use the ADM1 based mathematical model for the simulation of lab scale experiments was to prescribe a reasonable initial condition for the complete set of equations. First, the initial concentration of complex organic matter X_C, in terms of $kg_{COD}\ m^{-3}$, was derived from experimental measurements. It was fixed at $10\ kg_{COD}\ m^{-3}$ to reproduce bio-reactors A and B. The same amount of potato waste was fed again after 16 days to the bio-reactor A and B. This was reproduced by numerical simulations where the second organic load was considered at day 16. According to the experimental procedures, the initial concentration of the complex organic matter X_C was fixed to $8.5\ kg_{COD}\ m^{-3}$ to simulate the bio methane production of reactor C. After 17 days of simulation, the second organic load of $11\ kg_{COD}\ m^{-3}$ was applied. Similarly, the initial inorganic nitrogen S_{IN} and inorganic carbon S_{IC} were set in accordance with experimental measurements.

In ADM1 based models, a number of microbial species is hypothesized to perform the biochemical reactions for the conversion of organic matter into biogas. These species are usually categorized based on their contribution on the anaerobic bio-conversion, instead of classifying their specific phylum or genera. Initially, the conversion steps of AD lead to the production of VFAs, which depends on the concentration of the microbial species in the inoculum. Noteworthy, different inocula are characterized by different microbial species distribution, depending on the inoculum origin and the bioprocess performed at a real scale. For these reasons, it is very complicated to set the initial conditions for microbial species distribution in an ADM1 based model. In the present work, the initial condition for microbial species X_{su}, X_{aa}, X_{fa}, X_{c4}, X_{pro}, X_{ac}, and X_{h2}, was set based on numerical experiments. The hypothesized initial microbial concentrations and all the initial condition adopted for reactors A, B, and C, is resumed in Table 2.3. The modified ADM1 model was implemented in an original software developed on Matlab platform.

State Variable	Unit	Reactor A	Reactor B	Reactor C
X_C	$kg_{COD}\ m^{-3}$	10	10	8.5
X_{ch}	$kg_{COD}\ m^{-3}$	0.0	0.0	0.0
X_{pr}	$kg_{COD}\ m^{-3}$	0.0	0.0	0.0
X_{li}	$kg_{COD}\ m^{-3}$	0.0	0.0	0.0
X_i	$kg_{COD}\ m^{-3}$	0.0	0.0	0.0
S_i	$kg_{COD}\ m^{-3}$	0.0	0.0	0.0
S_{su}	$kg_{COD}\ m^{-3}$	0.0	0.0	0.0
S_{aa}	$kg_{COD}\ m^{-3}$	0.0	0.0	0.0
S_{fa}	$kg_{COD}\ m^{-3}$	0.0	0.0	0.0
S_{va}	$kg_{COD}\ m^{-3}$	0.001	0.001	0.001
S_{bu}	$kg_{COD}\ m^{-3}$	0.001	0.001	0.001
S_{pro}	$kg_{COD}\ m^{-3}$	0.0	0.0	0.0
S_{ac}	$kg_{COD}\ m^{-3}$	0.0	0.0	0.0
S_{IC}	$kmol\ m^{-3}$	0.055	0.055	0.055
S_{IN}	$kmol\ m^{-3}$	0.05	0.05	0.05
X_{su}	$kg_{COD}\ m^{-3}$	0.15	0.15	0.15
X_{aa}	$kg_{COD}\ m^{-3}$	0.10	0.10	0.10
X_{fa}	$kg_{COD}\ m^{-3}$	0.10	0.10	0.10
X_{c4}	$kg_{COD}\ m^{-3}$	0.01	0.01	0.01
X_{pro}	$kg_{COD}\ m^{-3}$	0.033	0.033	0.033
X_{ac}	$kg_{COD}\ m^{-3}$	0.10	0.10	0.10
X_{h2}	$kg_{COD}\ m^{-3}$	0.10	0.10	0.10

Table 2.3: Initial conditions for the state variables.

2.5.2 Sensitivity Analysis

Due to the consistent number of equation and parameters, a local sensitivity analysis (LSA) was carried out to investigate the parameters influencing the model outputs the most. LSA is able to investigate the effect of a single parameter variation on a specific model output [135, 27]. The influence of a varying parameter is studied by computing the output variable first-order partial derivative over time with respect to the the considered parameter [140] (Eq. (2.45)). For each parameter the maximum or the minimum value of the obtained partial derivatives can be used as sensitivity index (SI), depending on which one is higher in absolute terms (Eq. (2.46)).

$$W_{i,j}\left(t, \mathbf{C}, \mathbf{u}\right) = \frac{\partial C_i\left(t, \mathbf{C}, \mathbf{u}\right)}{\partial u_j}, \tag{2.45}$$

$$SI_{i,j} = \begin{cases} \max\limits_{t\in[0,\tau]} W_{i,j}\left(t, \mathbf{C}, \mathbf{u}\right) & if \quad \mid \max\limits_{t\in[0,\tau]} W_{i,j}\left(t, \mathbf{C}, \mathbf{u}\right) \mid \geqslant \mid \min\limits_{t\in[0,\tau]} W_{i,j}\left(t, \mathbf{C}, \mathbf{u}\right) \mid \\ \min\limits_{t\in[0,\tau]} W_{i,j}\left(t, \mathbf{C}, \mathbf{u}\right) & if \quad \mid \max\limits_{t\in[0,\tau]} W_{i,j}\left(t, \mathbf{C}, \mathbf{u}\right) \mid < \mid \min\limits_{t\in[0,\tau]} W_{i,j}\left(t, \mathbf{C}, \mathbf{u}\right) \mid \end{cases}, \tag{2.46}$$

where $SI_{i,j}$ is the j^{th} parameter sensitivity with respect to the i^{th} output state variable at the instant time t, $W_{i,j}$ is the value of the partial derivative of the i^{th} output state variable with respect to the j^{th} parameter at the instant time t, C_i is the i^{th} chosen output state variable concentration; $\mathbf{C}$ is the vector of the state variables concentration (in soluble, particle or gaseous phase), u_j is the j^{th} investigated parameter value, $\mathbf{u}$ is the vector of the model parameters and τ is the final instant time.

It is important to notice that some sensitivity analysis results may depend on the initial condition as some parameter could be characterized by a wide fluctuation range [140]. The cumulative methane production and the VFAs concentration over time were set as model output for Equation (2.45) and the sensitivity of three groups of biochemical parameters was evaluated: the first group included the kinetic parameters, such as maximum specific uptake rates ($k_{m,su}$, $k_{m,aa}$, $k_{m,fa}$, $k_{m,c4}$, $k_{m,pro}$, $k_{m,ac}$, $k_{m,h2}$), half-saturation constants ($K_{s,su}$, $K_{s,aa}$, $K_{s,fa}$, $K_{s,c4}$, $K_{s,pro}$, $K_{s,ac}$, $K_{s,h2}$), and first order decay rates ($k_{dec,all}$, $k_{dec,c4}$, $k_{dec,pro}$, $k_{dec,ac}$); the second group was constituted by stoichiometric parameters, such as yields of microbial species on substrates (Y_{su}, Y_{aa}, Y_{fa}, Y_{c4}, Y_{pro}, Y_{ac}, Y_{h2}); the third group included hydrolysis/disintegration-related parameters ($k_{hyd,ch}$, $k_{hyd,pr}$, $k_{hyd,li}$ and K_{sbk}). All non-biochemical related parameters, e.g. inhibiting constants, equilibrium constants for gas-transfer and acid-base reactions, were not investigated in the present study as their uncertainty can be attributed to the experimental design and the reactor configuration [117]. The sensitivity was performed by simulating the process dynamics of reactor A and setting the initial condition presented in Table (2.3). The initial values of the investigated parameters were set in accordance to the original ADM1 [10]. The initial value for the introduced surface based kinetic constant K_{sbk} was set in accordance to [108], where the same substrate and a similar equation were used. The Matlab tool *sens_sys* [86] coupled with an ODE solver were used to perform the numerical analysis.

2.5.3 Model calibration and validation

Based on the sensitivity analysis, a trial and error method was used to calibrate the model. This method is highly recommended for the calibration of complex mathematical models with a high number of parameters varying in a wide range [101]. Specifically, the selected parameters are calibrated individually. Once the first parameter is calibrated another parameter is allowed to vary in its specific variation range. The algorithm ends when a reasonable fitness with experimental data is reached [110]. The parameters with higher sensitivity indexes where calibrated before other parameters. To compare model prediction with experimental data during the calibration steps, the experimental cumulative methane production and VFAs trends data in bio-reactor A were used. The performance of the calibration was evaluated by three different methods [60]: the modeling efficiency (ME), the index of agreement (IoA), and the root mean square error (RMSE) method, including its normalized form (NRMSE). These methods require the computation of four different parameters (Eqs. (2.47)-(2.50)):

$$RMSE = \sqrt{\frac{\sum_{i=1}^{N} (P_i - O_i)^2}{N}} \tag{2.47}$$

$$NRMSE = \frac{RMSE(\mathbf{p})}{\bar{O}} \tag{2.48}$$

$$ME = 1 - \frac{\sum_{i=1}^{N} (P_i - O_i)^2}{\sum_{i=1}^{N} \left(O_i - \bar{O}\right)^2} \tag{2.49}$$

$$IoA = 1 - \frac{\sum_{i=1}^{N} (P_i - O_i)^2}{\sum_{i=1}^{N} \left(\left|P_i - \bar{O}\right| + \left|O_i - \bar{O}\right|\right)^2} \tag{2.50}$$

where: P_i is the i^{th} model predicted value, O_i and $\bar{O}$ are the i^{th} and the means observed value, and N is the number of observations.

The model validation consisted in verifying the agreement between simulated values and experimental data achieved from bio-reactors B and C, with particle sizes of 4 and 20 mm, respectively. The values of all parameters were obtained from the calibration step. The performance of the validation procedure was evaluated through the same parameters described above (Equations (2.47)-(2.50)).

2.6 Results and discussions

2.6.1 Sensitivity Analysis

The aim of AD is to maximize the production of methane from a given substrate with a stable biological process. On the other hand, VFAs concentration during the anaerobic conversion may be a useful index

to avoid bio-reactor acidification and decreased conversion efficiency. The cumulative methane production was chosen as the model output to perform the sensitivity analysis. The results of the sensitivity indexes for each investigated parameter are shown in Figure 2.2. The sensitivity analysis was also performed based on VFAs concentration, and the results are reported in Figure 2.3, 2.4 and 2.5.

The results related to methane production, Figure 2.2a, showed that the most sensitive parameter was the disintegration kinetic constant K_{sbk}, whose sensitivity index value was 0.339. This result is in accordance with the sensitivity analysis performed in [31], where the ADM1 was applied to simulate biogas production from a different organic substrate. Despite a different index was used, the most significant sensitivity was referred to the kinetic constant of the disintegration process. Another relevant result is related to the maximum specific uptake rate for acetic acid $k_{m,ac}$, which showed the higher SI than all the other parameters grouped in Figure 2.2a (SI$= 3.6 \times 10^{-5}$). However, this value is not comparable with respect to the SI of the disintegration constant K_{sbk}. This evidence is in contrast with the local sensitivity analysis reported in [87], where ADM1 was used to model the effects of thermal pretreatment on an AD process of food waste. In this study, the reported SI of $k_{m,ac}$ showed the same magnitude of the disintegration constant SI. In the present work, the sensitivity of $k_{m,ac}$ increased when the acetic acid concentration was considered as the model output of the sensitivity analysis (Figure 2.3a). However, it was lower than the sensitivity of K_{sbk}.

The SI of K_{sbk} showed the highest value also when using other VFAs concentration as output variables Figure 2.3. This can be explained by the crucial role of the disintegration during the first steps of the anaerobic bio-conversion. Indeed, low values of K_{sbk} lead to low kinetic rates due to the reduced availability of substrates. When high K_{sbk} values are applied, all the anaerobic kinetics are stimulated and the complexity and the particle size distribution of the substrates are completely neglected.

The SIs of all half-saturation constants with respect to the cumulative methane production are reported in Figure 2.2b in log-scale. The majority of the half-saturation constants showed SI values of around 10^{-3}, except for $K_{s,fa}$ and $K_{s,h2}$. For these parameters the sensitivity reached the extreme values of 1.42×10^{-6} and 1.21, respectively. The assimilation of fatty acids, regulated by $K_{s,fa}$, has a relatively negligible effect on methane production, while hydrogen kinetics strongly influences the final methane production. A similar result was also obtained by using VFA concentrations as output variable Figure 2.4a; the most sensitive half-saturation constant was $K_{s,h2}$ (SI $= 10^2$), and a negligible SI value was found for all the other parameters. In particular, $K_{s,fa}$ showed the lower SI value when valeric, propionic or acetic acid was selected as model output, while $K_{s,ac}$ showed the lowest sensitivity value in the case of butyric acid. The crucial role of $K_{s,h2}$ is due to the importance of hydrogen dynamics during AD. Indeed, hydrogen is able to affect the assimilation kinetic rates of fatty acids, valerate, butyrate and propionate (Equations 2.16-2.19). A partial inhibition of these processes leads to a slower acetate production and consequent negative effects on methane generation by acetoclastic methanogens (Eq. 2.20).

The SI values of yield coefficients with respect to the cumulative methane production (Figure 2.2c) revealed a significant influence of sugar and acetic acid consuming microorganisms. The values of -0.007 and -0.005 were obtained for Y_{su} and Y_{ac}, respectively. The low sensitivity of the majority of half-

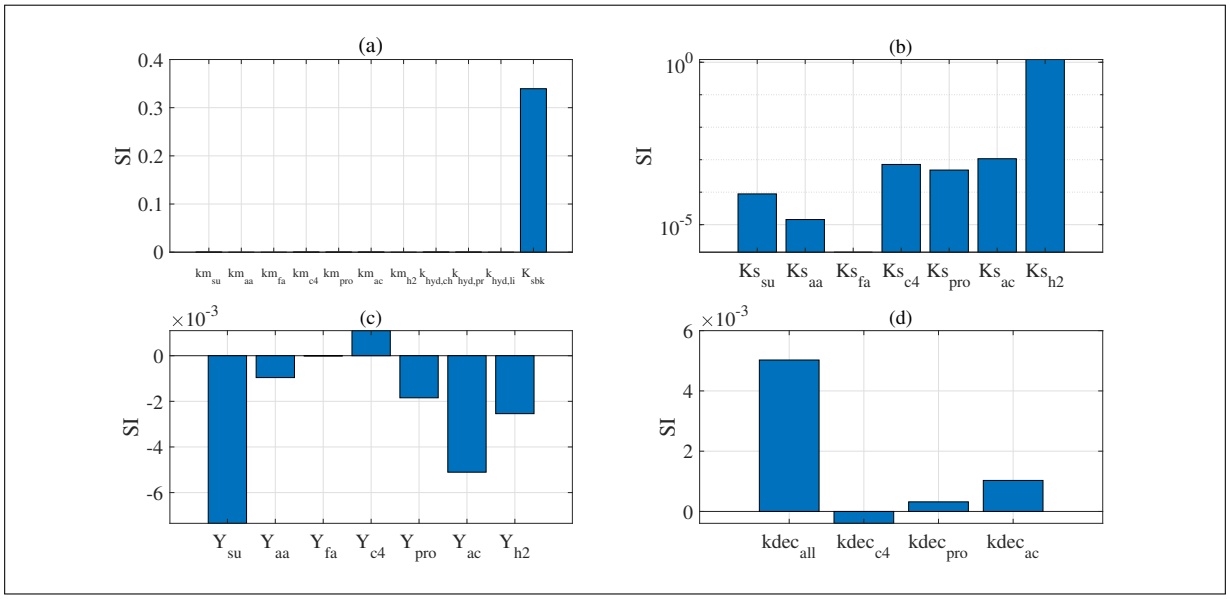

Figure 2.2: Absolute sensitivity referred to the produced methane concentration of: (a) Monod specific uptake rates and first order hydrolysis and disintegration constants; (b) half saturation constants (logarithmic scale); (c) yield of biomass on substrate; (d) first order decay rate.

saturation constants and yield coefficients is in accordance with the results of the local sensitivity analysis reported by [115]. In the case of VFAs used as sensitivity output (Figure 2.4b), the yields of valeric, butyric, propionic and acetic acid consuming species were relevant for the corresponding acid concentrations. Specifically, the propionic acid concentration S_{pro} resulted more sensitive to the yield Y_{pro} than Y_{su}. Such a result is in contrast with the sensitivity analysis performed by [8], where Y_{su} was one of the more influencing parameter on the propionic acid concentration. In addition, the yield of propionic acid consuming biomass was characterized by a very low sensitivity with respect to the same variable. This result can be due to the different structure of the model presented in [8], accounting for sulphate reduction during propionate uptake.

Finally, the SI values of all decay terms were reported in Figs. 2.2d and 2.5. Among them, the decay term related to sugar, amino acids, fatty acids and hydrogen consuming species ($k_{dec,all}$) showed the highest effect on the cumulative methane production. In the case the VFAs, the more sensitive decay rate was related to the microbial species involved in the degradation of each corresponding VFA.

2.6.2 Model calibration

Based on the results of the sensitivity analysis, the parameters K_{sbk}, $k_{hyd,ch}$, $k_{hyd,pr}$, $k_{hyd,li}$, $k_{m,pro}$, $k_{m,ac}$, $K_{s,su}$, $K_{s,c4}$, $K_{s,ac}$, $k_{dec,all}$, $k_{dec,c4}$, $k_{dec,pro}$, $k_{dec,ac}$ were selected for the calibration. Other sensitive parameters, such as $K_{s,h2}$ and all the yields coefficients, were set to the default ADM1 value as it was possible to appropriately fit the experimental data in all the studied cases. Table 2.4 reports the calibrated values for the investigated parameters compared to the ADM1 values.

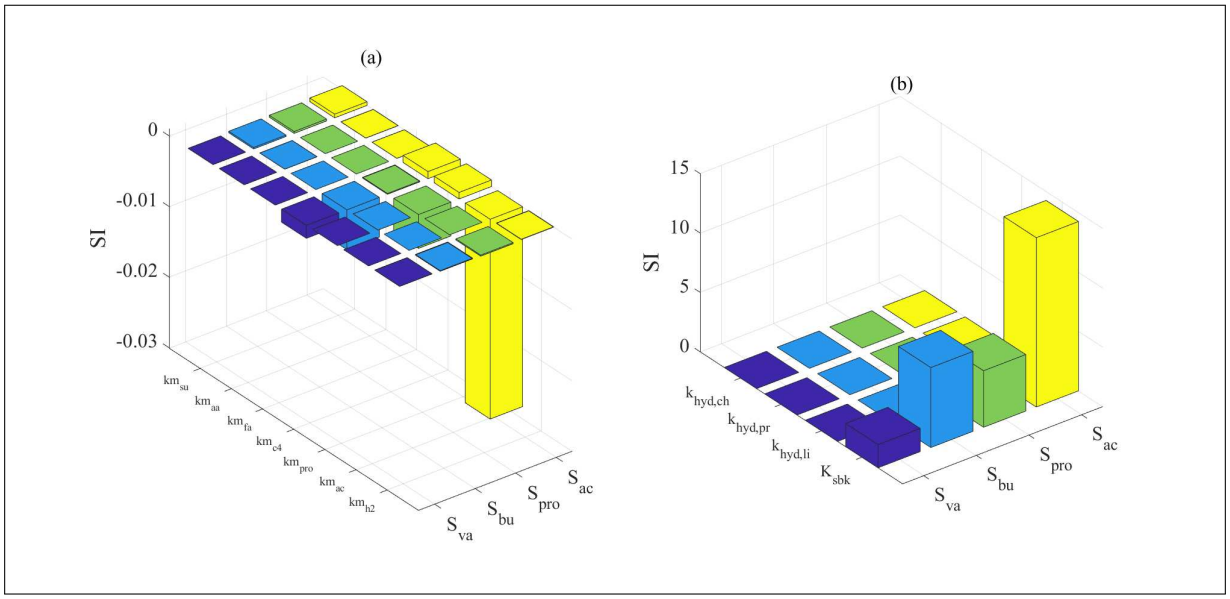

Figure 2.3: Absolute sensitivity referred to the produced VFAs concentrations of: (a) Monod specific uptake rates; (b) first order hydrolysis and disintegration constants.

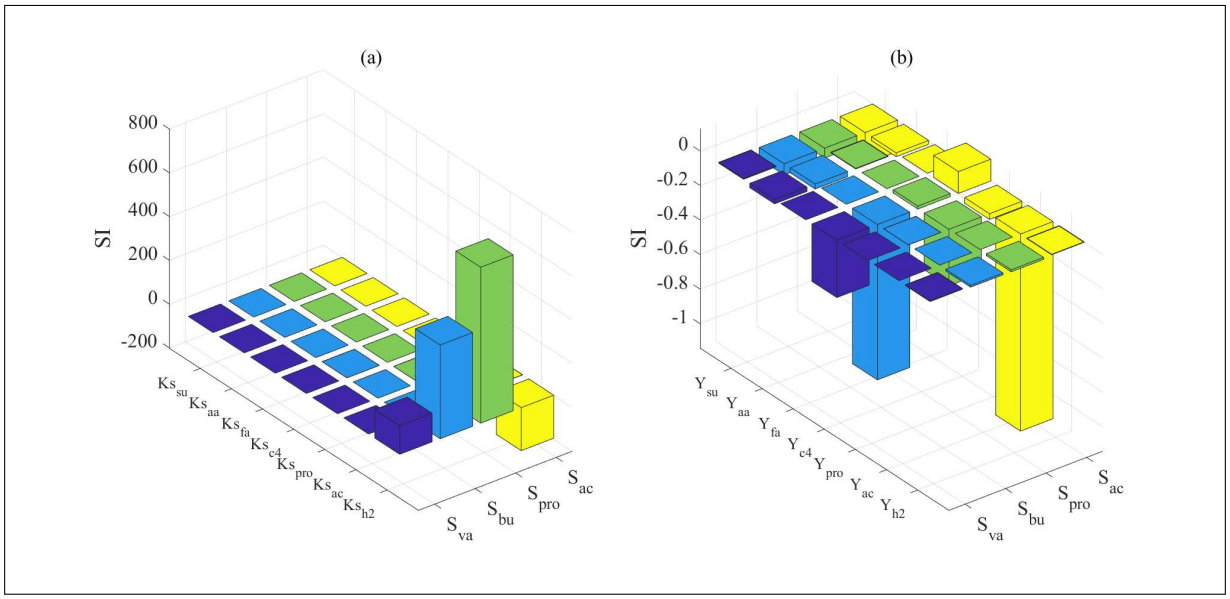

Figure 2.4: Absolute sensitivity referred to the produced VFAs concentrations of: (a) half saturation constants; (b) yields of biomass on substrate.

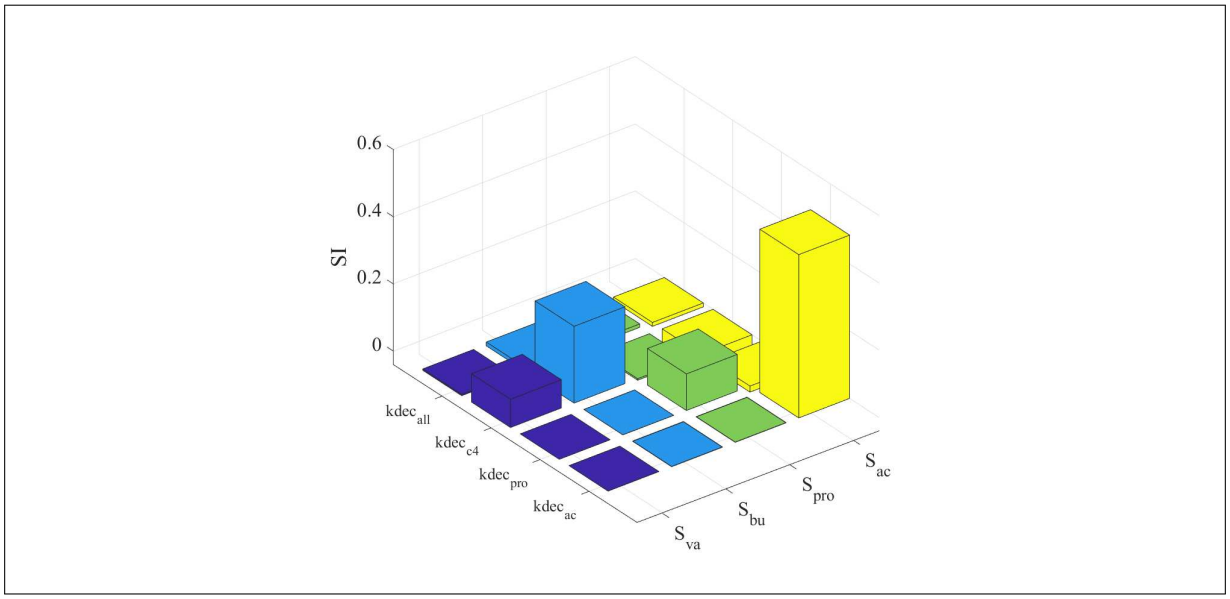

Figure 2.5: Absolute sensitivity referred to the produced VFAs concentrations of the first order decay rates.

The calibrated value of the disintegration constant K_{sbk} is not comparable with any ADM1 parameter as a different equation is assumed for the surface-based kinetic model. However, the K_{sbk} value has been investigated in very few cases in literature and its wide variation range strongly depends on the specific organic substrate converted. In the present case, the value of 0.72 $kg\ m^{-2}\ d^{-1}$ for this parameter allowed to achieve the best fit between experimental and simulated data. This value is higher with respect to 9.6×10^{-3}, 10.8×10^{-3} and 12.0×10^{-3} $kg\ m^{-2}\ d^{-1}$ used for a similar substrate by [108]. These authors reproduced experimental data of AD batch reactors operated by using particulate starch obtained from fresh potatoes as substrate. The specific particle size ranged from 45 and $125\,\mu m$. Conversely, the value of K_{sbk} calibrated in the present study is lower than $12.96 \times 10^3\ kg\ m^{-2}\ d^{-1}$ reported in [43], where the authors performed biomethane potential (BMP) experiments on synthetic organic waste with different particle size distributions. These differences in K_{sbk} value allows to confirm that it directly depends on the nature and characteristics of substrates.

Some differences with the ADM1 model have been observed with the maximum propionic and acetic acid uptake rate constants $k_{m,pro}$ and $k_{m,ac}$. These values were set to $60\ d^{-1}$ and $27\ d^{-1}$ in the modified model, differently from [46], where the increase of $k_{m,pro}$ and $k_{m,ac}$ with respect their baseline values of ADM1 was not required. In addition, Fatolahi et al. operated significant changes of the Monod maximum specific uptake rates $k_{m,su}$ and $k_{m,c4}$. In the present study, $k_{m,su}$ and $k_{m,c4}$ were set according to the ADM1 model. Moreover, the values of the calibrated half-saturation constants $K_{s,su}$, $K_{s,c4}$ and $K_{s,ac}$ were lower than ADM1. To better fit experimental data, the half-saturation constants for valerate, butyrate and acetate were reduced. A similar result was obtained in the calibration of a modified ADM1 used to reproduce starch wastewater and synthetic substrate bio-conversion in a lab scale upflow anaerobic sludge blanket (UASB) reactor [57].

Similarly, the calibrated values related to the hydrolysis constants $k_{hyd,ch}$, $k_{hyd,pr}$ and $k_{hyd,li}$, resulted lower than the same values reported in [10]. These values are in accordance with [12], where the range of $0.15 - 0.3$ d^{-1} was reported for BMP tests of hydrolyzed sludge samples. Decreased values for the hydrolysis parameters were also reported in [51]. The authors studied the disintegration and hydrolysis kinetics during the AD of fruit and vegetable waste. The differences with ADM1 can be mainly ascribed to the different substrate fed to the bioreactors: ADM1 was calibrated based on the AD of activated sludge, which is generally constituted by an hydrolyzed semi-solid matrix containing slow biodegradable compounds. On the other hand, potato waste needs to be hydrolyzed during AD, and its readily biodegradable organic content is higher than activated sludge. This fraction is able to stimulate biological kinetics during the bio-conversion and modify the kinetic constants.

The model was able to fit the experimental cumulative methane production data related to bio-reactor A as it is shown in Figure 2.6a. The performance indicators are reported in Table 2.5. The VFAs production (Figure 2.6b-e) accurately reproduced the experimental data except for butyric acid (Figure 2.6d). This can be due to the coupled kinetic uptake rates related to valeric and butyric acid assimilation reported in Equation 2.17-2.18. In some cases, two separate microbial species operating the valeric acid S_{va} and the butyric acid S_{bu} conversion separately were considered. In this study, a common microbial species was considered for S_{bu} and S_{va} degradation according to the original ADM1. This choice leads to a relative overestimation of butyric acid with respect to the experimental data, but it allows the possibility of comparing other ADM1 based works with the presented results.

Noteworthy, the calibration of the model was achieved by using the complete set of data related to the bio-reactor A. Based on the experimental feeding procedure, it should be possible to divide the data-set, and use the obtained partial set of data (from day 16 to the end of the experiment) to calibrate the model. Usually this procedure avoid any calibration error due to microbial species adaptation to the specific fed substrate, and it allows to obtain a more representative set of parameters. In the present case, this procedure was not required as no differences were observed when using the complete or the partial data set.

2.6.3 Model validation

Numerical simulations were run to validate the model using the data-sets related to bio-reactors B and C, where potato waste was fed at different particle sizes (4 and 20 mm) and comparable concentrations. Of course, the values of the calibrated parameters were used for numerical simulations and the validation results of the cumulative methane production and organic acids over time have been reported in Figures 2.7 and 2.8. Moreover, Table 2.5 shows the performance indicators values obtained during model calibration and validation steps using the different data-set.

The values of ME, IoA, RMSE, and NRMSE confirmed that the model is able to properly predict the cumulative methane production for a wide range of substrate particle size.

The VFA evolution curves were adequately fitted by model simulations, except for the butyric acid.

Calibrated parameter	Units	ADM1 default value	Modified Surface-Based Model value
K_{sbk}	$kg_{COD}\ m^{-2}\ d^{-1}$	/	0.72
$k_{hyd,ch}$	d^{-1}	10	0.95
$k_{hyd,pr}$	d^{-1}	10	0.25
$k_{hyd,li}$	d^{-1}	10	0.25
$k_{m,pro}$	d^{-1}	13	60
$k_{m,ac}$	d^{-1}	8	27
$k_{dec,all}$	d^{-1}	0.02	0.1
$k_{dec,c4}$	d^{-1}	/	0.05
$k_{dec,pro}$	d^{-1}	/	0.02
$k_{dec,ac}$	d^{-1}	/	0.02
$K_{s,su}$	$kg_{COD}\ m^{-3}$	0.5	0.05
$K_{s,c4}$	$kg_{COD}\ m^{-3}$	0.2	0.1
$K_{s,ac}$	$kg_{COD}\ m^{-3}$	0.15	0.015

Table 2.4: Calibrated parameters: ADM1 default values and Modified Surface-Based Model values.

Type of parameter analysis	Reactor	Performance measures			
		ME	IoA	RMSE	NRMSE
		(-)	(-)	(ml)	(-)
Calibration	A	0.99	0.998	209.51	0.039
Validation	B	0.99	0.997	256.19	0.049
Validation	C	0.92	0.979	710.15	0.157

Table 2.5: Performance indicators.

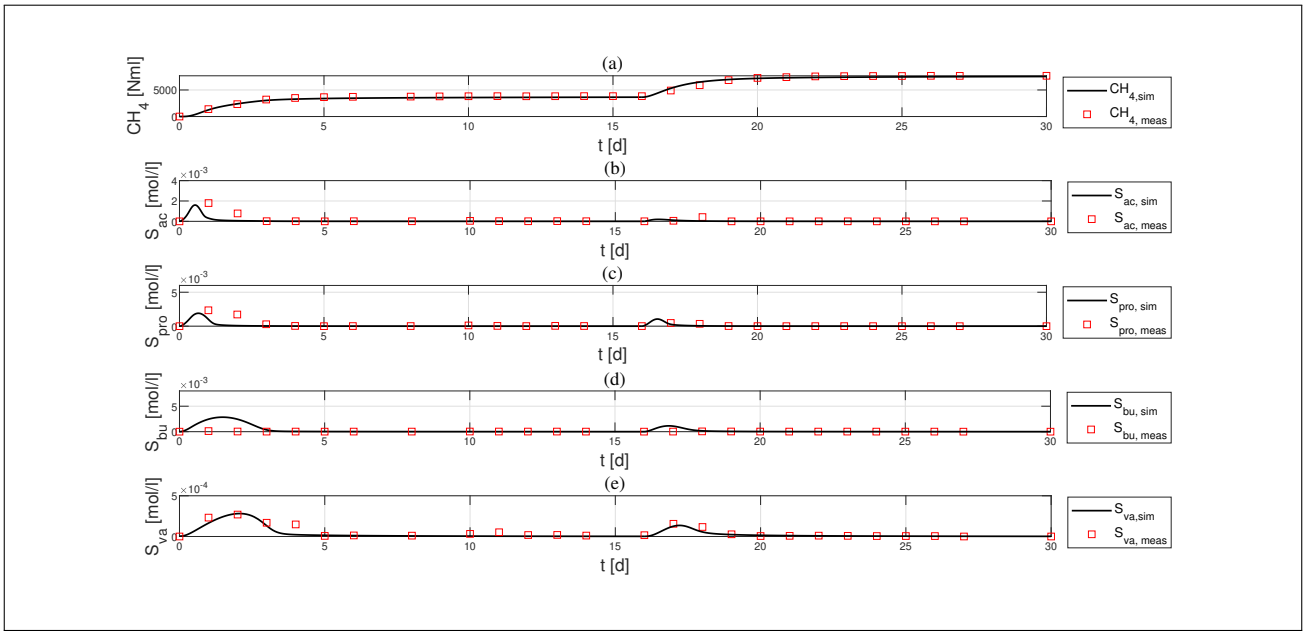

Figure 2.6: Reactor A: measured and simulated concentration values of (a) Methane; (b) Acetic acid; (c) Propionic acid; (d) Butyric acid; (e) Valeric acid.

As previously reported, the fitting with experimental data should be improved by uncoupling butyric and valeric acid degradation kinetics.

2.7 Conclusions

The aim of the present work was to calibrate and validate a modified surface-based model of an anaerobic digestion process of potato waste. The model consisted on a modified ADM1 model in which the disintegration kinetic was able to take into account the particle size of the composite substratum. Modifications concerning the kinetics parameters of the microbial species involved in the AD process have been discussed. A local sensitivity analysis highlighted the importance of choosing the correct set of parameters to model methane generation and volatile fatty acids concentrations in real AD bio-reactors. The introduced disintegration kinetic constant K_{sbk} presented the highest sensitivity among disintegration/hydrolysis related parameters and Monod specific uptake rates. The model was successfully calibrated and validated with ad-hoc AD experiments carried out using potato waste as organic substrate. The model properly predicted the cumulative methane production and VFAs concentration profiles achieved during lab-scale experiments. Finally, validation results showed the ability of the modified surface-based model to adequately describe real processes where a wide range of particle size characterizes the substrate fed to AD reactors.

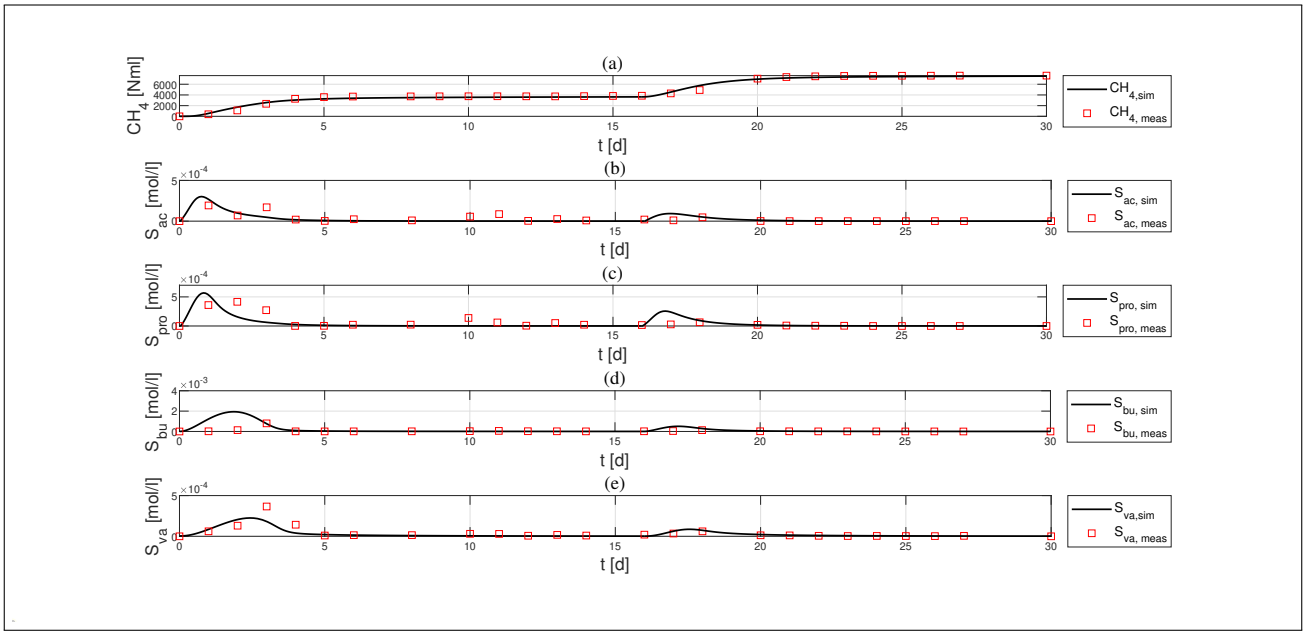

Figure 2.7: Reactor B: measured and simulated concentration values of (a) Methane; (b) Acetic acid; (c) Propionic acid; (d) Butyric acid; (e) Valeric acid.

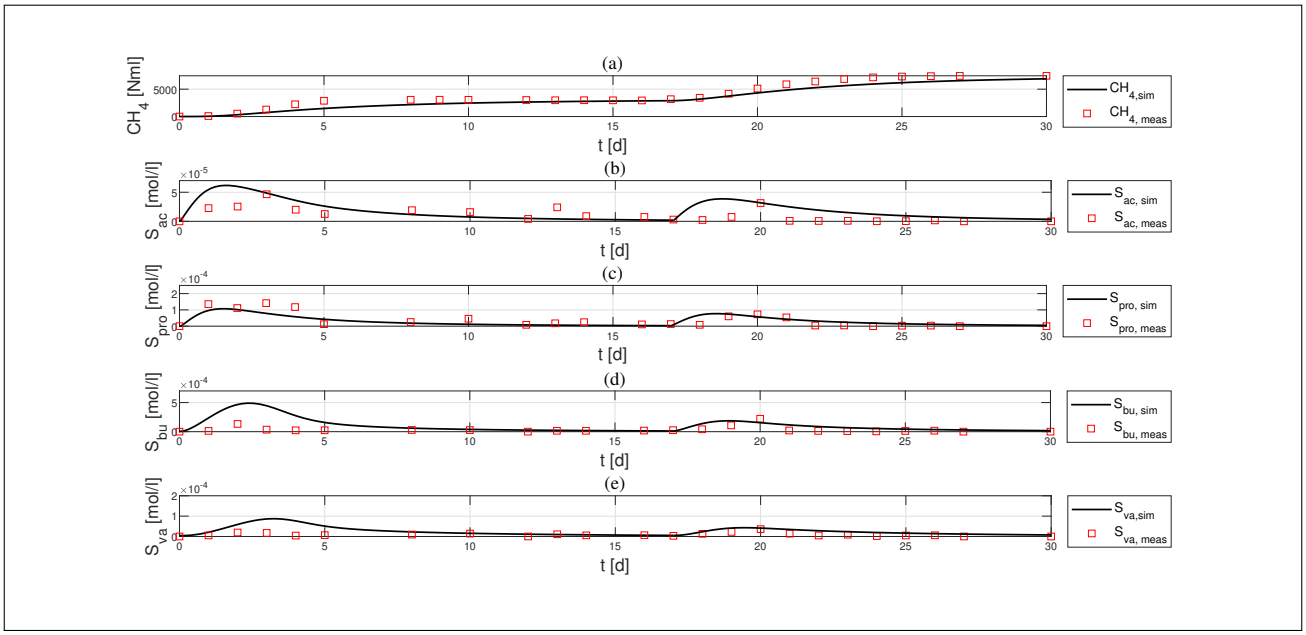

Figure 2.8: Reactor C: measured and simulated concentration values of (a) Methane; (b) Acetic acid; (c) Propionic acid; (d) Butyric acid; (e) Valeric acid.

2.8 Petersen Matrix

	Components →	1	2	3	4	5	6	7	8	9	10	11	12	Rate ρ_j
	Process ↓	S_{su}	S_{aa}	S_{fa}	S_{va}	S_{bu}	S_{pro}	S_{ac}	S_{H2}	S_{CH4}	S_{IC}	S_{IN}	S_I	$[\frac{kgCODm^{-3}d^{-1}}{kmolm^{-3}d^{-1}}]$
1	Disintegration												f_{x_i,x_c}	ρ_1
2	Hydrolysis of Carbohydrates	1												ρ_2
3	Hydrolysis of Proteins		1											ρ_3
4	Hydrolysis of Lipids	$1-f_{fa,li}$		$f_{fa,li}$										ρ_4
5	Uptake of Sugars	-1				$(1-Y_{su})f_{bu,su}$	$(1-Y_{su})f_{pro,su}$	$(1-Y_{su})f_{ac,su}$	$(1-Y_{su})f_{H2,su}$		$-\sum_{i=1-9,11-24} C_i\nu_{i,5}$	$-Y_{su}N_{bac}$		ρ_5
6	Uptake of AminoAcids		-1		$(1-Y_{aa})f_{va,aa}$	$(1-Y_{aa})f_{bu,aa}$	$(1-Y_{aa})f_{pro,aa}$	$(1-Y_{aa})f_{ac,aa}$	$(1-Y_{aa})f_{H2,aa}$		$-\sum_{i=1-9,11-24} C_i\nu_{i,6}$	$N_{aa}-Y_{su}N_{bac}$		ρ_6
7	Uptake of LCFA			-1				$(1-Y_{fa}0.7$	$(1-Y_{fa}0.3$		$-\sum_{i=1-9,11-24} C_i\nu_{i,7}$	$-Y_{fa}N_{bac}$		ρ_7
8	Uptake of Valerate				-1		$(1-Y_{C4})0.54$	$(1-Y_{C4})0.31$	$(1-Y_{C4})0.15$		$-\sum_{i=1-9,11-24} C_i\nu_{i,8}$	$-Y_{C4}N_{bac}$		ρ_8
9	Uptake of Butyrate					-1		$(1-Y_{C4}0.8$	$(1-Y_{C4}0.2$		$-\sum_{i=1-9,11-24} C_i\nu_{i,9}$	$-Y_{C4}N_{bac}$		ρ_9
10	Uptake of Propionate						-1	$(1-Y_{pro}0.57$	$(1-Y_{pro}0.43$		$-\sum_{i=1-9,11-24} C_i\nu_{i,10}$	$-Y_{pro}N_{bac}$		ρ_{10}
11	Uptake of Acetate							-1		$(1-Y_{ac})$	$-\sum_{i=1-9,11-24} C_i\nu_{i,11}$	$-Y_{ac}N_{bac}$		ρ_{11}
12	Uptake of Hydrogen								-1	$(1-Y_{ac})$	$-\sum_{i=1-9,11-24} C_i\nu_{i,12}$	$-Y_{H2}N_{bac}$		ρ_{12}
13	Decay of X_{su}										$-\sum_{i=1-9,11-24} C_i\nu_{i,13}$	$N_{bac}-N_{X_c}$		ρ_{13}
14	Decay of X_{aa}										$-\sum_{i=1-9,11-24} C_i\nu_{i,14}$	$N_{bac}-N_{X_c}$		ρ_{14}
15	Decay of X_{fa}										$-\sum_{i=1-9,11-24} C_i\nu_{i,15}$	$N_{bac}-N_{X_c}$		ρ_{15}
16	Decay of X_{C4}										$-\sum_{i=1-9,11-24} C_i\nu_{i,16}$	$N_{bac}-N_{X_c}$		ρ_{16}
17	Decay of X_{pro}										$-\sum_{i=1-9,11-24} C_i\nu_{i,17}$	$N_{bac}-N_{X_c}$		ρ_{17}
18	Decay of X_{ac}										$-\sum_{i=1-9,11-24} C_i\nu_{i,18}$	$N_{bac}-N_{X_c}$		ρ_{18}
19	Decay of X_{H2}										$-\sum_{i=1-9,11-24} C_i\nu_{i,19}$	$N_{bac}-N_{X_c}$		ρ_{19}
		Monosaccarides $kgCODm^{-3}$	Amino Acids $kgCODm^{-3}$	LCFA $kgCODm^{-3}$	Total Valerate $kgCODm^{-3}$	Total Butyrate $kgCODm^{-3}$	Total Propionate $kgCODm^{-3}$	Total Acetate $kgCODm^{-3}$	Liquid Hydrogen $kgCODm^{-3}$	Liquid Methane $kgCODm^{-3}$	Inorganic Carbon $kmolCm^{-3}$	Inorganic Nitrogen $kmolNm^{-3}$	Soluble Inerts $kmolPm^{-3}$	

Table 2.6: Petersen Matrix, part *a*.

	Components →	13	14	15	16	17	18	19	20	21	22	23	24	Rate ρ_j
	Process ↓	X_C	X_{ch}	X_{pr}	X_{li}	X_{su}	X_{aa}	X_{fa}	X_{c4}	X_{pro}	X_{ac}	X_{h2}	X_I	$[\frac{kgCODm^{-3}d^{-1}}{kmolm^{-3}d^{-1}}]$
1	Disintegration	-1	$f_{ch,xc}$	$f_{pr,xc}$	$f_{li,xc}$								f_{x_i,x_c}	ρ_1
2	Hydrolysis of Carbohydrates		-1											ρ_2
3	Hydrolysis of Proteins			-1										ρ_3
4	Hydrolysis of Lipids				-1									ρ_4
5	Uptake of Sugars					Y_{su}								ρ_5
6	Uptake of AminoAcids						Y_{aa}							ρ_6
7	Uptake of LCFA							Y_{fa}						ρ_7
8	Uptake of Valerate								Y_{C4}					ρ_8
9	Uptake of Butyrate								Y_{C4}					ρ_9
10	Uptake of Propionate									Y_{pro}				ρ_{10}
11	Uptake of Acetate										Y_{ac}			ρ_{11}
12	Uptake of Hydrogen											Y_{H2}		ρ_{12}
13	Decay of X_{su}	0.25				-1							0.75	ρ_{13}
14	Decay of X_{aa}	0.25					-1						0.75	ρ_{14}
15	Decay of X_{fa}	0.25						-1					0.75	ρ_{15}
16	Decay of X_{C4}	0.20											0.80	ρ_{16}
17	Decay of X_{pro}	0.20								-1			0.80	ρ_{17}
18	Decay of X_{ac}	0.20									-1		0.80	ρ_{18}
19	Decay of X_{h2}	0.25										-1	0.75	ρ_{19}
		Composites $kgCOD\ m^{-3}$	Carbohydrates $kgCOD\ m^{-3}$	Proteins $kgCOD\ m^{-3}$	Lipids $kgCOD\ m^{-3}$	Sugar degraders$kgCOD\ m^{-3}$	Amino acids degraders $kgCOD\ m^{-3}$	LCFA degraders $kgCOD\ m^{-3}$	Valerate and butyrate degraders $kgCOD\ m^{-3}$	Propionate degraders $kgCOD\ m^{-3}$	Acetate degraders $kgCOD\ m^{-3}$	Hydrogen degraders $kgCOD\ m^{-3}$	Particulate Inerts $kgCOD\ m^{-3}$	

Table 2.7: Petersen Matrix, part *b*.

Chapter 3

A modeling and simulation study of anaerobic digestion in plug-flow reactors*

*The results of this chapter will be submitted in the form of a manuscript entitled: *A modeling and simulation study of anaerobic digestion in plug-flow reactors.*

3.1 Abstract

In this work a mathematical model for the anaerobic digestion process in plug-flow reactors is proposed on the basis of mass balance considerations. The model consists of a system of non-linear parabolic partial differential equations for the variables representing the concentrations of the bio-components constituting the waste matrix and takes into account convective and diffusive phenomena. The plug-flow reactor is modelled as a one-dimensional domain; the waste matrix moves in the direction of the reactor axis and undergoes diffusive phenomena which reproduce the movement of the bio-components along the reactor axis due to a gradient in concentration. The velocity characterizing the convection of the waste matrix moving within the reactor is not fixed a priori but it is considered as an additional unknown of the mathematical problem. The variation in the convective velocity allows to account the mass variation occurring along a plug-flow reactor due to the conversion of solids, which is an aspect not much analysed in the literature of dry anaerobic digestion in plug-flow reactors. The equation governing the convective velocity is derived by considering the following hypothesis: the density of the waste matrix within the reactor is supposed constant over time and the sum of the volume fractions of the bio-components constituting the waste matrix are constrained to sum up to unity. The waste matrix undergoes biochemical transformations catalysed by anaerobic microbial species which lead to the production of gaseous methane, the final product of the anaerobic digestion process. Biochemical processes are modelled using a simplified scheme and a differential equation is used to describe the dynamics of the produced gaseous methane. A finite difference scheme is used for the numerical integration. Lastly, the model consistency is showed through numerical simulations which investigate the effect of the variation of some operating parameters on the process performance. The model is then applied to a case of engineering interest. Simulations produce results in agreement with the experimental observations. This highlights that the model can serve as a tool for the optimal management and sizing of an anaerobic digestion plug-flow reactor.

3.2 Introduction

Nowadays, Anaerobic Digestion (AD) process is a technology widely used for the treatment of the Organic Fraction of Municipal Solid Waste (OFMSW). The organic compounds are converted in biogas thanks to the activity of various microbial groups operating in an oxygen-free environment. The biogas, due to its high methane content, can be used to produce simultaneously heat and electricity through combined heat and power systems or directly injected in the gas grid (after cleaning) and is considered as a renewable energy. The residual substrate of the AD represents a by-product of the process, called digestate, which is used as fertilizer in agriculture.

The AD process is usually classified based on the Total Solids (TS) content of the substrate to be treated, where TS is the measure of all the suspended, colloidal and dissolved solids in a medium. If the TS content is less or equal to 10% the AD is classified as Wet-AD (WAD) otherwise, if it is greater or equal to 20%, it

is denoted as Dry-AD (DAD). Lastly, the AD is denoted as semi-dry AD (SDAD) when the TS content is between 10% and 20%. Moisture content is essential to the AD process because it dissolves nutrients and facilitates the contact between substrates and bacteria [68]. Compared to WAD, DAD has the advantage to reduce the needed reactor volume, the energy needs as there is less water to heat up and, moreover, the amount of by-product to be treated [136, 22]. However, DAD usually presents some drawbacks related to inhibition, accumulation of Volatile Fatty Acids (VFA) and long Hydraulic Retention Time (HRT) [65]. VFAs are short chain carboxylic acids having from 2 to 5 carbon atoms in the molecule and are among the essential intermediates of the AD process. HRT indicates the mean residence time of a certain substrate within a biological reactor [102], determining the contact time between the substrate to be treated and the microorganisms. One of the most used reactor configuration for DAD processes is the Plug-Flow Reactor (PFR), constituted by a reactor having a tubular or parallelepiped shape. In a plug-flow reactor, the waste movement along the digester is such that back-mixing is avoided [116] and a portion of the effluent is typically recycled to inoculate the influent and improve the AD process [73]. The hydrodynamics of a full-scale plug-flow reactor depends on the adopted configuration. For example Dranco systems work as vertical downflow digesters, where the mixing occurs via recirculation of the waste extracted at the bottom of the reactor; an horizontal flow is used in the Kompogas configuration, realized through slow rotation mixers that ensure the homogenization in radial direction and the stripping of the biogas; the horizontal plug-flow is circular in the Valorga configuration, where the mixing is realized injecting the biogas from the bottom of the reactor [77].

Mathematical modeling of AD process represents a powerful tool to enhance process control and optimization together with reactor sizing and plant management. The vast majority of models describing WAD process refers to Continuous Stirred Tank Reactor (CSTR) configuration and follows the approach of the Anaerobic Digestion Model No.1 (ADM1) [10, 50, 82]. ADM1 consists of a system of Ordinary Differential Equations (ODEs) which simulate the main biochemical processes occurring during anaerobic digestion. The latter can be classified into five main phases: disintegration, hydrolysis, acidogenesis, acetogenesis and methanogenesis. According to [9], one of the main limitations to mathematical modeling of AD is related to the lack of reliable mathematical models capable to describe this kind of process in PFRs. Contrary to CSTR, where the hypothesis of complete mixing of the compounds inside the reactor is considered, in a PFR model the state variables are functions both of time and space. Moreover, perfect mixing in radial direction is assumed, then reactant concentrations are uniform in any cross section and vary only along the flow path. The system of PDEs describing the phenomenon, is represented by mass balances on the state variables of the problem. In literature there exist a few number of works related to the modeling of AD in PFRs due to the uncertainty linked to some aspects of the problem such as dispersion, mixing, turbulence, variation of density and variation of the porosity of the medium. The existing PFR models make some simplifications to describe the phenomenon. For example in [39] the authors approximate the PFR as a tank-in-series system, solving a sequence of CSTR-type reactors; in [125] Vavilin et al. solved the convection-diffusion-reaction equation for a PFR using a constant convective velocity; Binxin

Wu in [132] faced the problem using a two-stage computational fluid dynamics (CFD) where the physical model, consisting of a system of PDEs, is solved under steady-state conditions while the biological model is represented by a system of ODEs.

Other works focus on the discussion of the boundary conditions for the convection-diffusion-reaction equations describing the PFR configuration. They mostly debate on the validity of the boundary conditions postulated by P.V. Danckwerts in 1953 [34]. In his work Danckwerts argues that for a convection-diffusion-reaction equation at the inlet section the flux continuity must be preserved while at the outlet the gradient in concentration must be zero. Several authors successfully used the Danckwerts' boundary conditions in their works [19, 96, 122, 36]), others criticized some aspect of Danckwerts' assertions, mostly claiming that the state variables should preserve the continuity across the inlet boundary [131] or that the mass and heat flux are not conserved if the contribution of dispersion to axial mass flow is important [37].
The aim of this work is to present a mathematical model capable to describe the DAD process of OFMSW in a PFR. The model considers the process being governed by one-dimensional convection-diffusion-reaction equations where the convective velocity is not a fixed value but it is considered as a function both of space and time. In the existing models, the general approach consists in neglecting the system mass variation due to the degradation processes that lead to the conversion of solids in gaseous compounds along the reactor. In this new kind of approach it is considered that this loss in mass is balanced by the variation of the convective velocity of the system, taking into account that these kind of processes are performed maximizing the working reactor volume, keeping constant the level of the treated substrate along the reactor. The equation governing the system velocity variation is derived through the hypothesis that the waste density is constant in time and space and the sum of the volume fractions of the bio-components constituting the waste matrix are constrained to sum up to unity. These statements imply that the mass of the waste mixture should remain constant in time and space, hence the solids mass reduction due to the degradation processes along the reactor, as aforementioned, has to be balanced by the variation of the convective velocity. Suitable initial-boundary conditions are prescribed. Biochemical processes are modelled using a simplified kinetic scheme where disintegration and methanogenesis are considered as the rate-limiting steps of the whole digestion process. Equations are numerically integrated by using a finite difference scheme and numerical simulations show different aspects that could be analysed during the management of an existing plant or the designing of new plants. They investigate the roles of some operating and physical parameters on process dynamics in terms of methane production, removal efficiency, bio-components constituting the waste matrix concentration trends and convective velocity trend. The investigated physical and operating parameters are the reactor length, the inlet convective velocity of the waste, the HRT and the diffusion coefficient. Finally, the model is applied to the case of a lab-scale experiment reproducing the DAD process in a PFR for different Organic Loading Rates (OLRs), where the OLR indicates a measure of the amount of organic material per unit reactor volume subjected to an AD process in a given unit time period [52].

3.3 Mathematical model

3.3.1 Model equations

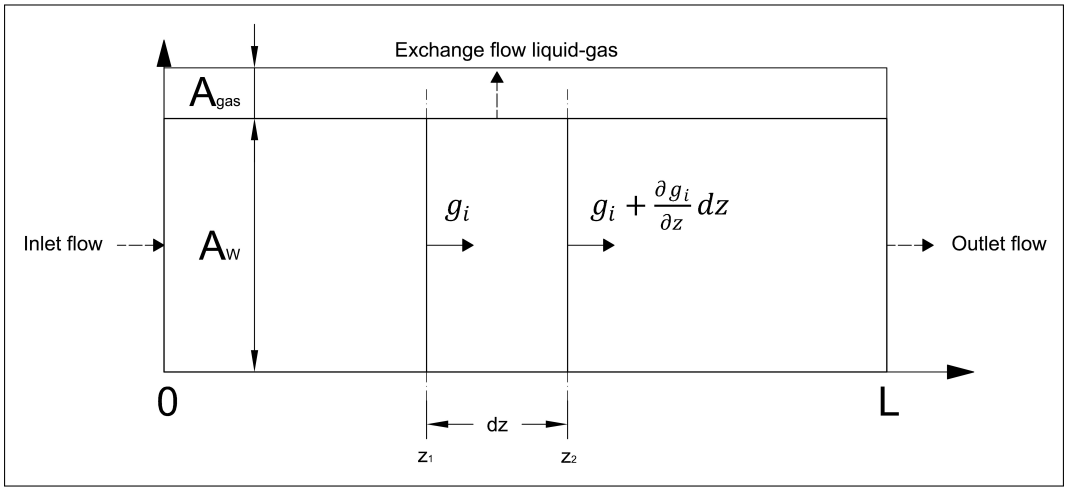

Figure 3.1: Control volume for the mass balance.

The mathematical model is derived in the framework of continuum mechanics and is based on mass balance considerations in one-dimensional case for n state variables $C_i\,(z,t)\,,\ i=1,...,n,\ \mathbf{C}=(C_1,...,C_n)$ which represent the concentrations of the bio-components constituting the waste mixture. The state variables are considered as functions of time t and space z, where z represents the spatial coordinate oriented along the reactor axis and directed from the inlet to the outlet section. Let us consider a control volume $A_w dz$ as represented in Figure 3.1, where A_w is the constant cross-sectional area of the reactor occupied by the waste. Taking into account the mass flux per unit area $g_i\,(z,t)$ crossing the surface A_w and the source/consumption term $F_i\,(z,t,\mathbf{C})$, the mass balance on the i^{th} compound gives:

$$A_w \frac{\partial}{\partial t}\int_{z_1}^{z_2} C_i\,(z,t)\ dz = A_w\left[g_i\,(z_1,t) - g_i\,(z_2,t)\right] + A_w\int_{z_1}^{z_2} F_i\,(z,t,\mathbf{C})\ dz,$$
$$0<z<L,\quad t>0,\quad i=1,...,n, \quad (3.1)$$

$$\int_{z_1}^{z_2}\frac{\partial C_i\,(z,t)}{\partial t}\,dz = -\int_{z_1}^{z_2}\frac{\partial g_i\,(z,t)}{\partial z}\,dz + \int_{z_1}^{z_2} F_i\,(z,t,\mathbf{C})\ dz,$$
$$0<z<L,\quad t>0,\quad i=1,...,n. \quad (3.2)$$

where:

- $g_i\,(z,t) = v_i\,(z,t)\,C_i\,(z,t) - \bar{D}_i\,(z,t)\,\partial C_i(z,t)/\partial z,\ i=1,...,n$;
- $F_i\,(z,t,\mathbf{C}) = \sum_{j=1}^{k}\alpha_{ij} r_j\,(z,t,\mathbf{C})\,,\ i=1,...,n$;

- k is the number of processes involved;

- α_{ij} is the stoichiometric coefficient of compound i on process j;

- $r_j\left(z,t,\mathbf{C}\right)$ is the kinetic rate of process $j,\ j=1,...,k$.

The convective flux of each compound of the waste matrix is characterized by a velocity $v_i\left(z,t\right)$ which is supposed to be a function of both space and time but the same for each compound. The diffusion coefficient $\bar{D}_i$ is assumed constant along the z-direction and on time and equal for all the compounds:

$$v_i = v, \quad \bar{D}_i = \bar{D}, \quad i = 1,...,n. \tag{3.3}$$

Differentiating equation (3.2) with respect to z_2 and considering $z_2 = z$ follows:

$$\frac{\partial C_i\left(z,t\right)}{\partial t} + \frac{\partial\left(v\left(z,t\right)C_i\left(z,t\right)\right)}{\partial z} - \bar{D}\frac{\partial^2 C_i\left(z,t\right)}{\partial z^2} = F_i\left(z,t,\mathbf{C}\right), \\ 0 < z < L, \quad t > 0, \quad i = 1,...,n. \tag{3.4}$$

Equation (3.4) represents the well known convection-diffusion-reaction equation in conservative form in one-dimensional case.

Now let us consider the composition of the waste matrix moving along the reactor. This matrix has a density $\rho\left(z,t\right) = \rho$ supposed to be constant with space and time and is constituted by water, particulate and dissolved components. The particulate fraction is composed of inerts, volatile solids (VS) (divided in bio-degradable and non bio-degradable material) and microbial biomass. VS represents the portion of the TS content that is volatilized at $550\ ^{\circ}\mathrm{C}$ and gives an idea on the amount of the readily vaporizing matter present in the solid fraction of a substrate. The sum of inerts and VS constitute the TS content of the waste. The dissolved components are soluble acetic acid and soluble methane, which are anaerobically produced from the degradation of VS performed by the microbial biomass. Their concentrations are usually expressed in terms of Chemical Oxygen Demand (COD) which is a measure of the amount of oxygen that is needed for the complete chemical oxidation of organic compounds of a medium. It is commonly expressed in mass of oxygen consumed over volume of the medium sample used for its measurement.

The volume of the head-space above the waste matrix is considered constant and the gas occupying this volume is composed only by gaseous methane, whose concentration is considered invariable along the space.

The following notations will be used:

- $X_1\left(z,t\right)$ is the water concentration within the reactor;

- $X_2\left(z,t\right)$ is the inerts concentration within the reactor;

- $X_3(z,t)$ is the concentration of bio-degradable VS;
- $X_4(z,t)$ is the concentration of non bio-degradable VS;
- $X_5(z,t)$ is the microbial biomass concentration within the reactor expressed in terms of VS;
- $S_1(z,t)$ is the soluble acetic acid concentration within the reactor expressed in terms of COD;
- $S_2(z,t)$ is the soluble methane concentration within the reactor expressed in terms of COD;
- $G(t)$ is the gaseous methane concentration within the head-space of the reactor expressed in terms of COD;
- $\mathbf{X} = (X_1, ..., X_5)$;
- $\mathbf{S} = (S_1, S_2)$;
- $F_{X,h}(z,t,\mathbf{X},\mathbf{S},G)$, $h = 1, ..., 5$, is the source/consumption term of the particulate compound X_h;
- $F_{S,l}(z,t,\mathbf{X},\mathbf{S},G)$, $l = 1, 2$, is the source/consumption term of the dissolved compound S_l.

The kinetic scheme of the model is reported in the Figure 3.2. The conversion of the bio-degradable VS X_3 in soluble acetic acid S_1, which takes place through different processes that are disintegration, hydrolysis, acidogenesis and acetogenesis, is summarized in a unique kinetic rate r_1, considering only the rate-limiting step that is the disintegration during AD of complex substrates [43, 49, 123]; from the degradation of the acetic acid through the non linear Monod-type kinetic rate r_2 are produced soluble methane S_2 and microbial biomass X_5; the microbial biomass die according to the decay law whose kinetic rate is indicated as r_4 and produce new bio-degradable and non-biodegradable VS X_4; lastly, the soluble and gaseous methane (S_2 and G), are in equilibrium according to the gas-transfer law expressed by the kinetic rate r_3.

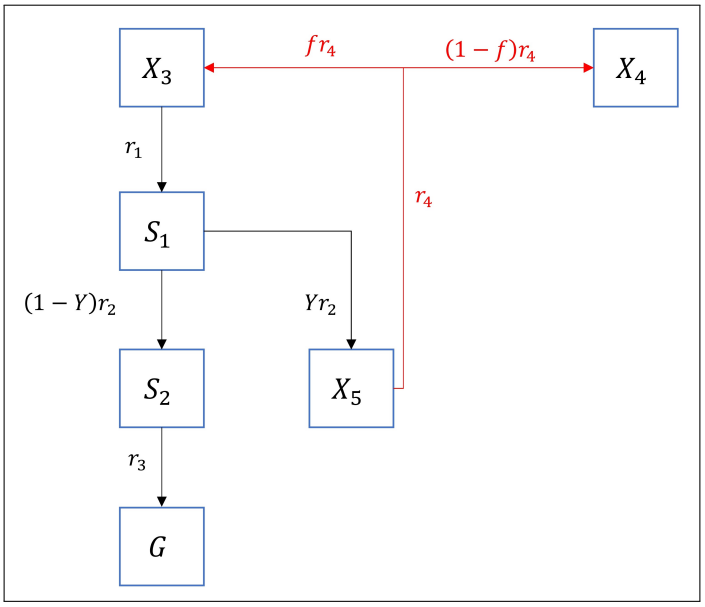

Figure 3.2: Kinetic scheme.

Applying equation (3.4) to the compounds $X_h,\ h = 1, ..., 5$, S_1 and S_2 the following non-linear system of PDEs is obtained.

$$\frac{\partial X_h(z,t)}{\partial t} + \frac{\partial (v(z,t)X_h(z,t))}{\partial z} - \bar{D}\frac{\partial^2 X_h(z,t)}{\partial z^2} = F_{X,h}\left(z,t,\mathbf{X},\mathbf{S},G\right), \quad 0 < z < L, \quad t > 0, \quad h = 1, ..., 5, \quad (3.5)$$

$$\frac{\partial S_l(z,t)}{\partial t} + \frac{\partial (v(z,t)S_l(z,t))}{\partial z} - \bar{D}\frac{\partial^2 S_l(z,t)}{\partial z^2} = F_{S,l}\left(z,t,\mathbf{X},\mathbf{S},G\right), \quad 0 < z < L, \quad t > 0, \quad l = 1, 2, \quad (3.6)$$

where:

- $F_{X,1}\left(z,t,\mathbf{X},\mathbf{S},G\right) = F_{X,2}\left(z,t,\mathbf{X},\mathbf{S},G\right) = 0$;
- $F_{X,3}\left(z,t,\mathbf{X},\mathbf{S},G\right) = fr_4 - r_1$;
- $F_{X,4}\left(z,t,\mathbf{X},\mathbf{S},G\right) = (1-f)r_4$;
- $F_{X,5}\left(z,t,\mathbf{X},\mathbf{S},G\right) = Yr_2 - r_4$;
- $F_{S,1}\left(z,t,\mathbf{X},\mathbf{S},G\right) = m(r_1 - r_2)$;
- $F_{S,2}\left(z,t,\mathbf{X},\mathbf{S},G\right) = m(1-Y)r_2 - r_3$;

- $r_1 = k_1 X_3$;
- $r_2 = k_2 X_5 S_1 / (K_1 + S_1)$;
- $r_3 = k_3 (S_2 - RTK_H G)$;
- $r_4 = k_4 X_5$;
- m is the conversion factor of VS in COD $\left[g_{COD}\ g_{VS}^{-1}\right]$;
- Y is the yield of biomass on substrate;
- f is the fraction of dead microbial biomass becoming new bio-degradable substrate;
- k_1 is the kinetic constant for the consumption of the volatile solids X_3, having the dimension of $[T^{-1}]$;
- k_2 is the Monod maximum specific uptake rate for the acetic acid $[T^{-1}]$;
- K_1 is the half saturation constant $[M\ L^{-3}]$ for the kinetics of consumption of the acetic acid;
- k_3 is the gas-liquid transfer coefficient $[T^{-1}]$;
- R is the gas law constant $[L^2\ T^{-2}\ \Theta^{-1}]$;
- T is the operating temperature $[\Theta]$;
- K_H is the Henry's law coefficient $[L^2\ T^{-2}]$;
- k_4 is the first order decay rate of the microbial biomass X_6 $[T^{-1}]$.

The velocity displacement of the waste matrix along the reactor axis constitutes an additional unknown of the problem, and a further equation is needed to describe its variation in space and time. To this aim, the following hypothesis is made: the sum of the volume fractions of the particulate components within the reactor is constrained to sum up to unity, that is:

$$\begin{cases} \sum_{h=1}^{5} X_h\,(z,t)\,/\rho_h = 1, \\ \rho_h = \rho, \quad h = 1, ..., 5 \end{cases} \quad \Longrightarrow \quad \sum_{h=1}^{5} X_h(z,t) = \rho. \tag{3.7}$$

Equation (3.7) implies that the mass of the mixture composed of water, inerts, VS and microbial biomass is constant over time. As a consequence, the convective velocity of the waste matrix varies along the reactor and its variation depends on the kinetics of the compounds constituting the mixture. In fact, the velocity variation has to balance the consumption of the VS to keep the mass of this particular mixture constant.

These considerations are used to derive the equation governing the velocity. Summing equation (3.5) on $h = 1, ..., 5$ and taking into account equation (3.7) follows:

$$\frac{\partial v(z,t)}{\partial z} = \frac{\sum_{h=1}^{5} F_{X,h}\left(z,t,\mathbf{X},\mathbf{S},G\right)}{\rho}, \tag{3.8}$$

$$\sum_{h=1}^{5} F_{X,h}\left(z,t,\mathbf{X},\mathbf{S},G\right) = Yr_2 - r_1. \tag{3.9}$$

In addition, a differential equation is derived from the mass balance for the volume $V_{gas} = A_{gas}L$ of the head-space where the biogas is stored. The dynamics of the gaseous methane $G\left(t\right)$ is described (Eq. (3.10)):

$$\frac{dG(t)}{dt} = \frac{A_w}{V_{gas}} \int_0^L r_3\left(z,t\right)\ dz. \tag{3.10}$$

This equation describes the fact that all the contributes to the gas-transfer in each point are summed to define a unique gas-transfer rate. The ratio between the cross-section occupied by the waste and the volume of gas is present to take into account the fact that the gas-transfer kinetic rate is waste volume-specific.

3.3.2 Boundary and initial conditions

With the aim to set a closed problem, initial-boundary conditions are prescribed. Firstly, the convective velocity of compounds moving along the reactor at the boundary $z = 0$ is assumed equal to the incoming flow velocity (Eq. (3.11)):

$$v(0,t) = v_0, \quad t \geqslant 0. \tag{3.11}$$

The value v_0 can be obtained by fixing the HRT of waste moving along the reactor of length L:

$$v_0 = \frac{L}{HRT}. \tag{3.12}$$

For the PDEs (3.5) and (3.6) Danckwerts' boundary conditions [34], which are Robin (Eqs. (3.13) and (3.15)) and Neumann (Eqs. (3.14) and (3.16)) conditions, are used. These conditions allow to preserve flux continuity in the first and last section of the reactor. Particularly, equations (3.13) and (3.15) indicate that, considering each particulate or dissolved compound constituting the mixture, the difference in concentration between the incoming flow rate and the first section of the reactor is linked to the diffusion phenomenon. Moreover, equations (3.14) and (3.16) imply that the diffusive flux has to be null in the last

section.

$$-\bar{D}\frac{\partial X_h(0,t)}{\partial z} = v_0(X_{h,IN} - X_h(0,t)), \quad h = 1, ..., 5, \quad t > 0, \tag{3.13}$$

$$\frac{\partial X_h(L,t)}{\partial z} = 0, \quad h = 1, ..., 5, \quad t > 0, \tag{3.14}$$

$$-\bar{D}\frac{\partial S_l(0,t)}{\partial z} = v_0(S_{l,IN} - S_l(0,t)), \quad l = 1, 2, \quad t > 0, \tag{3.15}$$

$$\frac{\partial S_l(L,t)}{\partial z} = 0, \quad l = 1, 2, \quad t > 0. \tag{3.16}$$

In (3.13) and (3.15) $X_{h,IN}$ and $S_{l,IN}$ are the concentrations of each particulate and dissolved compound in the incoming flow rate, respectively.

Lastly, the following initial conditions are considered (Eqs. (3.17), (3.18) (3.19)):

$$X_h(z,0) = X_{h,0}, \quad h = 1, ..., 5, \quad 0 \leqslant z \leqslant L, \tag{3.17}$$

$$S_l(z,0) = S_{l,0}, \quad l = 1, 2 \quad 0 \leqslant z \leqslant L, \tag{3.18}$$

$$G(0) = G_0. \tag{3.19}$$

3.4 Numerical simulations

3.4.1 Model input

The numerical method used for the integration of the system of PDEs stated in Section 3.3.1 with boundary and initial conditions presented in Section 3.3.2 follows the philosophy of the finite difference upwind method [33]. The method is conditionally stable and was implemented through an original software developed using Matlab platform.

Four sets of simulations A, B, C and D are performed to show model consistency. The effects of some operating and physical parameters on process performance are investigated in terms of methane production, bio-degradable VS removal efficiency, acetic acid concentration trend, microbial biomass concentration trend and convective velocity trend. The results are shown for a specific simulation time or, for one set (set C), for different simulation times. The investigated physical and operating parameters are the reactor length

L, the inlet convective velocity of the waste v_0, the HRT and the diffusion coefficient $\bar{D}$. In Table 3.1 are reported the kinetic parameters used in all simulations. The values of k_1 and k_3 were defined in this study. Particularly, the value of the gas-liquid transfer coefficient was decreased with respect to its value used in the ADM1 [10] to take into account the limitation to the gas-liquid transfer due to the high solids content [83, 1, 78]. Table 3.2 summarizes the initial and boundary conditions adopted for the various simulation sets. Such conditions have been obtained by fixing the TS content of the substrate to 20% and considering that the overall density of the treated substrate is equal to the density of water. Moverover, the VS content on TS base has been set equal to 70% and it is 50% non bio-degradable. The bio-degradable VS and the microbial biomass constitute the remaining 50% of the VS content. In all simulations the conversion coefficient of VS in COD has been set equal to $m = 1.5\ g_{COD}\ g_{VS}^{-1}$. The fraction of decayed microbial biomass becoming new bio-degradable substrate was set equal to $f = 0.2$.

Parameter	**Definition**	**Unit**	**Value**	**Reference**
k_1	Kinetic constant for the consumption of the volatile solids X_3	d^{-1}	0.10	This study
k_2	Monod maximum specific uptake rate for S_1	d^{-1}	8.00	[10]
k_3	Gas-liquid transfer coefficient	d^{-1}	20.0	This study
k_4	First order decay rate of the microbial biomass	d^{-1}	0.02	[10]
K_1	Half saturation constant	$g_{COD}\ l^{-1}$	0.15	[10]
Y	Yield of biomass on substrate	-	0.05	[10]
K_H	Henry's law coefficient	$Mbar^{-1}$	0.0011	[10]

Table 3.1: Kinetic parameters used in model simulations.

Parameter	Symbol	Unit	Value
Density of the waste	ρ	$g\ l^{-1}$	1000.0
Initial H_2O concentration	$X_{1,0}$	$g\ l^{-1}$	800.0
Initial inert concentration	$X_{2,0}$	$g\ l^{-1}$	60.0
Initial bio-degradable VS concentration	$X_{3,0}$	$g_{VS}\ l^{-1}$	69.3
Initial non-bio-degradable VS concentration	$X_{4,0}$	$g_{VS}\ l^{-1}$	70.0
Initial soluble acetic acid concentration	$S_{1,0}$	$g_{COD}\ l^{-1}$	0.0
Initial soluble methane concentration	$S_{2,0}$	$g_{COD}\ l^{-1}$	0.0
Initial microbial biomass concentration	$X_{5,0}$	$g_{VS}\ l^{-1}$	0.7
Initial gas-phase methane concentration	G_0	$g_{COD}\ l^{-1}$	0.0
Inlet H_2O concentration	$X_{1,IN}$	$g\ l^{-1}$	800.0
Inlet inert concentration	$X_{2,IN}$	$g\ l^{-1}$	60.0
Inlet bio-degradable VS concentration	$X_{3,IN}$	$g_{VS}\ l^{-1}$	69.3
Inlet non-bio-degradable VS concentration	$X_{4,IN}$	$g_{VS}\ l^{-1}$	70.0
Inlet soluble acetic acid concentration	$S_{1,IN}$	$g_{COD}\ l^{-1}$	0.0
Inlet soluble methane concentration	$S_{2,IN}$	$g_{COD}\ l^{-1}$	0.0
Inlet microbial biomass concentration	$X_{5,IN}$	$g_{VS}\ l^{-1}$	0.7

Table 3.2: Initial and boundary conditions used in model simulations.

Moreover, Table 3.3 present the values of the physical and operating parameters used in the simulation sets. The indicated HRT and OLR are referred to the inlet flow. In all simulations the cross section of the reactors is assumed equal to $1\,\mathrm{m}^2$ for simplicity. In the simulation set A, it is analysed the behaviour of the system when the process is performed using a constant HRT in reactors having different length and, as a consequence, a different inlet convective velocity of the waste v_0. In set B, a constant value is assumed for the inlet convective velocity of the waste v_0 while the reactor length and the HRT change. In set C the reactor length is constant but the inlet convective velocity of the waste, strictly related to the OLR, and the HRT are variable. It has to be highlighted that, since the same inlet VS concentration is used in all the simulations, when the HRT changes, the OLR changes too. Lastly, the value of the diffusion coefficient $\bar{D}$ is considered constant among the simulation sets A, B and C, while set D investigates the effects of the diffusion coefficient $\bar{D}$ on reactor performances.

3.4.2 Numerical results and discussion

For each simulation set, the results are reported in terms of the bio-degradable VS concentration $X_3\,(z,\tau)$, acetic acid concentration $S_1\,(z,\tau)$, microbial biomass concentration $X_5\,(z,\tau)$ trends and $v\,(z,\tau)$ profile after $\tau = 60$ days of simulation time. Furthermore, the methane production over time is shown. These

Parameter	Unit	Set A				Set B				Set C				Set D		
		A-1	A-2	A-3	A-4	B-1	B-2	B-3	B-4	C-1	C-2	C-3	C-4	D-1	D-2	D-3
$\bar{D}$	$10^{-7}\ m^2\ s^{-1}$	1.0	1.0	1.0	1.0	1.0	1.0	1.0	1.0	1.0	1.0	1.0	1.0	10^2	10^3	10^4
v_0	$cm\ d^{-1}$	8.33	16.67	25.00	33.33	33.33	33.33	33.33	33.33	20.0	25.0	33.33	50.0	33.33	33.33	33.33
L	m	2.5	5.0	7.5	10.0	2.5	5.0	7.5	10.0	10.0	10.0	10.0	10.0	10.0	10.0	10.0
HRT	d	30.0	30.0	30.0	30.0	7.5	15.0	22.5	30.0	50.0	40.0	30.0	20.0	30.0	30.0	30.0
OLR	$g_{VS}\ l^{-1}\ d^{-1}$	4.7	4.7	4.7	4.7	18.7	9.3	6.2	4.7	2.8	3.5	4.7	7.0	4.7	4.7	4.7

Table 3.3: Physical and operating parameters used during the four simulation sets A, B, C and D. $\bar{D}$ =Diffusion coefficient, v_0 =Inlet flow rate velocity, L =Reactor length, HRT =Hydraulic Retention Time and OLR =Organic Loading Rate.

trends are reported in Figures 3.3, 3.5 and 3.6 for simulation sets A, B and C respectively and in Figure 3.10 for set D.

Set A

Observing the results of the simulation set A (Figure 3.3), it can be noticed that, in this first case, a similar process of consumption of the bio-degradable VS takes place whatever is the reactor length (Figure 3.3a). This reveals that, treating a different substrate flow rate in reactors with different sizes keeping constant the HRT and OLR can be obtained the same concentration of bio-degradable VS in the outlet flow.

Figure 3.3b show the acetic acid concentration profiles along z after 60 days of simulation. The acetic acid profile presents a peak which is reached in a position very close to the inlet section for all the tested L values. The acetic acid is then consumed, assuming very low concentration values in the remaining part of the reactor. In this simulation set, where the HRT is kept constant, the values of the acetic acid concentration corresponding to the peaks of the curves decrease as the reactor length decreases.

The function $v(z)$ at simulation time $\tau = 60\,\mathrm{d}$ is plotted in Figure 3.3c. The function non-linearly decreases with z according to equation (3.8) resulting in a 6.5% lower velocity value in the outlet section for all the tested L values.

The concentrations of the microbial biomass for all the tested cases are reported in Figure 3.3e. A similar pattern is observed in all cases: in close proximity to the inlet section the concentration of the micro-organisms involved in the consumption of acetic acid is low. Then it increases, assuming its maximum values in the second half of the reactor. Hence, it can be considered that a stratification along the reactor is realized: the processes that lead to the production of acetic acid take place very close to the inlet section; then, thanks to the availability of the nutrients useful for the growth of the micro-organisms acting the uptake of the acetic acid, the acid is consumed and the soluble methane is produced.

Figure 3.3d shows the methane production in terms of liters in the head-space over time. The results suggest that, for the same period of observation time and under the same HRT and OLR, the longer is the reactor the higher is the methane production.

For the simulation set A are reported also the 3-D plots describing the dynamics of the variables $X_3(z,t)$, $S_1(z,t)$ and $X_5(z,t)$ over time and space in the simulation case A-4 (Figure 3.4). The constant initial concentration of bio-degradable VS X_3 along the reactor is reduced through the degradation process until the profile reported in Figure 3.3a (case with $L = 10\,\mathrm{m}$) is determined. Concerning the acetic acid dynamics it can be observed that it takes place an acid accumulation along the reactor during the initial days but then, with the growth of the concentration of the microbial biomass acting its uptake, the acid is consumed.

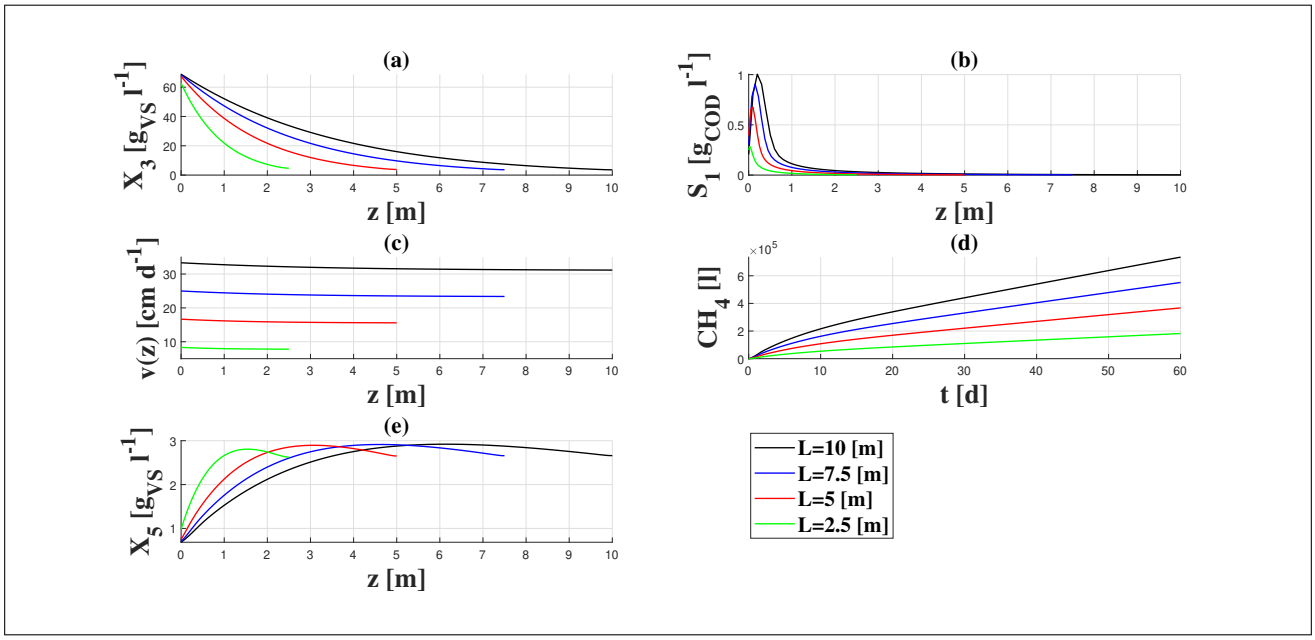

Figure 3.3: Bio-degradable VS $X_3\,(z,\tau)$ (3a), acetic acid $S_1\,(z,\tau)$ (3b), $v\,(z,\tau)$ (3c), methane production (3d) and microbial biomass $X_5\,(z,\tau)$ (3e) trends for simulations set A, at $\tau = 60\,\mathrm{d}$.

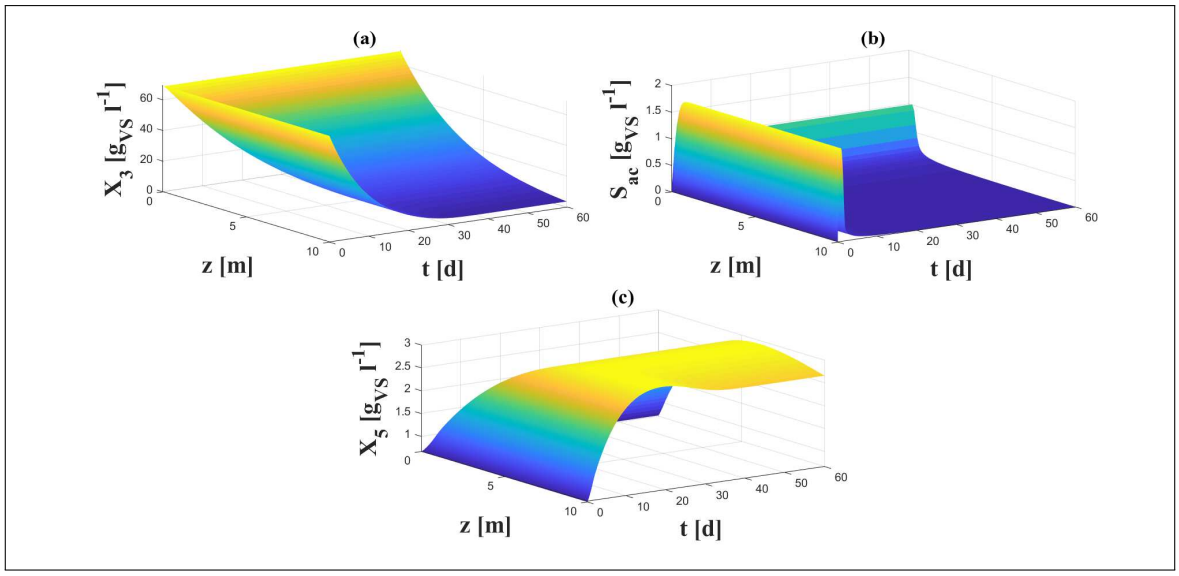

Figure 3.4: Bio-degradable VS $X_3\,(z,t)$ (4a), acetic acid $S_1\,(z,t)$ (4b) and microbial biomass $X_5\,(z,t)$ (4c) trends for simulations set A, case A-4.

Set B

The results of simulation set B are reported in Figure 3.5. In this case, the convective inlet velocity v_0 of the waste is supposed constant while the reactor length changes. This affects the values of both the HRT and the OLR. First of all, it is possible to observe that all the profiles of the variables along the space are aligned

on the same curve, except for the acetic acid. Concerning the bio-degradable VS conversion in acetic acid, it is clear that the shorter is the reactor length the higher is the residual bio-degradable VS concentration (Figure 3.5a). This is due to the fact that, feeding the waste inside the reactor with a constant inlet velocity, the shorter is the reactor length the lower is the HRT and, using the same concentration of VS, the higher is the OLR. Hence, a growing amount of bio-degradable compounds have less time to be degraded.

The acetic acid profiles show the same patterns established in the case of the simulation set A, with peaks located in close proximity to the inlet section and small residues of acid along the remaining part of the reactor. However, in this second case, the values corresponding to the peaks have a small decrease as the reactor length increases.

Moreover, also in the case of the simulation set B the velocity function trends are non-linear with z and it can be noticed a different percentage reduction in the velocity value between the inlet and outlet sections depending on the value of L. In particular, the longer is the reactor the higher is this percentage reduction: 3.52%, 5.24%, 6.07% and 6.49% for the reactor length $L = 2.5\,\mathrm{m}$, $L = 5.0\,\mathrm{m}$, $L = 7.5\,\mathrm{m}$ and $L = 10\,\mathrm{m}$ respectively.

The microbial biomass concentration profiles are similar to those observed for the simulation set A, with the highest concentration values achieved in the second half of the reactor for each simulation (Figure 3.5e).

Concerning the liters of produced methane over time (Figure 3.5d), the results show that, similarly to set A, the longer is the reactor the higher is the value of methane produced. This is mostly due to the different consumption of the bio-degradable VS content that takes place among the different operating conditions of the set B. Moreover, the initial mass of VS is higher the longer is the reactor, as a consequence of the initial conditions, and this affects the value of the produced methane. Furthermore, if reactors of the same size of the sets A and B are compared in terms of methane production, the investigated cases of the simulation set B during the same period of simulation time show an higher maximum value of produced methane with respect the cases of set A, except for the reactor length $L = 10\,\mathrm{m}$ where the operating conditions are the same between the two sets. This reveals that, considering a fixed reactor size, the methane production in absolute terms is improved when an higher volatile solids flow rate is fed into the reactor, even if a lower HRT is adopted, until inhibition phenomena occurs.

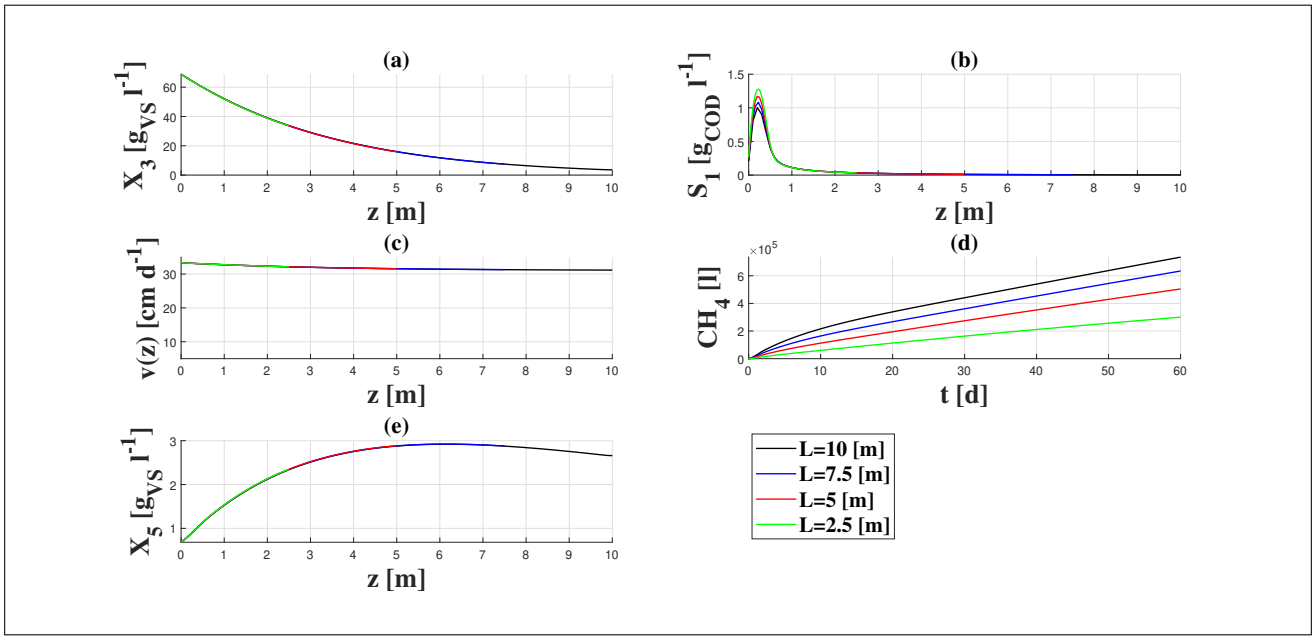

Figure 3.5: Bio-degradable VS $X_3\left(z,\tau\right)$ (5a), acetic acid $S_1\left(z,\tau\right)$ (5b), $v\left(z,\tau\right)$ (5c), methane production (5d) and microbial biomass $X_5\left(z,\tau\right)$ (5e) trends for simulations set B, at $\tau = 60\,\mathrm{d}$.

Set C

The results of simulation set C at simulation time $\tau = 60\,\mathrm{d}$, as in the previous cases, are reported in the Figure 3.6.

It can be observed that, for all simulations, the removal efficiency of the bio-degradable VS decreases as the inlet convective velocity of the waste increases (Figure 3.6a). If one analyses the removal efficiency of the bio-degradable VS in the three different simulation sets A, B and C at the simulation time $\tau = 60\,\mathrm{d}$ important informations for the designing of new plants of DAD can be obtained: keeping constant the HRT and considering a different reactor lengths and inlet velocities (simulation set A) the removal efficiency of the bio-degradable VS does not change so much ($92.5\% \leqslant \eta \leqslant 94.8\%$); passing from a length of $10\,\mathrm{m}$ to a length of $2.5\,\mathrm{m}$ (set B), keeping constant the inlet velocity of the waste, there is a reduction in the removal efficiency of the bio-degradable VS from $\eta = 94.8\%$ to $\eta = 50.7\%$; lastly, passing from an inlet convective velocity of the waste of $20\,\mathrm{cm\,d^{-1}}$ to an inlet velocity of $50\,\mathrm{cm\,d^{-1}}$ (set C), keeping constant the reactor length, there is a reduction in efficiency from $\eta = 98.7\%$ to $\eta = 85.6\%$. In the latter two cases, the reduction in efficiency means that if the reactor is not long enough or the inlet velocity is too high, respectively, and the process is performed with the objective to reach a certain volatile solids removal, there is the risk to fail.

In Figure 3.6b are reported the results referred to the acetic acid concentration profiles in the case of the simulation set C. It can be noticed that the lower is the inlet velocity the lower is the corresponding peak of the acetic acid concentration curve and the nearer to the inlet section this peak is reached. The residual acetic acid concentration show that, also in this simulation set, the acid is completely consumed along the

reactor.

The non-linearity characterizes the variation of the convective velocity along the reactor also in all cases of the set C (Figure 3.6c). Moreover, the curves describing the concentration of the micro-organisms involved in the consumption of acetic acid profile along the reactor length reported in Figure 3.6e present a visible decreasing pattern developed in the second half of the reactor, mainly in the cases where the inlet velocity is lower. These trends are the consequence of the differences in the convective transport phenomena and the acetic acid consumption dynamics occurring among the analysed cases.

Concerning the liters of methane in the head-space over time (Figure 3.6d), results confirm that, once fixed the reactor length, the higher is the adopted inlet velocity of waste fed into the reactor, which means also an higher OLR, the higher is the maximum value of produced methane.

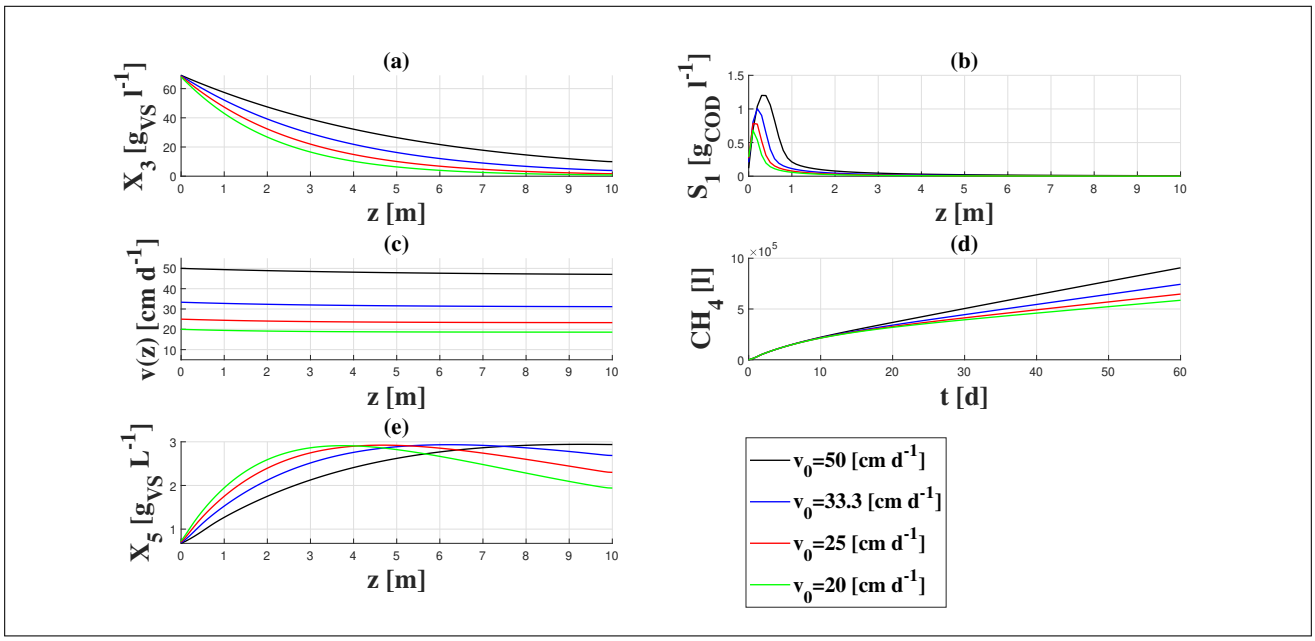

Figure 3.6: Bio-degradable VS $X_3\,(z,\tau)$ (6a), acetic acid $S_1\,(z,\tau)$ (6b), $v(z)$ (6c), methane production (6d) and microbial biomass $X_5\,(z,\tau)$ (6e) trends for simulations set C, at $\tau = 60\,\mathrm{d}$.

However, the results of methane production of the three simulation sets A, B and C can be analysed also monitoring the methane yields y, evaluated as the ratio between the value of the methane production curve at the instant time $\tau = 60\,\mathrm{d}$ $\alpha\ [l_{CH_4}]$ over the added mass of VS $\beta\ [g_{VS}\cdot]$ in the time interval $[0,\tau]$ (Eq. (3.20)) and reported in Figure 3.7.

$$y = \frac{\alpha(\tau)}{\beta(\tau)} \tag{3.20}$$

It is possible to observe that in the case of simulation set A the yields are constant with the reactor length (Figure 3.7a), while in the simulation set B the yield is about 2.5 times higher going from $L = 2.5\,\mathrm{m}$ to $L = 10.0\,\mathrm{m}$ (Figure 3.7b). Moreover, comparing the methane yields of the simulation sets A and B it can be concluded that, despite the absolute methane production increases when reactors of the same

length are fed with an higher amount of volatile solids, the yield decreases. A similar result is observed in simulation set C. Indeed, in this set is analysed the methane production of reactors having the same size fed using an increasing inlet velocity of the waste and an increasing OLR and, contrary to the maximum value of produced methane which increases as the adopted inlet velocity of waste increases, the methane yield decreases (Figure 3.7c).

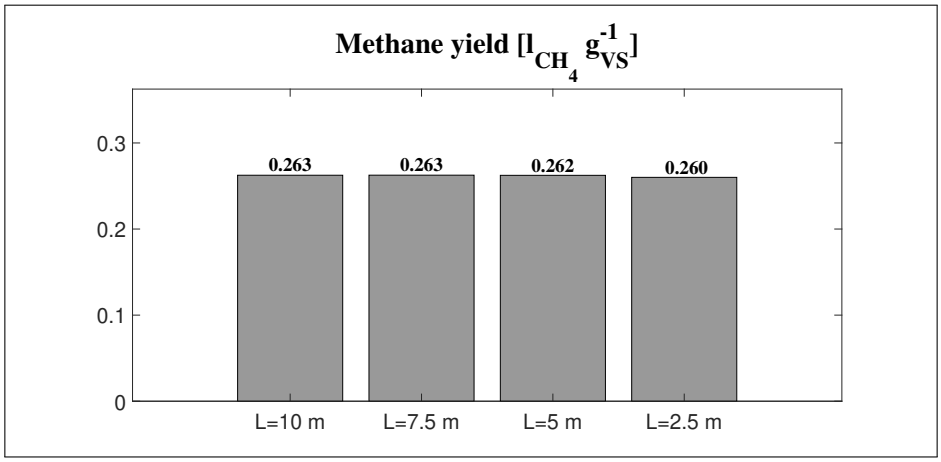

(a)

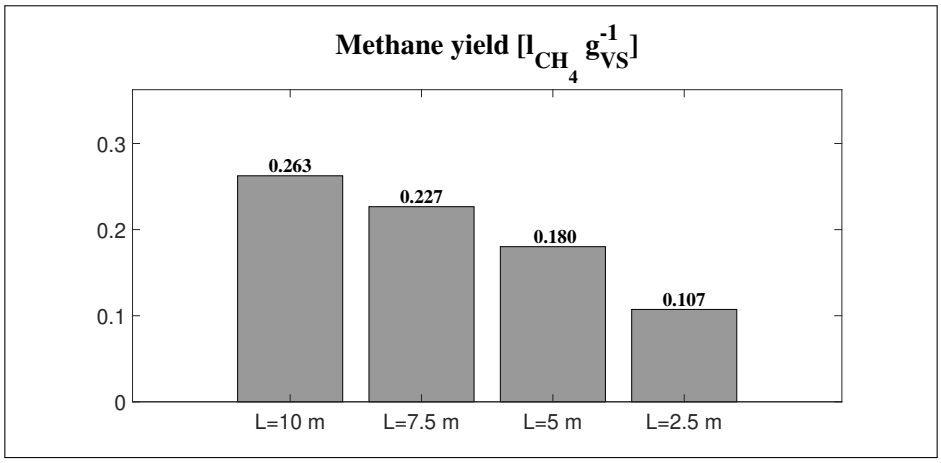

(b)

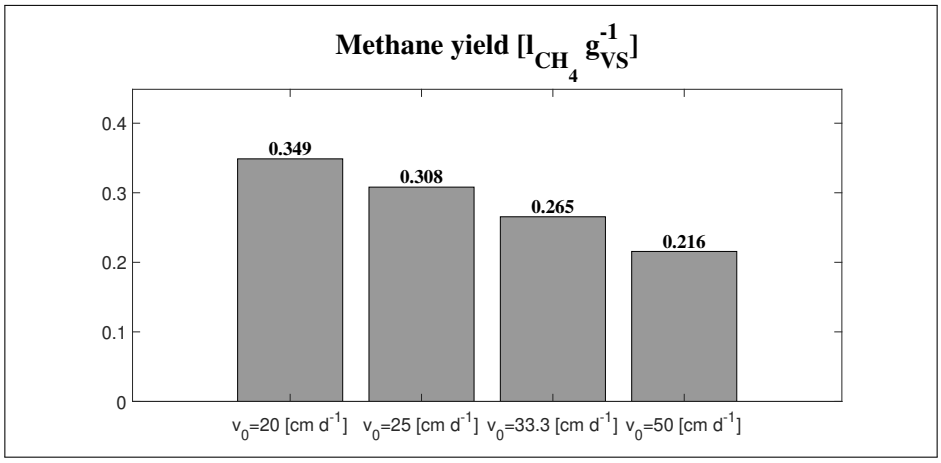

(c)

Figure 3.7: Methane yield for simulations sets A (3.7a), B (3.7b) and C (3.7c) after $\tau = 60\,\mathrm{d}$

Furthermore, for the simulation set C the bio-degradable VS concentration $X_3\,(z, \tau)$, microbial biomass

concentration $X_5(z,\tau)$, acetic acid concentration $S_1(z,\tau)$ trends and $v(z,\tau)$ profile at simulations times $\tau_1 = 15\,\mathrm{d}$, $\tau_2 = 30\,\mathrm{d}$, $\tau_3 = 60\,\mathrm{d}$ and $\tau_4 = 90\,\mathrm{d}$ are reported in Figures 3.8 and 3.9. Concerning the dynamics of the bio-degradable VS and microbial biomass concentrations reported in Figures 3.8a and 3.8b respectively, there are no differences between the 60th and 90th day, revealing that the process reached the steady state in all the investigated cases. On the contrary, the acetic acid concentration and velocity profiles along z appear to reach the steady state within the first 15 days (Figure 3.9a and 3.9b).

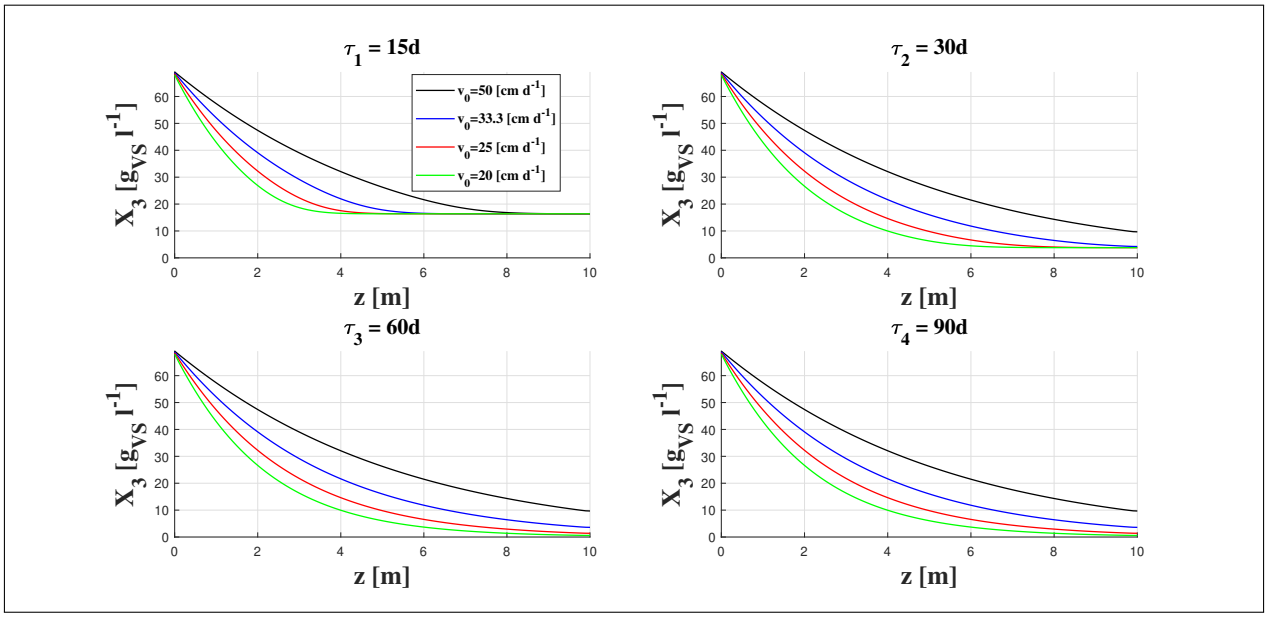

(a) Bio-degradable VS $X_3\,(z,\tau)$ concentration trend.

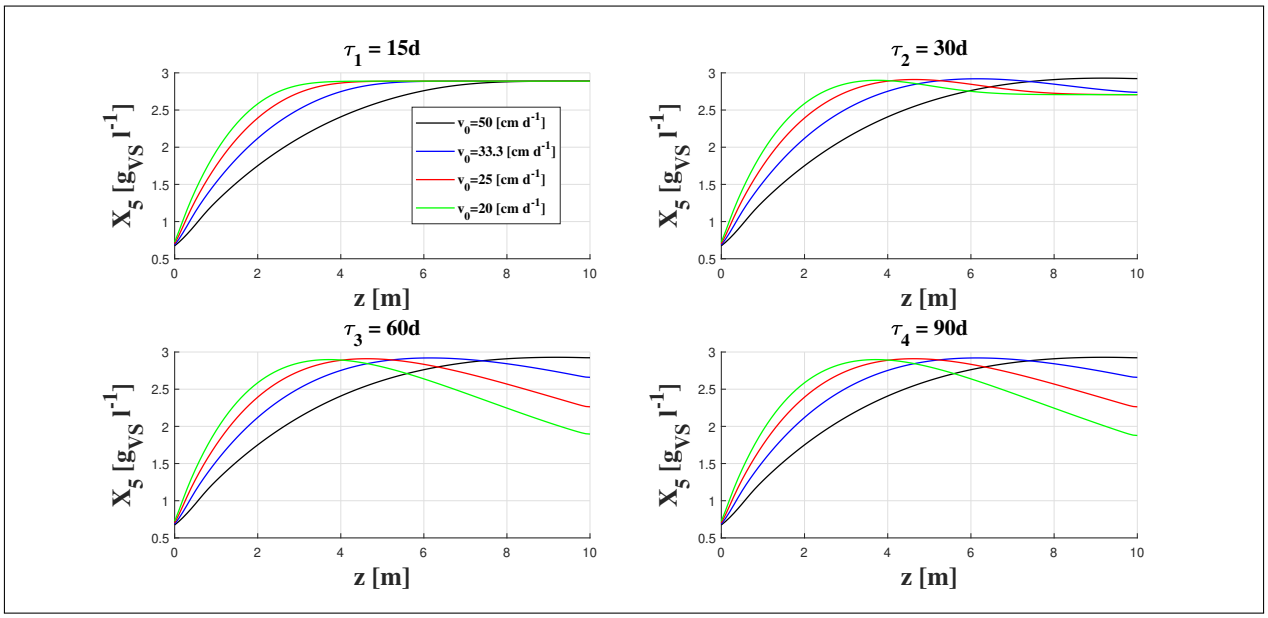

(b) Microbial biomass $X_5\,(z,\tau)$ concentration trend.

Figure 3.8: Bio-degradable VS $X_3\,(z,\tau)$ (3.8a) and microbial biomass $X_5\,(z,\tau)$ (3.8b) concentration trends at different time of simulation τ when $L = cost$ and v_0 varies, simulations set C.

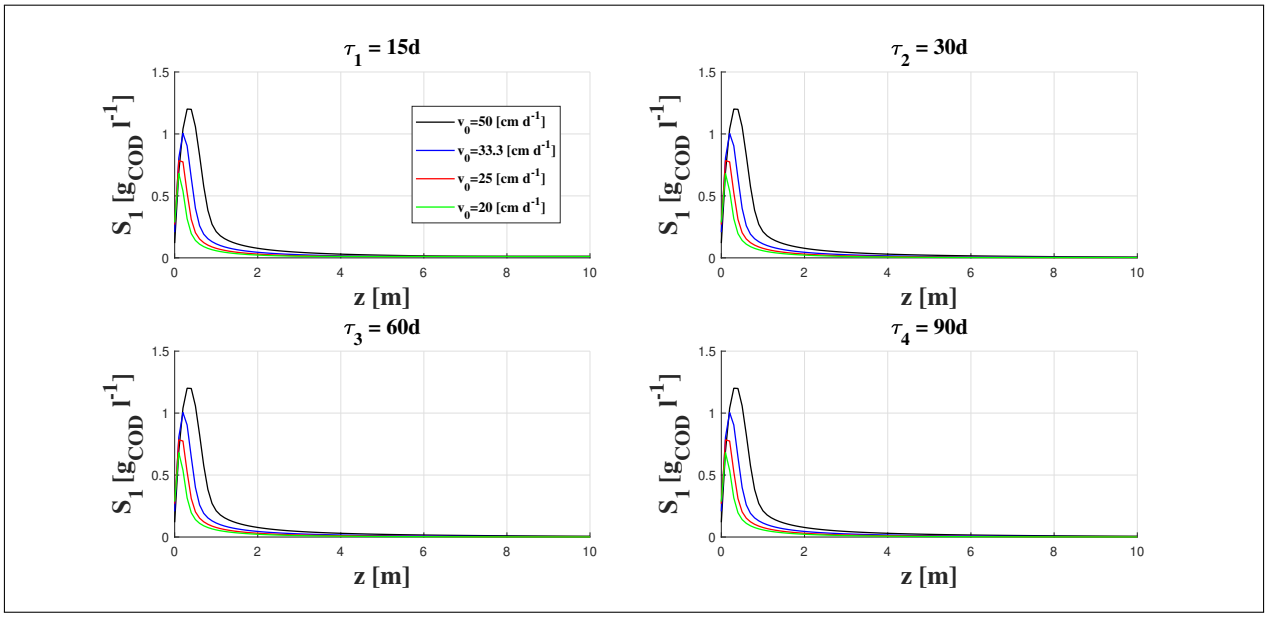

(a) Acetic acid $S_1\ (z, \tau)$ concentration trend.

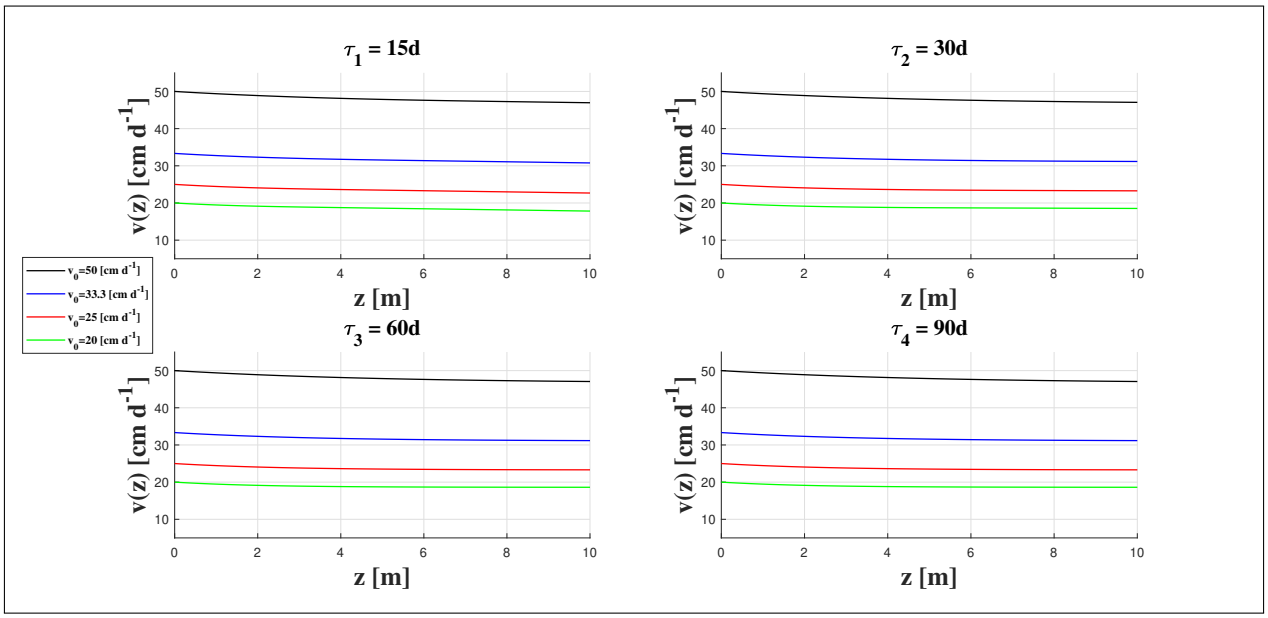

(b) $v\ (z, \tau)$ trend.

Figure 3.9: Acetic acid concentration $S_1\ (z, \tau)$ (3.9a) and $v\ (z, \tau)$ (3.9b) trends at different time of simulation when $L = cost$ and v_0 varies, simulations set C.

Set D

Figure 3.10 shows the results of the simulation set D, where the effects of the diffusion coefficient $\bar{D}$ are investigated, keeping constant the other operating and physical parameters. Based on the simulation results,

it is possible to state that the diffusion coefficient strongly affects the reactor performances. In fact, passing from an order of magnitude of 10^{-5} to 10^{-3} it is clear that diffusion contributes to the homogenization of the compounds along the reactor. Among the consequences there is the fact that, when the diffusion coefficient is higher, the velocity function assumes a linear trend with z, due to the constant concentrations along the reactor axis of the variables on which it depends. Moreover, it can be noticed that the homogenization of compounds inside the reactor explicitly show the difference between a CSTR and a PFR: there is a lower average concentration of substrates inside the reactor when the homogenization is high (CSTR behaviour), and this leads to have a lower uptaking rate for the substrates. As a consequence, the methane production is maximized the lower is the diffusion coefficient value (Figure 3.10d).

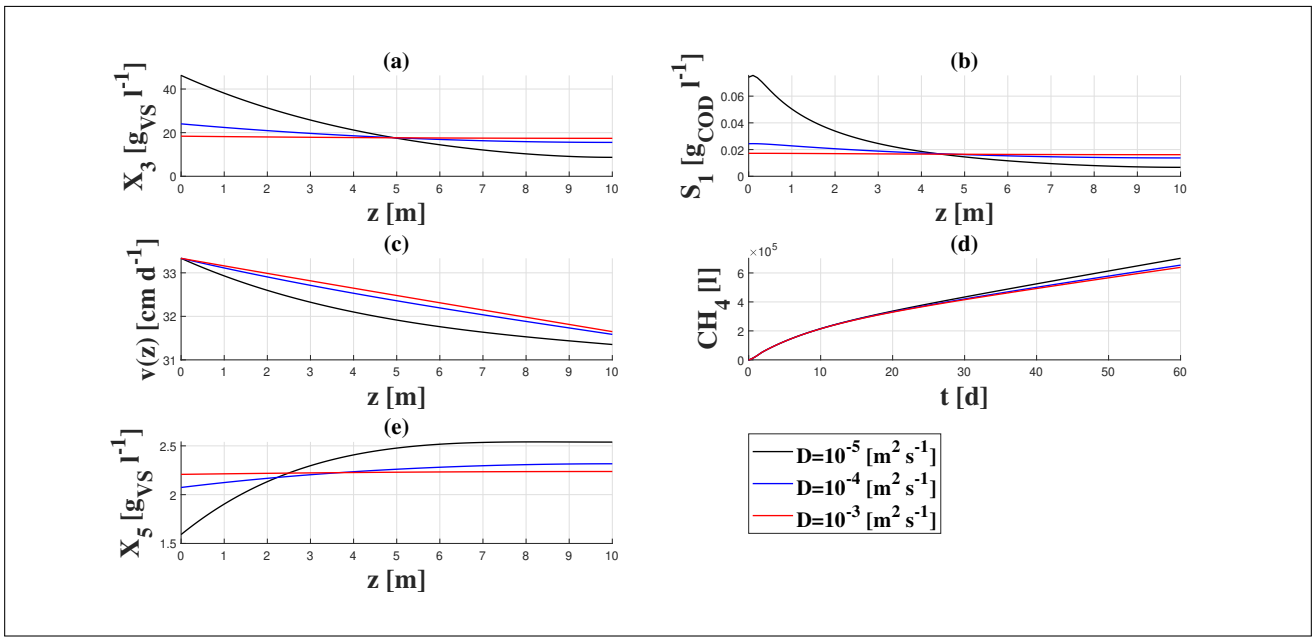

Figure 3.10: Bio-degradable VS $X_3\,(z,\tau)$ (10a), acetic acid $S_1\,(z,\tau)$ (10b), $v\,(z,\tau)$ (10c), methane production (10d) and microbial biomass $X_5\,(z,\tau)$ (10e) trends for simulations set D, at $\tau = 60\,\mathrm{d}$.

All these behaviours observed through the previous simulations are in accordance with the physics of the phenomenon, showing that the model is capable to correctly represent process dynamics. These informations could be used for the designing of anaerobic digestion in PFR plants. The optimal length or inlet velocity could be chosen depending on the result to be maximized: for example, the choice of a longer or shorter reactor depends on whether it is important to maximize the methane production or the OFMSW removal using a fixed value of the HRT. Furthermore, monitoring the acid concentrations inside the reactor could be crucial to avoid system failure. Lastly, the system velocity could be predicted gaining information useful to establish the outlet flow in order to avoid reactor emptying, which could cause system locking.

3.4.3 Application to a real case

To show model consistency with the bio-physics of a DAD process, the present model was used to simulate the dynamics of a laboratory scale digester. The reference experimental work is that presented by Regina J. Patinvoh et al. [95], who performed a DAD process of untreated manure bedded with straw at 22% of TS content under different OLRs. The experimental campaign started with a process of AD in batch conditions, established for reactor initialization. At this step, a mixture of inoculum and substrate in a ratio of 2:1 in terms of volatile solids content, was used as reactor feeding. This batch phase lasted 40 days and later the reactor was fed continuously according to the feeding conditions of Table 3.5. Firstly, the $OLR = 2.8\ \mathrm{g\,L^{-1}\,d^{-1}}$ was used and then it was increased gradually to 4.2 and 6.0 $\mathrm{g\,L^{-1}\,d^{-1}}$. The corresponding decreasing HRTs were of 60, 40 and 28 days. The feeding conditions were changed after a time period equal to the HRTs. Using the characteristics of the substrate and of the inoculum, reported in Table 3.4 and reproducing the feeding procedure of [95] results concerning daily methane production, cumulative biogas production and VFA concentration path were reproduced. The used reactor is an horizontal plug-flow with a total volume of $9.2\,\mathrm{L}$; the temperature regime is set to $37\,^{\circ}\mathrm{C}$. The values of model parameters used for reproducing experimental data are the same as reported in Table 3.1, except for the kinetic constant for the consumption of the volatile solids k_1, which was set equal to $0.035\ d^{-1}$. The values of the conversion coefficient of VS in COD m and the fraction of decayed microbial biomass becoming new bio-degradable substrate f were set as in the previous simulations.

Since no informations were available concerning the initial microbial biomass concentration, preliminary simulations of the batch case were run to build the missing initial condition. Later, the batch conditions of the experimental campaign were simulated, this time with the aim to reproduce the methane production using the built initial condition on the microbial biomass concentration. The values of the simulated variables at the end of this period were used as initial conditions for the simulation of the feeding condition 1.

$ND = not\ determined.$

	Symbol	Unit	Manure with straw	Inoculum
Moisture	f_1	g/g	0.7772	0.9220
TS content	$(1-f_1)$	g_{TS}/g	0.2229	0.078
VS content on TS base	f_2	g_{VS}/g_{TS}	0.7044	0.4046
Ash	$(1-f_2)$	g/g_{TS}	0.2956	0.5954
$COD_{content}$		g_{COD}/g_{VS}	0.73	ND
$BMP_{theoretical}$		L_{CH_4}/g_{VS}	0.290	ND

Table 3.4: Substrate and Inoculum characteristics used during the experimental campaign of [95].

Parameter	Unit	Condition		
		1	2	3
OLR	$g_{VS}\ L^{-1}\ d^{-1}$	2.8	4.2	6.0
HRT	d	60	40	28
Loading rate	$g_{VS}\ d^{-1}$	13.8	20.7	29.9

Table 3.5: OLRs, HRTs and Loading rates used in the experimental work of Patinvoh et al. and in the simulations used to reproduce its results.

The resulting dynamics determined the initial conditions for the feeding conditions 2 and so on.
It is possible to observe that the model results reasonably follow the experimental data (Figure 3.11).

In order to compare the experimental and simulated methane productions the experimental cumulative biogas production curve reported in [95] has been multiplied by the measured average methane content. The experimental daily methane production curve is not reported here, but to show that the simulated daily production well reproduces the experimental results, the simulated and experimental methane yields have been compared.

Feeding condition	Methane yield $\left[L_{CH_4}\ g_{VS}^{-1}\right]$	
	Experimental	Simulated
OLR 1	0.16	0.16
OLR 2	0.17	0.14
OLR 3	0.14	0.12

Table 3.6: Experimental and Simulated methane yield.

Table 3.6 show that the model is very good in predicting the system evolution. Similarly to the experimental case, the simulated daily methane production is decreasing during the development of the process in batch conditions. In the continuous feeding condition cases the profiles are increasing until a certain maximum value and then remain constant. The VFA path is well followed by the model. As in the experimental results, simulated acid concentration in the last section of the reactor is very low during all the simulation time (data not shown).

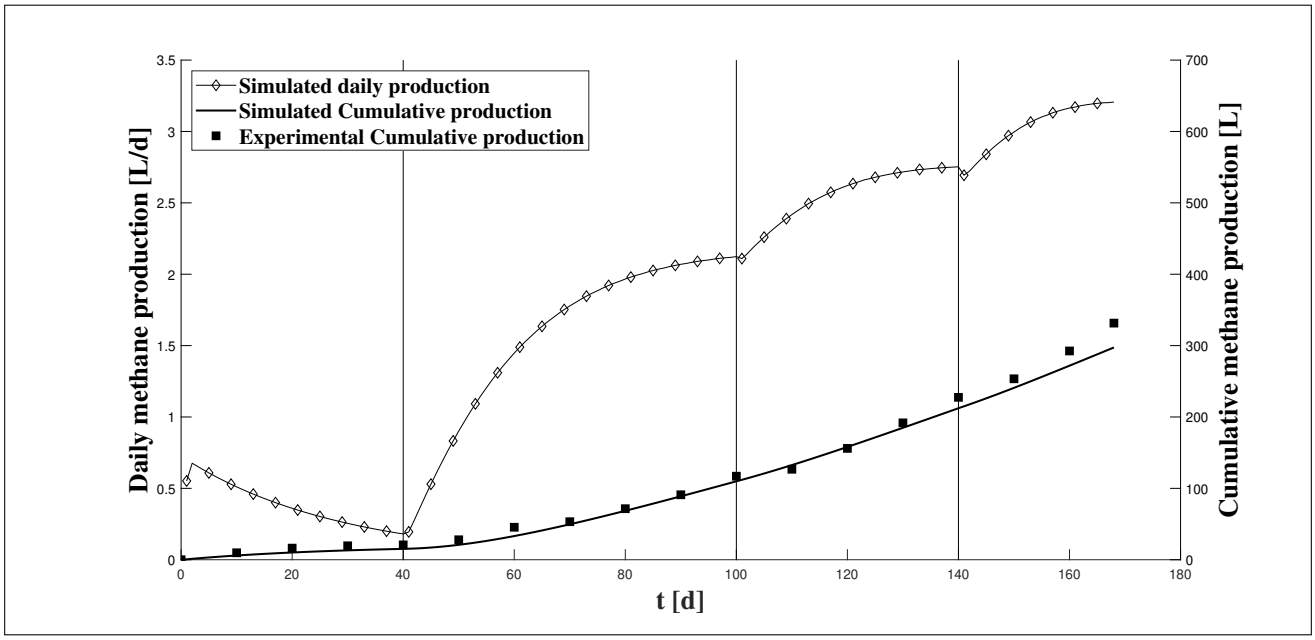

Figure 3.11: Daily and cumulative methane production in the experimental and simulated cases.

3.5 Conclusions

In this work a mathematical model for the dry anaerobic digestion process in PFRs based on the convection-diffusion-reaction equation in one-dimensional case was presented. The model predicts substances concentration along the reactor and it is also capable to describe the variation of the system velocity with time and space. The equation governing the convective velocity is derived by considering the hypothesis that density of the waste matrix within the reactor is constant over time and the sum of the volume fractions of the bio-components constituting the waste matrix are constrained to sum up to unity. The system of PDEs was integrated numerically. Results show model consistency with experimental evidence at laboratory scale and highlight the importance to have a mathematical tool useful to manage, size and improve real plants. For future development the kinetic model may be extended to the complete ADM1 framework. This will allow to predict all species dynamics, such as volatile fatty acids concentration profiles that can be used to predict the pH profile along the reactor and take into account inhibition processes on system dynamics. Moreover the composition of the biogas could be characterized, allowing to determine its effective energy power. Additionally, the equation describing methane concentration in the head-space may be modified by introducing a loss term that reproduces a certain gas tapping from the head-space of the reactor, bringing the model closer to the operative conditions of real plants. Another improvement of the model could consist in considering a variable density of the treated matrix. Kinetic processes could be linked to diffusion and the model could also be extended to 2D and 3D domains. This could allow to analyse other phenomena occurring along directions different from the system movement direction that may affect the anaerobic digestion process performance. Moreover, a sensitivity analysis is needed in order to investigate the most

influencing parameters of the model and a qualitative analysis of the solutions is needed to prove existence, uniqueness and stability of the solutions.

Nomenclature

HRT	Hydraulic Retention Time (d)
OLR	Organic Loading Rate $(g_{VS}\ l^{-1}\ d^{-1})$
α	Cumulative methane production value at a certain instant time (l_{CH_4})
β	Added mass of volatile solids in a certain time interval (g_{VS})
ρ	Waste density $(kg\ m^{-3})$
τ	Simulation time (d)
A_w	Cross-section of the reactor volume occupied by waste (m^2)
$\bar{D}$	Diffusion coefficient $(m^2\ s^{-1})$
F_i	Source/Consumption term of the i^{th} component $(kg\ m^{-3}\ s^{-1})$
g	Mass flux per unit area $(kg\ m^{-2}\ s^{-1})$
G	Gaseous methane concentration $(kg_{COD}\ m^{-3})$
k_1	Kinetic constant for the consumption of the volatile solids (d^{-1})
k_2	Monod maximum specific uptake rate (d^{-1})
k_3	Gas-liquid transfer coefficient (d^{-1})
k_4	First order decay rate of the biomass (d^{-1})
K_1	Half saturation constant $(kg_{COD}\ m^{-3})$
K_H	Henry's law coefficient $(Mbar^{-1})$
L	Reactor length (m)
m	Conversion factor of volatile solids in COD $\left(kg_{COD}\ kg_{VS}^{-1}\right)$
r_1	Kinetic rate for the process of consumption of volatile solids $(kg_{VS}\ m^{-3}\ d^{-1})$
r_2	Methanogenesis kinetic rate $(kg_{VS}\ m^{-3}\ d^{-1})$
r_3	Gas-transfer kinetic rate $(kg_{COD}\ m^{-3}\ d^{-1})$
r_4	Death rate of the microbial biomass $(kg_{VS}\ m^{-3}\ d^{-1})$
R	Gas law constant $(barM^{-1}K^{-1})$
S_1	Soluble acetic acid concentration $(kg_{COD}\ m^{-3})$
S_2	Soluble methane concentration $(kg_{COD}\ m^{-3})$
T	Temperature (K)
v	Velocity of the compounds moving along the reactor $(m\ s^{-1})$
v_0	Waste inlet velocity $(m\ s^{-1})$
V_{gas}	Head-space volume for the gas storage (m^3)
X_1	Water concentration $(kg\ m^{-3})$

X_2	Inert concentration $(kg\ m^{-3})$
X_3	Bio-degradable VS concentration $(kg_{VS}\ m^{-3})$
X_4	Non Bio-degradable VS concentration $(kg_{VS}\ m^{-3})$
X_5	Microbial biomass acting the uptake of acetic acid concentration $(kg_{VS}\ m^{-3})$
y	Methane yield $\left(l_{CH_4}\ g_{VS}^{-1}\right)$
Y	Yield of biomass on substrate $(-)$

Chapter 4

Global Sensitivity Analysis and Uncertainty Quantification for a mathematical model of dry anaerobic digestion in plug-flow reactors*

*The results of this chapter will be submitted in the form of a manuscript entitled: *Global Sensitivity Analysis and Uncertainty Quantification for a mathematical model of dry anaerobic digestion in plug-flow reactors.*

4.1 Abstract

In most applications, complex phenomena can be reproduced via models which depend on a (possibly) large set of input parameters, whose effect on the model outputs can be of paramount importance. Model calibration process is aimed at assessing the values of the model parameters in order to obtain the best fit between simulated and experimental data. Great uncertainty affects this procedure and sensitivity analysis and uncertainty quantification are used to estimate that uncertainty. Despite the significant number of applications of sensitivity analysis for models of wet anaerobic digestion, at the best of authors' knowledge there are no examples of global sensitivity analysis for mathematical modeling of dry anaerobic digestion in plug-flow reactors. In this study global sensitivity analysis and uncertainty quantification for a model of dry anaerobic digestion in plug-flow reactors have been performed. The selected model is the one presented in Chapter 3. There are very few works related to the modeling of this kind of process and the main novelty of the analysed model is the fact that it accounts the mass/volume variation that takes place in these systems because of the great amount of solids conversion in gaseous compounds. The convective velocity of the system is considered as a further unknown to be determined and it depends on the kinetics of the bio-components constituting the matrix of the treated substrate. Indeed, according to the model, the mass variation along the reactor is balanced by a variation in velocity. The study of the model trough uncertainty quantification and sensitivity analysis routines would be of great help for model calibration. A preliminary screening of model parameters through the Morris' method has been performed. A surrogate model (metamodel) has also been constructed in order to investigate the relation between input parameter and output without having to launch simulations from scratch. Sobol' indices of the input parameters obtained via surrogate model evaluations allowed to perform a quantitative global sensitivity analysis. Finally, uncertainty quantification has been performed to obtain the probability density function of the defined quantity of interest, by the means of the sampling of the metamodel.

4.2 Introduction

Anaerobic Digestion (AD) is a biological process applied to wastewater treatment sludge, that reduces Chemical Oxygen Demand (COD) of complex organic substrate and converts it into a gas, which is mainly composed by methane and carbon dioxide.

During such process organic matter is progressively converted into simpler and smaller-sized organic compounds, until biogas and digestate are obtained as final products. The digestate contains nutrients and microelements, therefore it can be employed in agricultural contexts [41, 42]. Since this practice is characterized by an eviromental impact, there is a pressing urge to correctly manage bio-waste from the generation stage to its ultimate disposal. For this purpose, AD can be adopted as biological treatment, since it can fulfill the objectives of the Kyoto Protocol and the EU Policies concerning organic waste disposal and renewable energy.

Depending on the solid content of the influent bio-waste, AD can be considered dry, semidry and wet. In dry AD (high-solids digestion), the feedstock to be digested has a Total Solids (TS) content higher than 15%, while in semidry AD the solid substrate to be digested has a TS content between 10% and 15%. At last, wet AD (low-solids digestion) is characterized by diluted feedstock having a TS content lower than 10% [70]. In the last decades, dry AD has got much attention since it features relevant advantages: a smaller reactor volume, reduced amount of water addition, easier management of digested residues, reduced nutrient loss [62] and simplified pre-treatments compared to wet systems. The only pre-treatment which is necessary before feeding the waste into a dry AD reactor is the removal of coarse materials larger than 40 mm [124].

The most used reactor configurations in AD are those of the Continuously Stirred Tank Reactor (CSTR) and Plug-Flow Reactor (PFR). In the ideal hydrodynamic model of CSTR the hypothesis of complete mixing holds. Hence, in a CSTR, the concentration of each compound into the reactor is homogeneous. This hypothesis is reproduced in real plants adopting the CSTR configuration by the continuous mixing systems installed and the more efficient is the mixing system, the closer is the real CSTR to the ideal one. The PFR is characterized by a continuous flow through the tubular shape of the reactor. There is a variation in concentration of components in the axial direction while in the radial direction it is supposed a complete mixing. For this reason the PFR could be interpreted as an infinite number of CSTR arrayed in series [39].

In real scale plants, CSTR configuration is mostly used for wet AD while PFR is preferred in dry AD due to the higher viscosity of the medium [65] and the consequent difficulty in mixing. Even though plug flow reactors are a simple and effective technical solution, to guarantee adequate inoculation and reduce acidification problems a correct internal mixing should be ensured. The economical differences between the implementation of wet and dry systems are small, both in terms of investment and operational costs. On the other hand, the differences between those systems are more remarked speaking in terms of environmental issues. While wet systems typically consume one m^3 of fresh water per ton of treated Organic Fraction of Municipal Solid Waste (OFMSW), the water consumption of dry AD reactors is about ten-fold less. Because of that, the volume of wastewater to be discharged is several-fold less for dry systems [124].

4.2.1 Modeling of AD

Due to its complexity, acting control and optimization of an AD process needs tools capable to describe its most important aspect. These tools are represented by mathematical models. One of the most used model for the description of the dynamics of wet AD is the Anaerobic Digestion Model n. 1 (ADM1) [10]. A great part of existing models of wet AD are based on ADM1 approach and try to take into account other mechanisms that it neglects adopting some modifications. Because of the CSTR configuration and its hypothesis, mathematical models of wet AD are based on systems of Ordinary Differential Equations (ODE). In fact, state variables depends only on time because concentrations of components are the same in each point of the reactor. On the other hand in a PFR model the mathematical problem consists in a

Partial Differential Equations (PDE) problem, since the state variables are function both of space and time. Because of the complexity of dry processes (turbulence, dispersion phenomena, accumulation of solids are aspects of the process carachterized by a great uncertainty) modeling of dry AD in PFRs is a less explored field and a few number of models have been developed. Some models try to avoid the PDE system by using the approximation of the PFR configuration as n CSTR in series [39, 45, 89], considers a fixed velocity inside the reactor [125] or couple Computational Fluid Dynamics analysis with steady state biological model of ODE [132].

In Chapter 3 has been proposed a one-dimensional mathematical model of dry AD in PFR based on mass balances on state variables resulting in a PDE system. The novelty of the model is the fact that the convective velocity of the substrate moving along the reactor is considered as a further unknown variable to take into account the mass/volume variation that takes place along the reactor. Indeed, in systems characterized by an high solids content, the solids conversion in gaseous compounds causes a mass variation that in wet systems is negligible due to the great quantity of water present in the system with respect to the solids amount. In the model of Chapter 3 the variation law of the system velocity is obtained through two main hypothesis: the density of the substrate matrix moving along the reactor is constant over time and the volume fractions of the bio-components constituting the treated substrate matrix are constrained to sum up to unity. These statements imply that the mass of the substrate mixture is constant along the reactor and, as a consequence, the mass reduction of Volatile Solids (VS) due to the degradation processes is balanced by a variation in velocity. The model is capable to describe the bio-physics of the phenomenon, predicting process performances depending on the reactor dimensions, input substrate characteristics and other key features that have a key role in determining the dynamics of the whole process.

4.2.2 Need for Uncertainty Quantification and Sensitivity Analysis

In models having an high number of equations and kinetic parameters, their selection is crucial to simulate a certain dynamics. With the aim to calibrate the model parameters to better fit the experimental data, Sensitivity Analysis (SA) studies are powerful tools used to obtain a screening of model parameters by their relevance and eventually fix to nominal values the least influential ones.

Saltelli et al. in [105] expressed some good practices in modeling, highlighting the need for a reliable Global Sensitivity Analysis (GSA). *Saltelli* pointed out that many works related to the uncertainty and sensitivity analyses explore the input space moving only along one-dimensional corridors (i.e Local Sensitivity analysis), leaving unexplored a great part of the space of parameters. In their literature review, Saltelli et al. demonstrate that a great part of cited papers (42%, according to their report) do not satisfy the requirement to properly explore the space of the input parameters. The result suggested that establishing good practices in SA and Uncertainty Quantification (UQ) procedures is strongly needed.

Despite the high number of mathematical models of AD, there are very few works related to global sensitivity analysis for them. The vast majority of available works are totally focused on local procedures,

thus neglecting more exhaustive global techniques [38].

In literature can be found several examples of procedures related to local sensitivity analysis. For example, Tartakovsky et al. (2008) [117] and Noykova and Gyllenberg (2000) [92] used relative sensitivity functions in order to obtain the reduction of the number of model parameters of their ADM1-based model for the waste water treatment through an Up-flow Anaerobic Sludge Blanket (UASB) reactor, the former, and the model of anaerobic waste water treatment process with substrate inhibition, the latter; Bernard et al., 2001 [18] performed a local sensitivity analysis for a model of waste water anaerobic digestion in an uplflow Fixed Bed Reactor (FBR) using sensitivity coefficients evaluated for the chosen output variable; Vavilin et al., 2003 performed local sensitivity analysis for their distributed model for the anaerobic digestion of solid waste in both batch and continuous 1-D reactors [127] to identify the key parameters changing their values by a certain percentage of their baseline values, as Lin and Wu (2011) [75] did, using the Least-Square (LS) method in their model of anaerobic degradation of phenol. However those works are based on analysis which overlook the effect of the possible interaction between parameters on the output of the model.

Concerning Global Sensitivity Analysis of AD models, few works have been published for models of wet AD using the CSTR configuration, none for models of dry AD in PFRs. Among those for the wet AD, K. Solon et al. (2015) [113] performed a GSA on the ADM1 implemented in the context of the Benchmark Simulation Model no. 2 (BSM2) using the methods of Standardized Regression Coefficients and Morris' Screening's Elementary Effects. They repeated the analysis at different temperature regimes and at different Solid Retention Time (SRT) revealing that those two methods are good measures of sensitivity when AD is performed at low SRT and mesophilic conditions. In the same context but in the open loop version of the BSM2 L. Benedetti et al. (2008) [17] by means of Monte Carlo (MC) experiments and linear regression of its results made a GSA study on the ADM1. They firstly focused on the discussion of the methods applied to reduce computational cost in terms of time and then on the choice of the optimal number of simulations that make the results of the sensitivity analysis acceptable. They revealed that it is useful to perform a numerical solver optimization to reduce the time required for computation by a factor of 5 and that the optimal number of simulations should be 50 times the number of parameters to be tested. Moving to studies of GSA on modified versions of ADM1 model we have an example in the work of Z. Zonta et al. (2012) [142]. The model considers new kinetics to describe the bio-physics of the inhibitory process in the ADM1 framework and they used the Bayesian sensitivity analysis tool for evaluating variance-based sensitivity analysis index. F. Carrera-Chapela et al. (2016) [29] developed a simplified mathematical model for the anaerobic digestion process that takes into account hydrogen sulphide formation in order to use the model also to assess the odor impact of the anaerobic digestion emissions. They carried out a GSA using ANOVA decomposition with dynamic changes on the inlet flow and concentration, determining the parameters having the highest sensitivity on the output. Among these parameters, they selected those whose sensitivity profile were least influenced by the interaction with the other parameters through a Collinearity Analysis.

Here we reported some examples of GSA for wet AD models. Unfortunately, at the best of authors'to knowledge there are no examples of GSA for mathematical modeling of dry AD in PFR. In this context, the aim of this work is to perform a GSA on the model presented in Chapter 3. The screening of model parameters is a mandatory activity for the future model calibration and validation, which should be performed having the purpose to apply the model to real cases. Moreover, through an analysis of this type, the aspects of the model that the most influence the model output are identified and, based on these results, the need of a deeper study of those aspects might be revealed.

The article structure is developed as follows: in Section 2, the model of dry anaerobic digestion in plug-flow reactors object of the study is presented. In Section 3, the selection of model parameters and the choice of the quantity of interest for the SA and UQ studies are introduced. Moreover, this Section describes also the studied test case and the used databases for the simulations. In Section 4 are described the adopted techniques for carrying out UQ and SA studies, i.e. the Morris' screening and the Surrogate-based SA technique. Section 5 recollect the main results of the study and their discussions and, lastly, Section 6 contains remarks and future perspectives.

4.3 Model of plug-flow reactor

4.3.1 Model equations

The mathematical model is based on mass balances in one-dimensional case for the concentrations of the components constituting the mixture of the substrate to be treated. These state variables are considered as functions of time t and space z, where z represents the spatial coordinate oriented along the reactor axis and directed from the inlet to the outlet section. The mass balances lead to define for each state variable an equation known as convection-diffusion-reaction equation, describing the movement along the reactor of each component due to convection and diffusion phenomena and their bio-chemical transformation. The convective and diffusive flux are characterized by a velocity $v(z,t)$ function of both space and time and by a diffusion coefficient D considered invariable along the z direction and the same for each compound, respectively. The model considers the substrate to be composed of water X_1, particulate (inerts X_2, bio-degradable X_3 and non bio-degradable X_4 VS and microbial biomass X_5) and dissolved compounds (soluble acetic acid S_1 and soluble methane S_2). One of the hypothesis of the model is that the described substrate matrix has a constant density within the reactor over time $\rho(z,t) = \rho$.

Moreover, in the head-space of the reactor is stored the biogas, supposed to be composed only of gaseous methane G.

The kinetic scheme describing the transformations occurring to the components of the substrate matrix is reported in the Figure 4.1. The conversion of the bio-degradable VS X_3 in soluble acetic acid S_1, is summarized through a unique kinetic rate r_1, considering only the rate-limiting step of disintegration among all the processes that lead to the production of acetic acid; the acetic acid is consumed through the

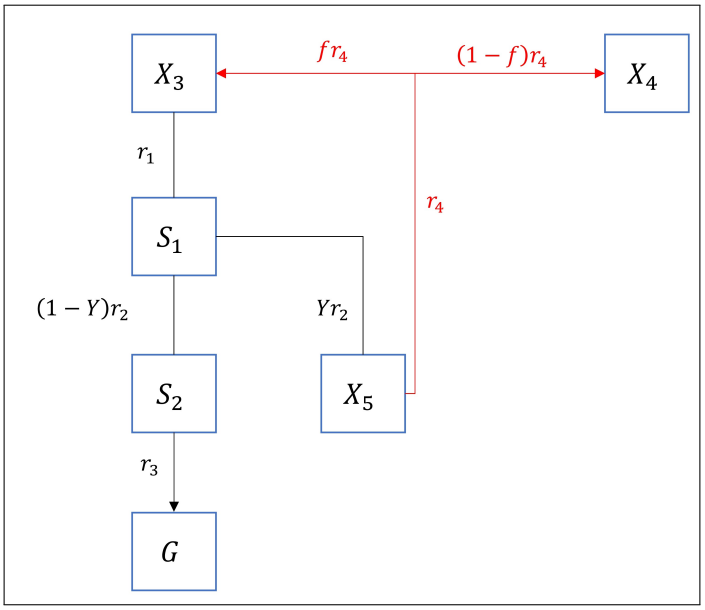

Figure 4.1: Kinetic scheme.

non linear Monod-type kinetic rate r_2 producing both soluble methane S_2 and microbial biomass X_5; the microbial biomass die according to the decay law whose kinetic rate is indicated as r_4 and produce new bio-degradable and non-biodegradable VS X_4; lastly, the soluble and gaseous methane (S_2 and G), are in equilibrium according to the gas-transfer law expressed by the kinetic rate r_3.

The application of the convection-diffusion-reaction equation the each described compound lead to the non-linear system of PDEs (4.1) and (4.2):

$$\frac{\partial X_h(z,t)}{\partial t} + \frac{\partial (v(z,t)X_h(z,t))}{\partial z} - D\frac{\partial^2 X_h(z,t)}{\partial z^2} = F_{X,h}\left(z,t,\mathbf{X},\mathbf{S},G\right), \quad 0 < z < L, \quad t > 0, \quad h = 1,...,5, \quad (4.1)$$

$$\frac{\partial S_l(z,t)}{\partial t} + \frac{\partial (v(z,t)S_l(z,t))}{\partial z} - D\frac{\partial^2 S_l(z,t)}{\partial z^2} = F_{S,l}\left(z,t,\mathbf{X},\mathbf{S},G\right), \quad 0 < z < L, \quad t > 0, \quad l = 1,2, \quad (4.2)$$

where:

- $\mathbf{X} = (X_1,...,X_5)$;
- $\mathbf{S} = (S_1, S_2)$;
- $F_{X,h}\left(z,t,\mathbf{X},\mathbf{S},G\right)$, $h = 1,...,5$, is the source/consumption term of the compound X_h;

- $F_{S,l}\left(z,t,\mathbf{X},\mathbf{S},G\right),\ l=1,2$, is the source/consumption term of the dissolved compound S_l.
- $F_{X,1}\left(z,t,\mathbf{X},\mathbf{S},G\right)=F_{X,2}\left(z,t,\mathbf{X},\mathbf{S},G\right)=0$;
- $F_{X,3}\left(z,t,\mathbf{X},\mathbf{S},G\right)=fr_4-r_1$;
- $F_{X,4}\left(z,t,\mathbf{X},\mathbf{S},G\right)=(1-f)r_4$;
- $F_{X,5}\left(z,t,\mathbf{X},\mathbf{S},G\right)=Yr_2-r_4$;
- $F_{S,1}\left(z,t,\mathbf{X},\mathbf{S},G\right)=m(r_1-r_2)$;
- $F_{S,2}\left(z,t,\mathbf{X},\mathbf{S},G\right)=m(1-Y)r_2-r_3$;
- $r_1=k_1X_3$;
- $r_2=k_2X_5S_1/\left(K_1+S_1\right)$;
- $r_3=k_3(S_2-RTK_HG)$;
- $r_4=k_4X_5$;
- m is the conversion factor of VS in COD $\left[g_{COD}\ g_{VS}^{-1}\right]$;
- Y is the yield of biomass on substrate;
- f is the fraction of dead microbial biomass becoming new bio-degradable substrate;
- k_1 is the kinetic constant for the consumption of the volatile solids X_3, having the dimension of $[T^{-1}]$;
- k_2 is the Monod maximum specific uptake rate for the acetic acid $[T^{-1}]$;
- K_1 is the half saturation constant $[M\ L^{-3}]$ for the kinetics of consumption of the acetic acid;
- k_3 is the gas-liquid transfer coefficient $[T^{-1}]$;
- R is the gas law constant $[L^2\ T^{-2}\ \Theta^{-1}]$;
- T is the operating temperature $[\Theta]$;
- K_H is the Henry's law coefficient $[L^2\ T^{-2}]$;
- k_4 is the first order decay rate of the microbial biomass X_6 $[T^{-1}]$.

The velocity displacement of the bio-components along the reactor axis constitutes an additional unknown of the problem, and the equation describing its variation in space and time is derived using the following hypothesis: the sum of the volume fractions of the particulate components and water within the reactor is constrained to sum up to unity, that is:

$$\begin{cases} \sum_{h=1}^{5} X_h\left(z,t\right)/\rho_h = 1, \\ \rho_h = \rho, \quad h = 1,...,5 \end{cases} \quad \Longrightarrow \quad \sum_{h=1}^{5} X_h(z,t) = \rho. \tag{4.3}$$

Equation (4.3) implies that the mass of the mixture composed of water, inerts, VS and microbial biomass is constant over time. As a consequence, the convective velocity varies along the reactor and its variation depends on the kinetics of the compounds constituting the mixture. In fact, the velocity variation has to balance the consumption of the VS to keep the mass of this particular mixture constant.

Summing equation (4.1) on $h = 1, ..., 5$ and taking into account equation (4.3) follows:

$$\frac{\partial v(z,t)}{\partial z} = \frac{Y r_2 - r_1}{\rho}. \tag{4.4}$$

In addition, the mass balance on the head-space volume $V_{gas} = A_{gas}L$ leads to a differential equation describing the dynamics of the gaseous methane $G\left(t\right)$ (Eq. (4.5)):

$$\frac{dG(t)}{dt} = \frac{A}{V_{gas}} \int_0^L r_3\left(z,t\right)\ dz. \tag{4.5}$$

where:

- A is the constant cross-sectional area occupied by the treated substrate.

The integral in the equation (4.5) describes the fact that all the contributes to the gas-transfer in each point are summed to define a unique gas-transfer rate. The ratio between the cross-section occupied by the treated substrate and the volume of gas is present to take into account the fact that the gas-transfer kinetic rate is referred to the volume of the treated substrate.

Lastly, boundary and initial conditions are prescribed according to equations (4.6) to (4.13).

$$v(0,t) = v_0, \quad t \geqslant 0. \tag{4.6}$$

$$-D\frac{\partial X_h(0,t)}{\partial z} = v_0(X_{h,IN} - X_h(0,t)), \quad h = 1,...,5, \quad t > 0, \tag{4.7}$$

$$\frac{\partial X_h(L,t)}{\partial z} = 0, \quad h = 1,...,5, \quad t > 0, \tag{4.8}$$

$$-D\frac{\partial S_l(0,t)}{\partial z} = v_0(S_{l,IN} - S_l(0,t)), \quad l = 1,2, \quad t > 0, \tag{4.9}$$

$$\frac{\partial S_l(L,t)}{\partial z} = 0, \quad l = 1,2, \quad t > 0. \tag{4.10}$$

$$X_h(z,0) = X_{h,0}, \quad h = 1,...,5, \quad 0 \leqslant z \leqslant L. \tag{4.11}$$

$$S_l(z,0) = S_{l,0}, \quad l = 1,2 \quad 0 \leqslant z \leqslant L. \tag{4.12}$$

$$G(0) = G_0. \tag{4.13}$$

The value v_0 in the (4.6) can be obtained by fixing the HRT of the components moving along the reactor of length L:

$$v_0 = \frac{L}{HRT}. \tag{4.14}$$

In (4.7) and (4.8) $X_{h,IN}$ and $S_{l,IN}$ are the concentrations of water and each particulate and dissolved compound in the incoming flow rate, respectively.

4.4 Sources of uncertainty, quantities of interest and data-bases

In the presented model, the state variables whose dynamics is described through the system of equations (4.1), (4.2), (4.4) and (4.5) coupled with boundary conditions (4.6) to (4.10) and initial conditions (4.11) to (4.13) depend on a set of parameters. Since it is a model recently introduced, knowledge about the response of such model on variations of parameters is mandatory in order to calibrate the model with experimental data. In this study 7 parameters have been selected: a group of parameters consisting in the first order parameter for the conversion process of bio-degradable VS in acetic acid k_1, the Monod maximum specific uptake rate for acetic acid k_2, the first order decay rate for the microbial biomass k_4, the half-saturation constant K_1 and the yield of biomass on substrate Y linked to bio-chemical processes; a second group including the gas-transfer coefficient k_3 and the diffusion coefficient D, related to physics phenomena occurring along the reactor.

Uniform distributions have been selected for the input parameters, reported in Table 4.6 (second column).

4.4.1 Quantity of Interest

The state of the PFR digestion model evolves in time $t \in (0,\tau)$ and space $x \in (0,L)$. It is characterized through the state variables $X_h(z,t)$, $h = 1,...,5$, $S_1(z,t)$, $S_2(z,t)$ and $G(t)$.

Since many of the latter set of variables are spatially distributed, it is mandatory to focus on a small set of scalar outputs in order to better catch the relation between the uncertain inputs and the behaviour of the

PFR Model.

A single quantity of interest (QoI) has been considered in this study: we shall denote with y the time integral of the value of the liters of methane in the head-space in Normal Temperature and Pressure conditions from time $t = 0$ to time $t = \tau$.

$$y = \int_0^\tau \frac{RT_0}{P_0} V_{gas} \frac{G(t)}{64} dt \qquad [l_{CH_4} d], \tag{4.15}$$

where:

- G is the variable of the gaseous methane concentration expressed in $g_{COD}\ l_{gas}^{-1}$;
- T_0 and P_0 are the values of the temperature and the pressure at Normal Temperature and Pressure conditions;
- 64 are the grams of COD per moles of methane.

The choice of this QoI is linked to the main objective of this kind of process: the energy recovery trough the methane production. Hence, the uncertainty related to the modeling of this output needs a strong reduction.

4.4.2 Description of test case

With the purpose to run simulations to have useful datasets for the sensitivity analysis, a test case has been considered. The selected test case is based on experimental procedures aimed to have informations on the methane production from anaerobic digestion processes in dry conditions in PFRs. For example it can be studied the variation of the methane production based on tests conducted in various temperature regime or using different inlet conditions: growing Organic Loading Rates (OLRs), growing TS content, different pretreatment on the substrate and so on. OLR represents a measure of the amount of VS fed into the reactor, evaluated as the ratio between the concentration of VS in the inlet flow and the Hydraulic Retention Time (HRT), which gives informations on the average time spent by a bio-component inside a reactor.

The reactor length L, the cross-sectional area occupied by the substrate being treated A, the head-space volume V_{gas}, the HRT, the inlet convective velocity v_0, the OLR and the temperature T used in the simulations are reported in Table 4.1. The value of the conversion coefficient of VS in COD m was fixed equal to $1.5\ g_{COD}\ g_{VS}^{-1}$ while the fraction of dead microbial biomass becoming new bio-degradable substrate was set at $f = 0.2$. The characteristics of the initial and the entering substrate were chosen in such a way to have very similar to lab-scale experiments values and are reported in Table 4.2. The considered initial substrate consists of a mixture of digestate and inoculum. The initial compounds concentrations are supposed constant along the reactor. Initial and boundary conditions used in the simulations are summarized in Table 4.3. The simulation time was fixed equal to three times the HRT.

Parameter	Description	Dimension	Value
L	Reactor length	m	1.34
A	Reactor cross-section	m^2	0.0224
V_{gas}	Volume of the head-space	l	10.0
HRT	Hydraulic Retention Time	d	40.0
v_0	Incoming flow rate velocity	$cm\ d^{-1}$	3.35
OLR	Organic Loading Rate	$g_{VS}\ l^{-1}\ d^{-1}$	6.0
T	Reactor temperature regime	°C	37.0

Table 4.1: Operating parameters of the test case.

Parameter	Dimension	Initial mixture	Inlet substrate
Total solids	$g_{TS}\ g^{-1}$	0.15	0.30
Volatile solids	$g_{VS}\ g_{TS}^{-1}$	0.80	0.80
Bio-degradable VS	$g_{VS}\ g_{VS}^{-1}$	0.07	0.396
Non bio-degradable VS	$g_{VS}\ g_{VS}^{-1}$	0.905	0.60
Microbial biomass	$g_{VS}\ g_{VS}^{-1}$	0.025	0.004

Table 4.2: Initial mixture and inlet substrate characterization.

4.4.3 Experimental designs and databases

The space where the uncertain parameters vary (also known as the "hypercube") $Z_\Theta \in \mathbb{R}^d$ (where $d = 7$ in this study) is discretized by the means of a design of experiments. In this way N realizations of the parameters $\boldsymbol{\theta}_i$ are defined and the PFR model is integrated as a "black-box" to obtain N functional outputs $\mathbf{y}$. These functional outputs are analysed and useful statistics are obtained. The ensemble is compiled into a database $\mathcal{D}_N$:

$$\mathcal{D}_N = \left\{ \left(\boldsymbol{\theta}^{(l)}, \mathbf{y}^{(l)} \right)_{1 \leqslant l \leqslant N} \right\}, \tag{4.16}$$

where $\mathbf{y}^{(l)} = \mathcal{F}\left(\boldsymbol{\theta}^{(l)}\right)$ is the integration of the PFR model $\mathcal{F}$ obtained fixing the lth set of input parameters $\boldsymbol{\theta}^{(l)}$.

In the present work, the parameter set used to carry out the model parameters screening $\boldsymbol{\theta}_{\text{Morris}}$ consisted in a set composed of $N_M = 400$ samples. The randomized algorithm proposed in [88] has been used to generate it. For the sake of the surrogate-based study, quasi-Monte Carlo sampling methods have been selected to compile two databases of size $N = 2^{10}$. A first database is generated using Halton's sampling and is used as a training set. Faure's sampling has been used to generate the second database, the validation one. This last database has been used to evaluate the accuracy of the different surrogate techniques. Table 4.4 summarizes the compiled databases.

It is remarked that that the considered digestion model features non-linearities for the QoI y when $\boldsymbol{\theta}$

Parameter	Symbol	Unit	Value
Density of the treated substrate	ρ	$g\ l^{-1}$	1000.0
Initial H_2O concentration	$X_{1,0}$	$g\ l^{-1}$	850.0
Initial inert concentration	$X_{2,0}$	$g\ l^{-1}$	30.0
Initial bio-degradable VS concentration	$X_{3,0}$	$g_{VS}\ l^{-1}$	8.4
Initial non bio-degradable VS concentration	$X_{4,0}$	$g_{VS}\ l^{-1}$	108.6
Initial soluble acetic acid concentration	$S_{1,0}$	$g_{COD}\ l^{-1}$	0.0
Initial soluble methane concentration	$S_{2,0}$	$g_{COD}\ l^{-1}$	0.0
Initial microbial biomass concentration	$X_{5,0}$	$g_{VS}\ l^{-1}$	3.0
Initial gas-phase methane concentration	G_0	$g_{COD}\ l^{-1}$	0.0
Inlet H_2O concentration	$X_{1,IN}$	$g\ l^{-1}$	700.0
Inlet inert concentration	$X_{2,IN}$	$g\ l^{-1}$	60.0
Inlet bio-degradable VS concentration	$X_{3,IN}$	$g_{VS}\ l^{-1}$	95.04
Inlet non-bio-degradable VS concentration	$X_{4,IN}$	$g_{VS}\ l^{-1}$	144.0
Inlet soluble acetic acid concentration	$S_{1,IN}$	$g_{COD}\ l^{-1}$	0.0
Inlet soluble methane concentration	$S_{2,IN}$	$g_{COD}\ l^{-1}$	0.0
Inlet microbial biomass concentration	$X_{5,IN}$	$g_{VS}\ l^{-1}$	0.96

Table 4.3: Initial conditions and inlet flow compound concentrations used in model simulations.

varies in Z_Θ. Figure 4.2 portrays 40 representative PFR snapshots sampled from Morris Database.

Sampling Strategy	Purpose	Sample size
Randomized algorithm of [88]	Morris Screening	400
Halton's sequence	Surrogate Training	2^{10}
Faure's sequence	Surrogate Validation	2^{10}

Table 4.4: Datasets $\mathcal{D}_N$ of AD PFR model simulations used in this work whether for the sake of performing Morris screening, or building surrogates ("training"), or for validating them ("validation").

4.5 Surrogate-Based Sensitivity Analysis

The Sensitivity Analysis of the model presented in Section 4.3.1 consisted in a two phases study: on the one hand, a faster preliminary screening analysis through the *Elementary Effect Test* (EET), proposed by Morris in [88]; on the other hand, an exhaustive surrogate-based GSA (see Subsection 4.5.2), aimed to get more accurate results.

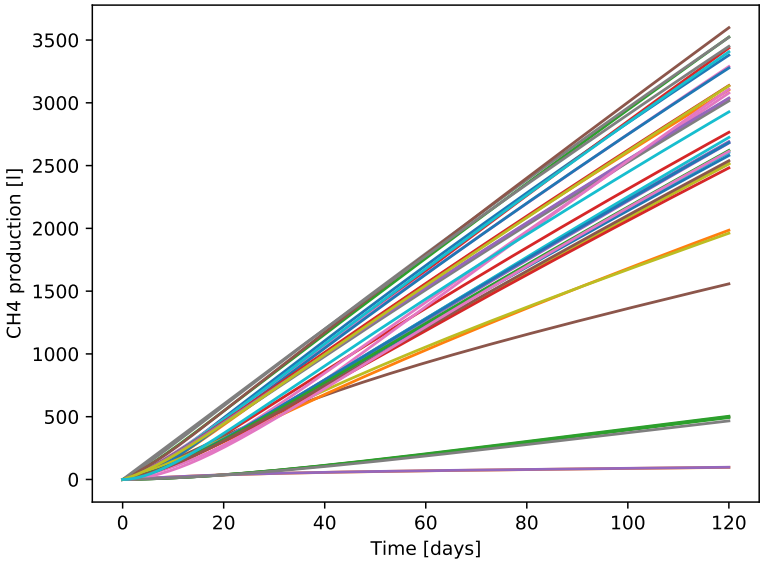

Figure 4.2: An ensemble of 40 different CH_4 profiles extracted from the Morris' algorithm sampling database, with different values of θ.

4.5.1 Screening of influential parameters via Morris' Scheme

According to Morris [88] a useful screening sensitivity measure used to identify the most important parameters of a model is the so called Elementary Effect (EE). The method proposed by Morris is based on the computation for each parameter of incremental ratios (the EEs indeed), whose mean is used as a measure of global sensitivity, determining the overall importance of each input parameter on the QoI. The analysis is conducted adopting randomized One-At-Time (OAT) experiments. In the following, we assume that input parameters are uniformly distributed in $[0, 1]$ and then transformed from the unit hypercube to their respective distribution.

For a given value of $\theta_i \in \boldsymbol{\theta}$, the associated elementary effect EE_i is expressed as:

$$EE_i = \frac{y(\theta_1^*, \ldots, \theta_i^* + \delta_i, \ldots, \theta_d^*) - y(\theta_1^*, \ldots \theta_i^*, \ldots, \theta_d^*)}{\delta_i}, \tag{4.17}$$

where $\delta \in \left\{\frac{1}{n_l - 1}, 1 - \frac{1}{n_l - 1}\right\}$, n_l is the number of levels, $\boldsymbol{\theta}^* = (\theta_1^*, \ldots, \theta_d^*)$ is a random value in the hypercube Z_θ such that the point $(\boldsymbol{\theta}^* + \boldsymbol{e}_i\delta)$ still maps to a point in Z_θ for each $i \in 1, \ldots, d$ and $\boldsymbol{e}_i$ is a zero valued vector except for its i-th component $e_i = 1$.

For each input parameter θ_i is derived the empirical distribution of elementary effects EE_i with a random sampling of $\boldsymbol{\theta}$, s.t. $EE_i \sim F_i$ and its mean μ_i and standard deviation σ_i are used as sensitivity measures.

In the following is adopted a correction to the μ_i, introduced by Campolongo and Saltelli in [25]. In their alternative measure the absolute value of the EEs is adopted instead of the mean μ_i, in order to avoid

that increments of different signs would cancel out. Their measure reads

$$S_i = \mu^*_{\text{Morris}} = \frac{1}{n}\sum_{j=1}^{n} EE^j = \frac{1}{n}\sum_{j=1}^{n} \left| \frac{y(\theta_1^j, \dots \theta_i^j + \delta_i^j, \dots, \theta_d^j) - y(\theta_1^j, \dots \theta_i^j, \dots, \theta_d^j)}{\delta_i^j} \right| c_i \tag{4.18}$$

To estimate these quantities without constructing large databases of experiments and/or simulations, Morris suggested sampling r elementary effects from each F_i via an efficient design that constructs r trajectories of $(d+1)$ points in the input parameter space, each one providing d elementary effects, one per input factor. The total cost of the experimental set is thus $r(d+1)$ model evaluations.

Apart from the mean (and its eventual corrections) also standard deviation of the EEs provides useful information. It may constitute a proxy of the level of interaction between the parameters and it allows to understand if a certain factor has non-linear effects on the Quantity of Interest.

4.5.2 Surrogate Modeling

In this work, an emulator, (also known as metamodel, or surrogate model) of the PFR model described in Section 4.3.1 is built adopting two distinct algorithms: generalized Polynomial Chaos (gPC) expansion or Gaussian Process (GP) model. gPC-expansion and GP model are robust and widely spread techniques, well described in literature. In particular, the mathematical setting is explained in detail when applied in distinct Sensitivity Analysis of environmental models in the two recent paper of Trucchia and coauthors [121],[120] and the previous work of Roy and coauthors [104] . Both approaches create a surrogate for the quantity of interest y using a (finite) sum of basis functions:

$$y = \sum_{\boldsymbol{\alpha} \in \mathcal{A}} \gamma_{\boldsymbol{\alpha}} \, \Psi_{\boldsymbol{\alpha}}. \tag{4.19}$$

The Halton's training database $\mathcal{D}_N$ with $N = 2^{10}$ (see Section 4.4.3) is used to determine the coefficients $\{\gamma_{\boldsymbol{\alpha}}\}_{\boldsymbol{\alpha}\in\mathcal{A}}$ and the basis functions $\{\Psi_{\boldsymbol{\alpha}}\}_{\boldsymbol{\alpha}\in\mathcal{A}}$ of equation (4.19). The coefficients can be determined using different methods.

In this work, three algorithms are tested: two variations of gPC expansion and an implementation of GP. While performing a Polynomial Chaos, the basis functions of Equation (4.19) are multivariate orthonormal polynomial functions (see e.g. [134]). The two implementations of gPC differ by the rule that determines the finite sum of polynomial basis in Equation (4.19). One variant of gPC, referred to as Standard Least Squares, used a linear truncation scheme to determine the choice of the polynomial basis, while the second attempt employs a sparse strategy with for the truncation scheme, via Least Angle Regression [20].

The implementation of GP used as correlation kernel the squared exponential (also known as radial basis function) [100].

Workflow for gPC-expansion

The algorithm to compute a gPC-expansion can be resumed as follows:

1. choose the polynomial basis [121] [120] $\{\Psi_{\boldsymbol{\alpha}}\}_{\boldsymbol{\alpha}\in\mathcal{A}}$ according to the prescribed input marginal PDFs of the inputs $\theta_i \in \boldsymbol{\theta} \in \mathbb{R}^d$ $(d = 7)$;

2. choose the total polynomial order P according to the complexity of the digestion processes;

3. truncate the gPC-expansion to r_{lin} terms using linear truncation according to the problem dimension d and the total polynomial order P;

4. if LAR sparse truncation is selected, compute a smaller set of indices for the orthonormal polynomials, with cardinality $r \leqslant r_{\text{lin}}$. Otherwise, $r = r_{\text{lin}}$;

5. compute the coefficients $\{\gamma_{\boldsymbol{\alpha}}\}_{\boldsymbol{\alpha}\in\mathcal{A}}$ with least-square minimization, using $N = 2^{10}$ snapshots from the simulation database $\mathcal{D}_N$ (the experimental design is based on Halton's low-discrepancy sequence);

6. formulate the surrogate $\mathcal{F}_{\text{pc}}$, which can be evaluated for any new vector of parameters $\boldsymbol{\theta}^*$.

Workflow for GP surrogate

The scheme of the construction of the GP surrogate is summarized in the following:

1. choose the kernel function $\pi_{\boldsymbol{\alpha}}$ suitable for the input vector $\boldsymbol{\theta} \in \mathbb{R}^d$ $(d = 7)$ – we consider RBF in the present study, see Eq. 31 of [121]

2. optimize the GP-hyperparameters $\{\ell_{\boldsymbol{\alpha}}, \sigma_{\boldsymbol{\alpha}}, \tau\}$ associated with the kernel $\pi_{\boldsymbol{\alpha}}$ using maximum likelihood;

3. formulate the surrogate $\mathcal{F}_{\text{gp}}$, which can be evaluated for any new vector of parameters $\boldsymbol{\theta}^*$.

4.5.3 Numerical implementation

From the implementation point of view, the computation of Morris Screening, gPC-expansion and GP-model have been pursued thanks to the Python package *OpenTURNS* [14] (see www.openturns.org).

Moreover, the model equations (4.1), (4.2), (4.4) and (4.5) are integrated with the aid of the `MATLAB` programming language through an original code based on the finite difference upwind method.

4.6 Results

4.6.1 Morris screening

In Figure 4.3 are reported the results of Morris' screening procedure applied to the QoI y. The ranking between parameters resulting from this analysis is reported in Table 4.6. Based on Morris' screening results we can divide the parameters in three groups in terms of importance. Firstly, it can be noticed that the most important parameters in determining the value of the QoI are the kinetic constant of the conversion process of the bio-degradable VS in acetic acid k_1 and the Monod maximum uptake rate of acetic acid k_2. This was to be expected due to the fact that k_1 affects the kinetics of the disintegration process, determining the rate at which the substrate is available to be converted in the intermediate product, and k_2 directly affects the methane production rate. Moreover, this suggests that it could be more appropriate to model the disintegration kinetics taking also into account the particle size of the bio-degradable components, when it represents the bottleneck of the entire process, as during the degradation of complex particulate compounds.

A second group made of physical parameters k_3 and D are in the middle in terms of importance in determining the QoI value. The gas-transfer coefficient k_3 determines the quantity of soluble methane released in the gas-phase. When its value is very small, a small amount of soluble methane passes in the gas-phase. When the value of k_3 exceeds a certain threshold, all the methane is released in the gas-phase and the value of the gas-transfer coefficient does not affect the QoI value anymore. The diffusion coefficient D was not expected to be so less important with respect to kinetic parameters in determining the QoI value in a process modelled considering convective-diffusive-reactive phenomena. These results suggests that, if one wants to model also the effect of diffusion on the development of the process, the dependence of kinetics on the diffusion coefficient must be incorporated. Indeed, it has been demonstrated that in dry anaerobic digestion diffusion affects hydrolysis of complex material [128, 137], for example. Moreover, the fact that the model is a one-dimensional model and that it is neglected a different value of diffusion along the other directions influence the role of such a coefficient in determining the QoI value. In 2D and 3D models could emerge the importance of the diffusion coefficient in determining the rate of conversion of substrate in methane. Indeed, different diffusion processes in the other directions influencing acid distribution in the reactor could be analysed.

The last qualitative information obtained through the Morris screening is that the group of parameters consisting in the half-saturation constant K_1, the microbial biomass decay rate k_4 and the yield of biomass on substrate Y present very small sensitivity. The roles of the half-saturation constant and the yield of biomass on substrate are not emerging in the qualitative preliminary screening obtained through the Morris method. Indeed, when the half-saturation constant assumes very small values the kinetic of consumption of the acetic acid becomes linear, indicating that the process becomes faster and it is not limited by substrate availability. The yield of biomass on substrate determines directly the amount of acetic acid that becomes methane and, even if it varies among 0 and 1, it is expected to influence methane production. These aspects

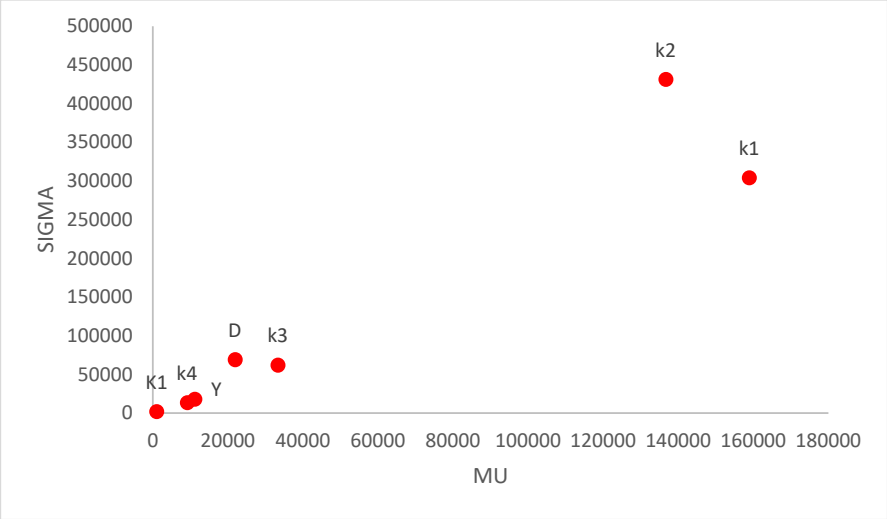

Figure 4.3: Morris algorithm applied with respect to y.

need to be investigated deeply with the quantitative variance based GSA.

4.6.2 A posteriori error estimation of the surrogate models

Since metamodels of the PFR will be used for UQ and SA, measuring their effectiveness in reproducing the real model variability is mandatory. The construction of the surrogate model would in fact introduce an approximation error, which can be computed in an *a posteriori* fashion as

$$\epsilon_{\text{emp}} = \frac{1}{N_{\text{halton}}} \sum_{l=1}^{N_{\text{halton}}} \left(y^{(l)} - \widehat{y}^{(l)} \right), \tag{4.20}$$

where $y^{(l)}$ is the lth element of the training set, $\widehat{y}^{(l)}$ is the corresponding prediction by the surrogate model (gPC or GP), and $N = 2^{10}$ (see Table 4.4). However, this estimator for the metamodel error suffers from *overfitting* issues and may thus severely underestimate the mean square error [20]. In addition, the GP-model is interpolating the the training set points and therefore it will always achieve $\epsilon_{\text{emp}} = 0$ (when noise free kernel are adopted). In the following, for any tested surrogate model, algorithm and configuration, we have $\epsilon_{\text{emp}}/\overline{y} < 4.0 \times 10^{-3}$, with $\overline{y}$ the empirical mean of the QoI over the Halton's dataset.

To make up for the aforementioned shortcomings, the surrogates are validated using the so called Q_2 predictive coefficient, that corresponds to a cross-validation error metric using the independent dataset

based on Faure's low discrepancy sequence (see Table 4.4). In formulas, this coefficient reads

$$Q_2 = 1 - \frac{\sum_{l=1}^{N_{\text{faure}}} \left(y^{(l)} - \widehat{y}^{(l)}\right)^2}{\sum_{l=1}^{N_{\text{faure}}} \left(y^{(l)} - \overline{y}\right)^2}, \tag{4.21}$$

with $\overline{y}$ the empirical mean over the Faure's validation set ($N_{\text{faure}} = 2^{10}$). Q_2 predictor coefficient furnishes a normalized estimate of the generalization error, that is, the surrogate error when considering points outside of the Halton's training set [85]. The target value for Q_2 is 1: the closer the result to unity, the better is the surrogate in reproducing the dynamical system of PFR.

The Q_2 indicator performs thus the function of ranking the surrogates by their effectiveness in reproducing the dynamics of the studied PFR model. In particular, when gPC techniques is applied, we consider the results of the surrogate with total polynomial order P that gives the best results. In our study, P varied from 1 to 7.

Figure 4.4, first panel, shows the adequacy plots, i.e. the plots of metamodel computed over points of the DOE over actual forward model $\mathcal{F}$ runs. In the second panel, the robustness of LAR-gPC algorithm with respect to the choice of P is given by the plots of Q_2 values over the tested values for the maximum polynomial degree. When $P > 4$, the dimensionality of the underlying statistical model hinders the convercence. In Table 4.5, the different error estimators for the adopted surrogate techniques are tabulated.

Metamodel	Q_2	$\epsilon_{emp}/\overline{y}$
SLS-gPC $(P = 4)$	0.972	$3.40e-03$
LAR-gPC $(P = 4)$	0.975	$3.79e-03$
GP (RBF Kernel)	0.993	$0.$

Table 4.5: Errors relative to built surrogates. For LAR-gPC and SLS-gPC, the best results for the spanned values for P are reported.

4.6.3 Quantitative SA with Sobol' indices

Variance decomposition-based global sensitivity analysis is usually performed by means of Sobol' indices [112, 106]. These indices allow to quantify the weight of the uncertainty of a single input parameter, considered as an independent variable with respect to the other parameters, on the variance of the quantity of interest y. Indicating the variance of the output random variable y and the one linked to the variability of the ith parameter as $\mathbb{V}(y)$ and $\mathbb{V}_i(y)$, respectively, the first-order Sobol' index S_i referred to the ith

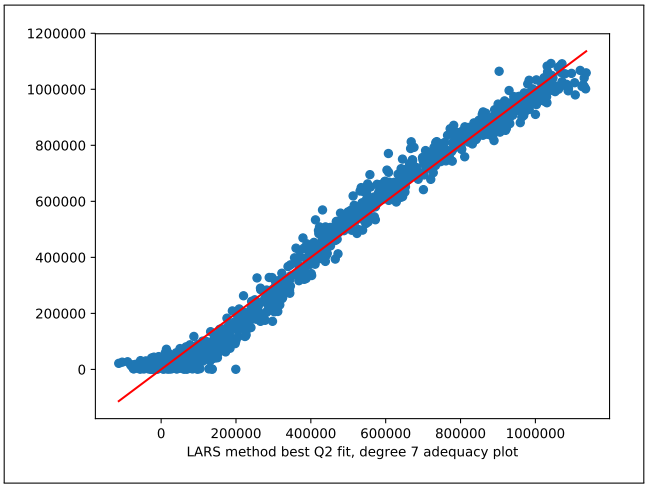

(a) Adequacy plot for LAR gPC algorithm.

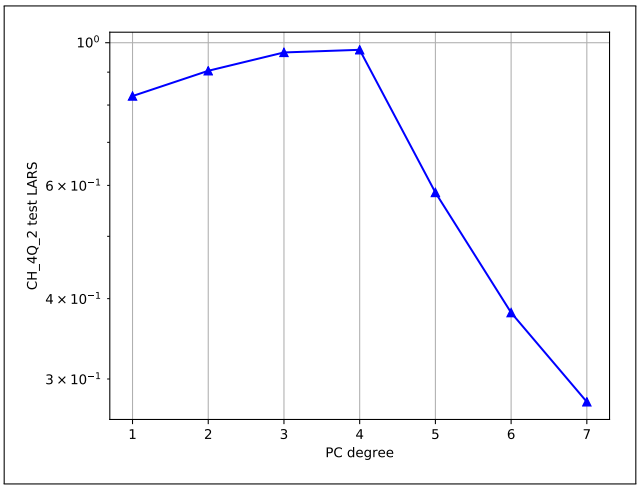

(b) Q_2 test for varying maximum order of gPC from $p_0 = 1$ to $p_1 = 7$.

Figure 4.4: Adequacy plots for the prediction of QoI y. For the Q_2 test, we showed the results of several maximum degrees p of LAR-based gPC algorithm.

parameter of $\boldsymbol{\Theta}$ is defined as:

$$S_i = \frac{\mathbb{V}_i(Y)}{\mathbb{V}(Y)}. \tag{4.22}$$

S_i ranges then between 0 and 1. In order to include the interactions with the other parameters while defining the measure of the contribution of the ith input parameter on the output variance, the total Sobol' index S_{T_i} is introduced:

$$S_{T_i} = \sum_{\substack{I \subset \{1,\dots,d\} \\ I \ni i}} S_I. \tag{4.23}$$

By definition, $S_{T_i} \geqslant S_i$. The presence of interactions between input parameters in determining the output variance is stated observing if the first-order and total indices differ. In the GP-surrogate approach, Sobol' indices are estimated stochastically adopting Martinez' formulation as a stable estimator [13]. For the LAR gPC-expansion, the first-order and total Sobol' indices are directly derived from the gPC-coefficients, for instance the first-order Sobol index reads (see e.g. [121], [120]) :

$$S_{i,\text{pc}} = \frac{1}{\sigma_y^2} \sum_{\substack{\boldsymbol{\alpha} \in \mathcal{A}, \\ \alpha_i > 0 \text{ and } \alpha_{k \neq i} = 0}} \gamma_{\boldsymbol{\alpha}}^2, \tag{4.24}$$

with σ_y the empirical output sample STD.

Figure 4.5 presents the first-order and total Sobol' indices obtained with the three adopted algorithms. However, since the best performing algorithm with respect to Q_2 error has been GP surrogate, in the following we shall discuss only the SA and UQ results concerning this algorithm.

It is worth noting that first-order and total Sobol' indices are not identical, implying that some interactions take place between the factors.

Regarding CH_4 production, Sobol' indices analysis confirmed the results of the Morris screening concerning the sensitivity of k_2. Both the Sobol' index and the Total Sobol' index of the Monod maximum uptake rate k_2 are the highest between all the parameters. The kinetic constant k_1 maintains its importance while the half-saturation constant K_1 and the yield of biomass on substrate Y gain positions with respect to k_3, k_4 and D, as expected. Indeed, as said before, the half-saturation constant K_1 and the yield of biomass on substrate Y directly determines the maximum consumption rate of acetic acid and the amount of the consumed acetic acid that becomes methane, respectively. The effects of the variation of these parameters on the QoI were not appreciable with the Morris screening and have been highlighted by the quantitative SA.

Lastly, the small sensitivity of the microbial decay rate kinetic constant k_4 and the physical parameters k_3 and D is remarked by the quantitative SA with Sobol' indices.

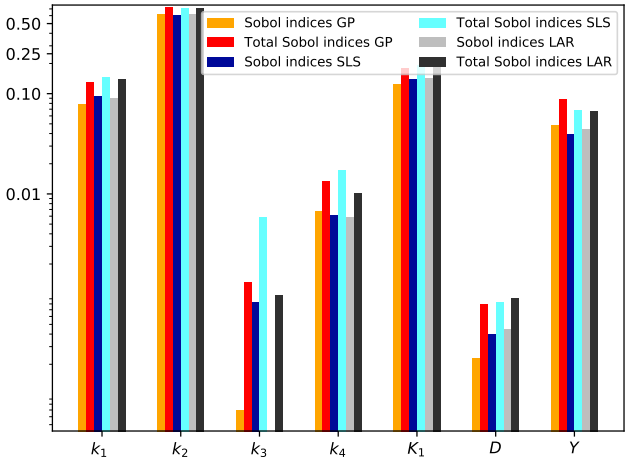

Figure 4.5: First-order and total Sobol' indices (in logarithmic scale) associated with uncertain parameters $\boldsymbol{\theta}$ and their effect on y. The three different tested algorithm are presented. For GP, orange color stands for first-order Sobol' indices; red colors stands for to total Sobol' indices. For SLS-gPC, light blue colors represent first-order Sobol' indices; dark blue colors represent instead total Sobol' indices. For LAR-gPC, gray colors stand for first-order Sobol' indices; dark gray colors stand for to total Sobol' indices.

4.6.4 Uncertainty Quantification

For the sake of Uncertainty Quantification, we restrict the study at the surrogate that behaved best with respect to the Q_2 error estimator, that is Gaussian Process metamodel.

In order to obtain a statistical description of the Quantity of Interest (statistical moments and Probability Density Function) a sampling of the uncertain input space Z_Θ (with sample size of 10,000 members) is performed, adopting a Monte Carlo random sampling and then evaluating the GP surrogate for all these points.

Mean, standard deviation, skewness and kurtosis of the QoI computed from such Montecarlo sample are given in Table 4.7.

Figure 4.6 presents the PDF of the QoI related to CH_4 net production. Some information can be deducted from the shape of such PDF (and more concretely from the higher order moments of its respective distribution). There are two visible peaks indicating that, depending on the model parameters values and the fixed initial and inlet conditions, there is an high probability to have a small amount of produced methane (corresponding to a failure of the system) and a medium-high probability to succeed in having an high methane production. This behaviour is mostly due to the fact that, if the input parameters vector is characterized by unfavorable values, with the combination of constants that implies a small conversion of the bio-degradable COD in acetic acid or a slow conversion of the acetic acid in methane, it is very difficult to produce methane. On the other hand, if the vector of parameters exhibits a good combination of input factors, more favorable to the reactor working conditions, there is a good chance to have methane

Parameter	Description	Uniform distribution	Morris rank (CH_4)	Sobol' Indices rank (CH_4)
k_1	Kinetic constant for the consumption of the volatile solids	$\mathcal{U}(0.005, 0.5)$	1	3
k_2	Monod maximum specific uptake rate for the acetic acid	$\mathcal{U}(0.08, 8.0)$	2	1
k_3	Gas-liquid transfer coefficient	$\mathcal{U}(0.3, 300)$	3	6
k_4	First order decay rate of the microbial biomass	$\mathcal{U}(0.001, 0.05)$	6	5
K_1	Half saturation constant	$\mathcal{U}(0.015, 1.5)$	7	2
D	Diffusion coefficient	$\mathcal{U}(1 \times 10^{-8}, 1 \times 10^{-6})$	4	7
Y	Yield of biomass on substrate	$\mathcal{U}(0.04, 0.1)$	5	4

Table 4.6: In the third column the complete list of Uniform marginal PDFs associated with vector θ is reported. Note that $\mathcal{U}(a, b)$ stands for the uniform distribution with a the minimum value of the parameter and b the maximum one. The last two columns show the ranking of the parameters according to Morris' preliminary screening test and Sobol' Indices given by metamodels.

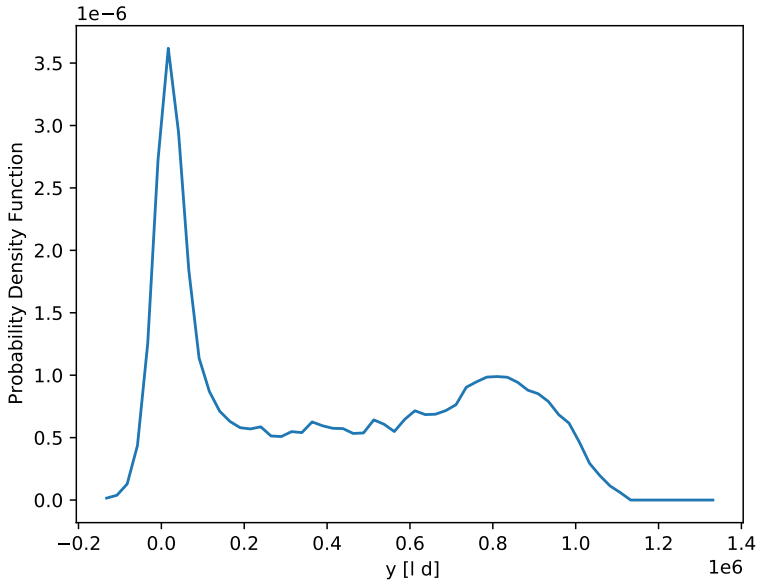

Figure 4.6: Probability density function for the quantity of interest y obtained with the GP metamodel.

production. The fact that the PDF drops to zero after the value of approximately 1×10^6 $[l_{CH_4} \cdot d]$ it is due to the fact that it is impossible to produce more than that quantity of methane in the considered period of time with the used values of HRT, v_0 and OLR.

4.7 Conclusions

In this paper, uncertainty quantification and global sensitivity analysis non-intrusive methods were applied to a novel model for dry anaerobic digestion in plug-flow reactors for a test case of engineering relevance. The model depends on a conspicuous set of input parameters of different nature and lacked up to now a global sensitivity analysis and uncertainty quantification to help predicting the overall effect of uncertainty

Moment	$y\ (l_{CH_4}d)$
Mean	398514.91
St. Deviation	353356
Skewness	0.275
Kurtosis	1.5638

Table 4.7: Statistical moments for the PDF of the two QoI y.

of the input parameters on the net CH_4 production. The Morris screening test and the quantitative sensitivity analysis with Sobol' indices showed, with a good accordance, that the model output concentration of methane in the head-space is mostly sensitive to the values of parameters linked to the kinetics describing the conversion of the particulate bio-degradable volatile solids in acetic acid k_1 and to the kinetics of uptake of acetic acid, k_2. The importance in determining the quantity of interest value of the half-saturation constant K_1 and the yield of biomass on substrate Y is highlighted only by means of the quantitative sensitivity analysis through the Sobol' indices. The values of the QoI are less sensitive to the values assumed by the physical parameters. This result emerged from both the qualitative and quantitative studies of the Morris preliminary screening and the variance decomposition-based global sensitivity analysis through the Sobol' indices. In fact, the variations of the gas-transfer coefficient k_3 beyond a fixed threshold have no effects on the output as all the methane is released in the gas-phase. Moreover, according to the results of the study it is possible to claim that in a 1-D model of this type, where the diffusion is not linked to kinetic processes, the sensitivity of the diffusion coefficient on the model output is very low with respect to the sensitivity of the kinetic parameters. Lastly, the first order decay rate of the biomass acting the uptake of the acetic acid k_4 determines indirectly the quantity of new bio-degradable substrate available to be converted in methane but the uncertainty linked to this parameter does not affect model results in a considerable way.

In the end, this analysis revealed that during the calibration and validation of a complex plug-flow reactor model, characterized by a high number of interacting parameters, sensitivity analysis and uncertainty quantification routines, that ranged from simple screening analysis to more complex, and computationally demanding, variance-based metamodel analysis, constitute a robust asset for modellers and practitioners. In the specific case of anaerobic digestion performance evaluation, the group of parameters it should be paid most attention to are the ones linked to the kinetic processes, i.e. k_1, k_2, K_1 and Y.

Chapter 5

High-solids anaerobic digestion in plug-flow reactors: model calibration and validation*

*The results of this chapter will be submitted in the form of a manuscript entitled: *High-solids anaerobic digestion in plug-flow reactors: model calibration and validation.*

5.1 Abstract

Mathematical modelling of high-solids anaerobic digestion in plug-flow reactors is a little explored field in literature. Mathematical models constitute important tools to support managing, designing and optimizing real plants because they allow to predict methane production, substrate conversion, bio-components concentration trends and other key parameters of the process. This paper focuses on the calibration and validation of a mathematical model recently proposed by authors describing the high-solids anaerobic digestion process in plug-flow reactors. The model is based on a system of partial differential equations and tries to describe the convective-diffusive-reactive phenomena that rule the process. The most important aspect of the model is the fact that the convective velocity of the substrate moving along the reactor is a further unknown of the problem. The conversion of the bio-degradable fraction of the volatile solids into methane is described through a simple biochemical scheme. A global sensitivity analysis revealed the most important parameters affecting methane production, which is the final output of the model. These parameters are the kinetic constant of the process describing the conversion of the bio-degradable solids in acetic acid and three parameters linked to the uptake of the acetic acid: the Monod maximum specific uptake rate, the half-saturation constant and the yield of biomass on substrate. Their calibration and validation is mandatory for the model application to real-scale processes. Laboratory scale experiments on a 30L plug-flow digester fed with cattle manure were carried out for more than 6 months by varying the applied organic load, and thus the velocity of the material all along the experiment. These experiments were used to calibrate model parameters. The calibration procedure showed a good agreement between simulated and experimental methane production curves. Other experimental data were used to validate the model. The study showed the capability of the model in predicting the output of the process.

5.2 Introduction

Anaerobic Digestion (AD) is an affirmed biological treatment process used to convert various kind of organic waste (waste water sludge, organic fraction of municipal solid waste, agricultural and industrial waste etc.) in energy, with a low environmental impact [26]. The biogas, which is a biologically produced gas with an high methane content, is the main product of the AD process while the digestate is a by-product that can be used for agronomic purposes. Based on the Total Solids (TS) content, where TS is the measure of all the suspended, colloidal and dissolved solids in a medium, AD is classified as Wet AD (WAD) (TS content $< 10\%$), Dry AD (DAD) (TS content $> 20\%$), also called High-solid or solid-state AD and Semi-dry AD (SAD) ($10\% \leqslant$ TS $\leqslant 20\%$). During the last decades, WAD and DAD are equally used technologies for new plants performing the AD process [23]. AD in wet conditions is usually performed in Continuous Stirred Tank Reactor (CSTR) configurations and implies the usage of a great amount of water when substrate with high solids content is used with the subsequent need of wide reactor volume and large amount of by-product to be treated. AD in dry conditions, performed mainly in Plug-Flow Reactors

(PFR), requires lower pretreatment of feedstocks for the reduction of size or removal of inert materials, usually performed to avoid the clogging of pumps or pipes [32]. DAD is characterized by less wastewater production [22] and, furthermore, it is attractive for the opportunity to have very robust performances, less energy needs for mixing and heating [61] and does not present problems of sedimentation of surface crust [32]. Hence, economic savings for both public and private companies and greater environmental advantages can be achieved preferring DAD to WAD in some cases, depending on the substrate to be treated. However, optimization techniques are needed in order to overcome some difficulties that occur performing DAD, such as inhibition due to acidification and high ammonia content [94, 63], great amount of inocula, dispersion problems, mechanical problem linked to the high viscosity [15] and so on. Moreover, effort in developing mathematical models capable to describe the dynamics of such a process must be done in order to improve the designing and managing of plants of this type. At the best of authors' knowledge, there are a few works related to the mathematical modelling of DAD in PFRs. These works are based on some simplifications, such as approximating the PFR as a chain of CSTR-in-series [39, 16] or consider a constant velocity along the reactor [127, 125], neglecting the mass variation that takes place because of solids conversion in gaseous compounds along the reactor.

The lack of scientific literature on the mathematical modelling of DAD in PFRs inspired authors to propose a new mathematical model (Chapter 3) based on mass balances on the state variables of the problem, taking into account their variation in both space and time. The mass balances considerations lead to define a system of Partial Differential Equations (PDEs), represented by convection-diffusion-reaction equations, describing the bio-physics of the phenomenon. The novelty of the model is the fact that the convective velocity of the bio-components constituting the matrix of the treated substrate is considered as an unknown function. Indeed, thanks to the variation of the velocity the loss in mass of the treated substrate along the reactor is accounted for. This aspect must be considered in systems treating a substrate having an high solids content and the used approach reflects what happens during the management of real plants. Indeed, since these kind of processes are performed maximizing the working reactor volume, keeping constant the level of the treated substrate along the reactor, the velocity variation balances the described loss in mass. The equation describing the velocity variation along the reactor is derived as a consequence of the principal hypothesis of the model: the density of the treated substrate is constant in time and space and the sum of the volume fractions of the bio-components constituting the matrix of the treated substrate are constrained to sum up to unity. From these statements it follows that the mass of the treated mixture has to be constant along the reactor and then the solids mass reduction due to the degradation processes has to be balanced by the variation of the convective velocity. The bio-chemical scheme considers the conversion of the biodegradable fraction of Volatile Solids (VS) of the treated mixture in methane. VS represents the portion of the TS content that is volatilized at $550\,^{\circ}\mathrm{C}$ and gives an idea on the amount of the readily vaporizing matter present in the solid fraction of a substrate and it corresponds to the organic matter. Such a conversion is considered to occur through two main processes: a unique step of disintegration, that leads to the production of acetic acid, followed by the methanogenesis process, whose result is the production of soluble

methane and microbial biomass. The equilibrium between the soluble methane and the gaseous methane is described by a gas-transfer law. Moreover, a differential equation describes the gaseous methane dynamics and suitable boundary and initial conditions are prescribed to close the mathematical problem.

The Global Sensitivity Analysis (GSA) reported in Chapter 4 identified the parameters of the aforementioned model that affect the most methane production. According to the results of the GSA, the calibration and validation of model parameters must focus on the values of the kinetic parameters describing the conversion of the bio-degradable VS in acetic acid and the subsequent consumption of the produced acetic acid. The calibration and validation of these parameters is a mandatory activity to set up a model that is able to correctly describe the dynamics of AD processes in PFRs.

The aim of this study is to use results related to the methane production of a laboratory-scale plug-flow digester treating cattle manure, to calibrate and validate the mentioned model parameters and to show that the model is capable to emulate the performance of a real DAD process. To this purpose, two experimental campaigns were carried out to compare modelling results with real data. The substrate used in the two experimental campaigns was characterized by a TS content in total weight of 30% and 25%, respectively. In the two campaigns the reactor was fed using increasing Organic Loading Rates (OLRs), where OLR is a measure of the amount of organic material per unit reactor volume subjected to an AD process in a given unit of time period [52]. The first campaign was used to calibrate the model. The second one was used to validate it. The calibration procedure involved the maximization of an objective function related to the difference between the simulated and experimental methane productions. This maximization was obtained varying the chosen model parameters in a fixed range of variation and observing the model results. The validation was performed evaluating some functions able to describe the quality of the accordance between experimental and simulated data.

5.3 Material and methods

5.3.1 Experimental design

A DAD process was performed in a laboratory-scale horizontal plug-flow reactor. Two experimental campaigns A and B were aimed to study the dependence of the methane production on the OLR. The PFR was fed with cattle manure bedded with straw, mixed with water in order to set the TS content of the feeding at 30% in total weight for the campaign A and 25% for the campaign B. Inoculum was used in the start-up phase of the campaign A and digestate recirculation was meant to adjust the pH in the initial sections of the reactor adding ammonia and microbial biomass to the feeding. The campaign B was carried out after a period of inactivity during which the reactor was not fed but just heated. The OLR referred to the substrate was increased almost every week, following the scheme reported in the Table 5.1 and 5.2 for the two campaigns A and B respectively. In such tables, for each feeding condition, are reported also the values of the used Hydraulic Retention Time (HRT), which indicates the mean residence time of a certain substrate

Time (d)	**Progressive time** ($week$)	**OLR** ($g_{VS}\ l^{-1}\ d^{-1}$)	**HRT** (d)
7	1	0.714	349.1
7	2	0.714	349.1
7	3	0.857	290.9
7	4	1.029	242.4
7	5	1.234	202.0
7	6	1.481	168.4
7	7	1.422	175.4
7	8	2.136	116.8
7	9	2.046	121.9
7	10	3.071	81.2
7	11	3.686	67.7
7	12	4.423	56.4
7	13	4.864	51.3
7	14	5.350	46.6
7	15	5.136	48.5
7	16	5.136	48.5
7	17	6.420	38.8
1		9.887	25.2
6	18	5.853	42.6
7	19	6.420	38.8
7	20	6.420	38.8
1		7.490	33.3
6	21	6.247	39.9
7	22	6.421	38.8
7	23	6.421	38.8
7	24	6.421	38.8
7	25	6.421	38.8
7	26	6.421	38.8

Table 5.1: Campaign A: OLR and HRT referred to the substrate used during the experiment.

within a biological reactor and it is obtained from the ratio between the the reactor volume and the volumetric flow rate. Methane production was monitored during the whole duration of the experiment. The minimum and maximum values of the used OLRs were 0.714 and 9.887 $g_{VS}\ l^{-1}\ d^{-1}$ and 1.029 and 6.421 $g_{VS}\ l^{-1}\ d^{-1}$ for the campaigns A and B respectively. A part of the digestate was analysed to establish the Volatile Fatty Acids (VFA) concentration and pH. The process was performed in a temperature regime of (37 °C).

5.3.2 Digester setup

Reactor configuration used in this study was an horizontal PFR, with a reactor length and volume of $1.34\,\mathrm{m}$ and $45\,\mathrm{L}$, respectively. The total working volume was $30\,\mathrm{L}$ and head space volume was $15\,\mathrm{L}$. This is

Time (d)	**Progressive time** ($week$)	**OLR** ($g_{VS}\ l^{-1}\ d^{-1}$)	**HRT** (d)
7	1	1.029	241.4
7	2	1.543	115.4
7	3	2.007	103.8
7	4	1.927	74.0
7	5	2.893	46.0
7	6	4.343	33.3
7	7	6.421	22.5
7	8	6.421	22.5
7	9	6.421	22.5

Table 5.2: Campaign B: OLR and HRT referred to the substrate used during the experiment.

a double walled reactor made of stainless steel maintained at $37\,^{\circ}\mathrm{C}$ by using regulated bath of calorific liquid. Substrate was inserted into a tube separated from the digester by a hermetic system which consists in a clamp. The reactor was equipped with a motor rotating paddle axel at a speed of 4 rpm which stirred discontinuously (1 min every hour). The digestate was discharged using a vertical rod by pushing the digestate downward into an airtight withdrawal box which was previously purged with N_2. The reactor was operated semi-continuously with a daily supply from Monday to Friday. Feeding was supplemented by the recirculation of a part of the digestate in order to promote colonization of microorganisms on the newly introduced substrate. Biogas produced in the reactor passed through a moisture trap and then measured using a drum gas meter (RITTER ® TG05). The reactor was weighted every week in order to maintain constant the reactor mass.

5.3.3 Digester feed and inoculum

The digester feed was collected from a cattle farm. Its size was reduced to approximately $1\,\mathrm{cm}$ size in a Blik BB 230 crusher equipped with stainless steel rotating blades. Crushed cow manure was aliquoted stored at $-20\,^{\circ}\mathrm{C}$. Frozen substrate was transferred to $4\,^{\circ}\mathrm{C}$ temperature 1 day prior to use. The TS content and VS content were 46.21% and 38.39%, respectively. Tap water was used to reduce the TS content before reactor feeding. The final TS content of the substrate fed into the reactor was fixed at 30% and 25% for the experimental campaign A and B, respectively. PFR was inoculated with a mixture of different inocula: i) a granular sludge sampled from an UASB reactor treating a sugar industry wastewater, ii) a solid digestate sampled from a pilot batch reactor treating chicken manure and straw. The inoculum mixture was $10\ gVS_{granularsludge}\ :\ 1\ kg_{digestate}$. The main characteristics of substrate and digestate used are listed in Table 5.3. The final characteristics in terms of water, TS, VS and inert concentrations of the substrate used in the experiments are reported in Table 5.4.

Parameters	Unit	Manure with straw	Digestate
Total solids	%	46.21 ± 0.57	15.73 ± 0.21
Volatile solids-Wet basis	%	38.40 ± 1.30	8.83 ± 0.40
Moisture	%	53.79 ± 0.57	84.27 ±0.21
Ash – Wet basis	%	7.82 ± 0.77	6.90 ± 0.41
pH		7.78	7.95
BMPexperimental	$l_{CH_4}\ g^{-1}_{VSadded}$	0.218 ± 0.01	0.048 ± 0.001

Table 5.3: Characteristics of substrate and digestate used during the experiment (Standard deviation based on triplicate measurements).

Parameters	Unit	Campaign A	Campaign B
Total solids content - Wet basis	$g_{TS}\ g^{-1}$	0.30	0.25
VS content on TS basis	$g_{VS}\ g^{-1}_{TS}$	0.83	0.83
Water concentration	$g\ l^{-1}$	700.00	750.00
Total solids concentration	$g_{TS}\ l^{-1}$	300.00	250.00
Volatile solids concentration	$g_{VS}\ l^{-1}$	249.35	207.79
Inerts concentration	$g\ l^{-1}$	50.65	42.21

Table 5.4: Final characteristics of the feed used in the experimental campaigns A and B.

5.3.4 Analytical measurements

Volatile Fatty Acids and pH

pH was measured directly from the digestate using WTW pH electrode senlix 41 probe. Digestate was centrifuged using Beckman Coulter brand centrifuge before measuring VFA. It was programmed for JA-25.50 mode at $20\,^{\circ}\mathrm{C}$ under 15000 rpm for 12 minutes. VFA was measured using a gas chromatograph (CPG3900 VARIAN) equipped with a flame ionization detector and an automatic sampler (CP8400 VARIAN). The column used was a semi-capillary FFAP (Alltech) column with $15\,\mathrm{m}$ in length, $0.53\,\mathrm{cm}$ in diameter and $1.2\,\mu\mathrm{m}$ phase ECTM 1000 film, where temperature increased from $80\,^{\circ}\mathrm{C}$ to $250\,^{\circ}\mathrm{C}$ isothermally. The carrier gas is N_2. Sample was centrifuged again at 134×1000 rpm for 1 minute before analysis. The temperature of the injector was $210\,^{\circ}\mathrm{C}$.

Methane production

Biogas produced in the reactor passed through a moisture trap and then measured using a drum gas meter (RITTER ® TG05). Biogas composition was determined using a gas chromatograph (GC Perkin Clarus 580). The equipment consists of 2 different columns. The first column, RtU-Bond was filled with silica gel which separates CO_2 from other gases while the second column, Rt-Molsieve 5A was filled with argon as the carrier gas which separates H_2, O_2, N_2 and CH_4. The length as the diameter of two columns were $30\,\mathrm{m}$ and $0.32\,\mathrm{cm}$ respectively. The temperatures were $65\,^{\circ}\mathrm{C}$ for the oven, $200\,^{\circ}\mathrm{C}$ for the injector and

the detector. The detection of gaseous compounds was done using a thermal conductivity detector. The volume of biogas injected was $2\,\mathrm{mL}$. Gas measurements were done in triplicates. Methane production was determined using biogas production and the biogas composition.

5.3.5 Mathematical Model

The mathematical model is based on 1-D mass balances for the state variables represented by the concentration of each bio-component considered in the model. The matrix of the substrate to be treated is supposed to have a density $\rho\,(z,t) = \rho$ constant with space and time. This matrix is supposed to be constituted by water, particulate and dissolved compounds. The particulate compounds are inerts, VS (divided in bio-degradable and non bio-degradable material) and microbial biomass. The dissolved compounds are soluble acetic acid and soluble methane, anaerobically produced from the degradation of VS taking place within the reactor. The gas occupying the head-space of the reactor is composed only by gaseous methane, whose concentration is considered invariable along the space.

The following notations are used:

- $X_{H_2O}\,(z,t)$ is the water concentration within the reactor;
- $X_I\,(z,t)$ is the inerts concentration within the reactor;
- $X_{BVS}\,(z,t)$ is the concentration of bio-degradable VS;
- $X_{NBVS}\,(z,t)$ is the concentration of non bio-degradable VS;
- $X_{ac}\,(z,t)$ is the microbial biomass concentration within the reactor expressed in terms of VS;
- $S_{ac}\,(z,t)$ is the soluble acetic acid concentration within the reactor expressed in terms of Chemical Oxygen Demand (COD);
- $S_{CH_4}\,(z,t)$ is the soluble methane concentration within the reactor expressed in terms of COD;
- $G_{CH_4}\,(t)$ is the gaseous methane concentration within the head-space of the reactor expressed in terms of COD;

COD is a measure of the amount of oxygen that is needed for the complete chemical oxidation of organic compounds of a medium. It is commonly expressed in mass of oxygen consumed over volume of the medium sample used for its measurement.

Figure 5.1 summarizes the kinetic scheme of the model. Disintegration, hydrolysis, acidogenesis and acetogenesis which lead to the conversion of bio-degradable VS X_{BVS} in soluble acetic acid S_{ac} are summarized in a unique kinetic rate r_{BVS}, taking into account only the rate-limiting step of the whole conversion process. This limiting step is represented by the disintegration process when the substrate to be treated is

in particulate form [43]. Soluble methane S_{CH_4} and microbial biomass X_{ac} are produced from the degradation of the acetic acid, which takes place through a process described by a non linear Monod-type kinetic rate r_{ac}. The decay of the microbial biomass is described by the kinetic rate r_{dec} and from this decay are produced new bio-degradable and non-biodegradable VS; lastly, the soluble and gaseous methane (G_{CH_4}) are in equilibrium according to the gas-transfer law expressed by the kinetic rate r_{CH_4}.

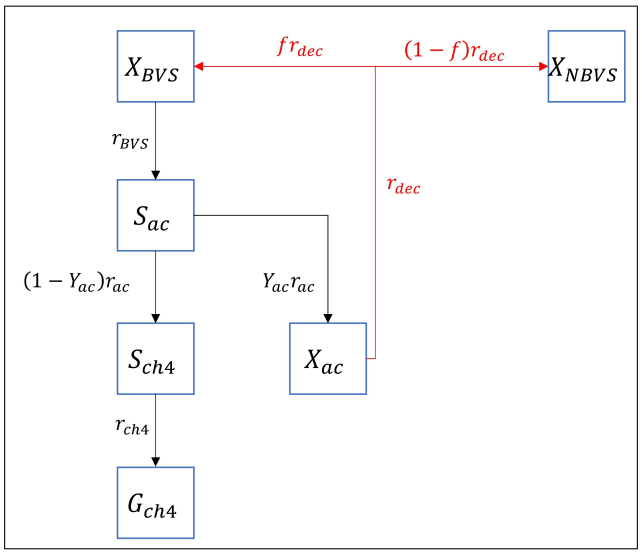

Figure 5.1: Kinetic scheme of the model.

The model is constituted by a system of convection-diffusion-reaction equations (Eq. (5.1)-(5.7)), which holds for $0 < z < L$, where L is the reactor length, and $t > 0$. Moreover, the mass balance on the volume of gas leads to a differential equation describing the gaseous methane dynamics (Eq. (5.8)).

$$\frac{\partial X_{H_2O}(z,t)}{\partial t} + \frac{\partial (v(z,t)X_{H_2O}(z,t))}{\partial z} - D\frac{\partial^2 X_{H_2O}(z,t)}{\partial z^2} = 0, \tag{5.1}$$

$$\frac{\partial X_I(z,t)}{\partial t} + \frac{\partial (v(z,t)X_I(z,t))}{\partial z} - D\frac{\partial^2 X_I(z,t)}{\partial z^2} = 0, \tag{5.2}$$

$$\frac{\partial X_{BVS}(z,t)}{\partial t} + \frac{\partial (v(z,t)X_{BVS}(z,t))}{\partial z} - D\frac{\partial^2 X_{BVS}(z,t)}{\partial z^2} = -r_{BVS} + fr_{dec}, \tag{5.3}$$

$$\frac{\partial X_{NBVS}(z,t)}{\partial t} + \frac{\partial (v(z,t)X_{NBVS}(z,t))}{\partial z} - D\frac{\partial^2 X_{NBVS}(z,t)}{\partial z^2} = (1-f)r_{dec}, \tag{5.4}$$

$$\frac{\partial S_{ac}(z,t)}{\partial t} + \frac{\partial (v(z,t)S_{ac}(z,t))}{\partial z} - D\frac{\partial^2 S_{ac}(z,t)}{\partial z^2} = m\left(r_{BVS} - r_{ac}\right), \tag{5.5}$$

$$\frac{\partial X_{ac}(z,t)}{\partial t} + \frac{\partial (v(z,t)X_{ac}(z,t))}{\partial z} - D\frac{\partial^2 X_{ac}(z,t)}{\partial z^2} = Y_{ac}r_{ac} - r_{dec}, \tag{5.6}$$

$$\frac{\partial S_{ch4}(z,t)}{\partial t} + \frac{\partial (v(z,t)S_{ch4}(z,t))}{\partial z} - D\frac{\partial^2 S_{ch4}(z,t)}{\partial z^2} = m\left(1-Y_{ac}\right)r_{ac} - r_{ch4}, \tag{5.7}$$

$$\frac{dG_{CH_4}(t)}{dt} = \frac{A_w}{V_{gas}}\int_0^L r_{ch4}\, dz, \tag{5.8}$$

where:

- the diffusion coefficient D $[L^2\ T^{-1}]$ is assumed to be the same for each compound and invariable along the z direction;
- the convective velocity of the system $v(z,t)$ is the same for each compound and it is a furtner unknown;
- $r_{BVS} = k_{BVS} X_{BVS}$;
- $r_{ac} = k_{ac} X_{ac} S_{ac} / (K_{s,ac} + S_{ac})$;
- $r_{dec} = k_{dec} X_{ac}$;
- $r_{ch4} = kLa\,(S_{ch4} - K_H RTG_{CH_4})$;
- f is the fraction of dead microbial biomass becoming new bio-degradable substrate;
- m is the conversion factor of VS in COD $\left[g_{COD}\ g_{VS}^{-1}\right]$;
- Y_{ac} is the yield of biomass on substrate;
- k_{BVS} is the kinetic constant for the consumption of the bio-degradable volatile solids X_{BVS}, having the dimension of $[T^{-1}]$;
- k_{ac} is the Monod maximum specific uptake rate for the acetic acid $[T^{-1}]$;
- $K_{s,ac}$ is the half saturation constant $[M\ L^{-3}]$ for the kinetics of consumption of the acetic acid;
- k_{dec} is the first order decay rate of the microbial biomass X_{ac} $[T^{-1}]$;
- kLa is the gas-liquid transfer coefficient $[T^{-1}]$;
- K_H is the Henry's law coefficient $[L^2\ T^{-2}]$;
- R is the gas law constant $[L^2\ T^{-2}\ \Theta^{-1}]$;
- T is the operating temperature $[\Theta]$;
- A_w $[L^2]$ is the constant cross-sectional area occupied by the substrate to be treated along the reactor;
- V_{gas} is the head-space volume where the gas is stored $[L^3]$.

In the equation (5.8) the contributes to the gas-transfer in each point are summed to define a unique gas-transfer rate for the gaseous variable. Moreover, the gas-transfer kinetic rate r_{ch4} is referred to the volume occupied by the matrix of the treated substrate. Hence, to take into account the fact that the gaseous variable must be gas-volume specific, the ratio between the cross-section occupied by the substrate to be treated and the head-space volume is present.

A further equation is needed to describe the variation in space and time of the convective velocity. Such equation is obtained considering that the volume fractions of the water and the particulate components within the reactor is constrained to sum up to unity and that the densities of these components are equal to the density of the whole matrix of substrate to be treated ρ, that is:

$$\begin{cases} \frac{X_{H_2O}(z,t)}{\rho_{H_2O}} + \frac{X_I(z,t)}{\rho_I} + \frac{X_{BVS}(z,t)}{\rho_{BVS}} + \frac{X_{NBVS}(z,t)}{\rho_{NBVS}} + \frac{X_{ac}(z,t)}{\rho_{ac}} = 1, \\ \rho_{H_2O} = \rho_I = \rho_{BVS} = \rho_{NBVS} = \rho_{ac} = \rho, \end{cases} \tag{5.9}$$

which leads us to consider that the sum of the concentrations of water and particulate components is equal to the density ρ of the substrate to be treated (Equation (5.10)).

$$X_{H_2O}(z,t) + X_I(z,t) + X_{BVS}(z,t) + X_{NBVS}(z,t) + X_{ac}(z,t) = \rho. \tag{5.10}$$

Equation (5.10) implies that the mass of the mixture composed of water, inerts, VS and microbial biomass is constant over time. As a consequence, the convective velocity of the matrix of the treated substrate varies along the reactor and its variation depends on the kinetics of the compounds constituting the mixture. In fact, the velocity variation has to balance the consumption of the VS to keep the mass of this particular mixture constant.

Now summing equations (5.1) to (5.4) and equation (5.6), remembering the (5.10), the equation governing the velocity is derived (Eq. (5.11)):

$$\frac{\partial v(z,t)}{\partial z} = \frac{Y_{ac} r_{ac} - r_{BVS}}{\rho}. \tag{5.11}$$

Lastly, boundary and initial conditions (Eq. (5.12)-(5.19)) are prescribed to set a closed mathematical problem

$$v(0,t) = v_0, \quad t \geqslant 0, \tag{5.12}$$

$$-D\frac{\partial X_i(0,t)}{\partial z} = v_0 \left(X_{i,IN} - X_i(0,t)\right), \quad t > 0 \quad i = 1, ..., n_1, \tag{5.13}$$

$$-D\frac{\partial S_i(0,t)}{\partial z} = v_0 \left(S_{i,IN} - S_i(0,t)\right), \quad t > 0 \quad i = n_1 + 1, ..., n_2, \tag{5.14}$$

$$\frac{\partial X_i(L,t)}{\partial z} = 0, \quad t > 0 \quad i = 1, ..., n_1, \tag{5.15}$$

$$\frac{\partial S_i(L,t)}{\partial z} = 0, \quad t > 0 \quad i = n_1 + 1, ..., n_2, \tag{5.16}$$

$$X_i(z,0) = X_{i,0}, \quad 0 \leqslant z \leqslant L, \quad i = 1, ..., n_1, \tag{5.17}$$

$$S_i(z,0) = S_{i,0}, \quad 0 \leqslant z \leqslant L, \quad i = n_1 + 1, ..., n_2, \tag{5.18}$$

$$G_{CH_4}(0) = G_{CH_4,0}, \tag{5.19}$$

where:

- v_0 is the inlet flow velocity;
- n_1 is the number of the particulate compounds plus water;
- $n_2 - n_1$ is the number of dissolved compounds;
- $X_{i,IN}$ is the concentration of the i^{th} particulate compound and water in the incoming flow rate;
- $S_{i,IN}$ is the concentration of the i^{th} dissolved compound in the incoming flow rate;
- $X_{i,0}$, $S_{i,0}$ and $G_{CH_4,0}$ are the initial concentrations of each particulate compound, dissolved compound and gaseous methane, respectively.

5.3.6 Model Inputs

For the experimental campaign A, the reactor was initially filled with a mixed inoculum, containing microorganisms, low-degradable organic matter and inerts. Hence, the characteristics of the inoculum represented the initial conditions for the numerical simulations performed for model calibration (Table 5.7). No stratification of substrates was observed at $t = 0$ and thus it is possible to assume that the initial concentrations of the compounds are homogeneous along the reactor. Biochemical Methane Potential (BMP) is a measure of the portion of organic material which can be anaerobically converted to methane [103] and is established through specific tests [48]. This parameter was used to evaluate the initial concentration of bio-degradable VS of the inoculum while the initial microbial biomass concentration was obtained assuming that the sum of the concentrations of the bio-degradable VS and the microbial biomass represented the 15% of the VS content of the inoculum. The start-up phase was simulated considering only diffusion as transport phenomenon. The values of the compounds concentrations resulting from the simulation of this

start-up phase (lasted for 3 days) represented the initial condition for the simulation of the process in continuous conditions. Indeed, starting from $t = 4$ days the reactor was continuously fed with fresh influent. These boundary conditions were evaluated considering the weighted average between the characteristics of the fed substrate (Table 5.4) and the recirculated digestate. In particular, it was assumed that no microbial biomass is present in the fresh substrate while the 15% of the VS content of the digestate was assumed to be constituted by a 2/3 of low-degradable substrate and 1/3 of microbial biomass. The characteristics of the recirculated digestate in terms of TS and VS content are reported in Table 5.5 and 5.6 for campaigns A and B, respectively.

The inactivity period between the two campaigns A and B (lasted for two months) was simulated using a feeding condition characterized by a very small OLR (0.1 $g_{VS}\ l^{-1}\ d^{-1}$), with the diffusion as unique transport phenomenon. The experimental campaign B was simulated in continuous feeding conditions, using as initial conditions the concentration values resulting from the simulation of the period of inactivity and as boundary conditions the values obtained as weighted average between the characteristics of the fed substrate (Table 5.4) and the recirculated digestate (Table 5.6).

Some aspects of the experimental procedure needed an adaptation to the model structure. First of all, during the experiments, for practical aspects, the feeding was performed in semi-continuous conditions. Hence, it was necessary to reallocate the amount of the fed mixture to obtain a day-by-day reactor feeding. Moreover, the flow rate of the recirculated digestate affects the OLR and HRT of the substrate alone. Hence, depending on the amount of recirculated digestate, the OLR and HRT of the mixture composed of substrate and digestate were evaluated and used in the simulations. Lastly, the value of the conversion factor m of VS in COD used in model simulations for the fresh substrate was set to 1.50 $g_{COD}\ g_{VS}^{-1}$ [53] while for the inoculum and the digestate it was set to 1.25 $g_{COD}\ g_{VS}^{-1}$ [74, 107]).

5.3.7 Model calibration and validation

According to the results of the GSA for the model reported in Chapter 4, a calibration procedure was applied to find the best values of the most influencing parameters of the model which allow the model to achieve the optimal fit between observed and simulated data of a certain output. The screening of model parameters performed through the aforementioned GSA established that k_{BVS}, k_{ac}, $K_{s,ac}$ and Y_{ac} are the parameters that the most affect the values of the quantity of interest. Despite this, it is feasible to consider the values of $K_{s,ac}$ and Y_{ac} equal to the values used in the Anaerobic Digestion Model n° 1 (ADM1) [10] in mesophilic temperature regime. Indeed, the half-saturation constant $K_{s,ac}$, which recollects the influence of the acetic acid concentration on its maximum uptake rate, and the yield of biomass on substrate Y_{ac}, which represents the quantity of acetic acid that is converted in new microbial biomass, are two parameters that are basically function of temperature and the kind of substrate they refer to [47, 55] (acetic acid in this case). Moreover, the values of the other parameters that were not object of model calibration were set as in the ADM1 (Table 5.8), except for the value of the liquid-gas transfer coefficient kLa that was decreased to 2.0 d^{-1} respect to

Time (d)	**Progressive time** ($week$)	**TS content** ($g_{TS}\ g^{-1}$)	**VS content on TS base** ($g_{VS}\ g_{TS}^{-1}$)
7	1	-	-
7	2	-	-
7	3	-	-
1	-	-	-
6	4	0.145	0.579
1	-	-	-
6	5	0.144	0.569
1	-	-	-
6	6	0.143	0.579
1	-	-	-
6	7	0.147	0.578
1	-	-	-
6	8	0.148	0.610
1	-	0.148	0.610
1	-	-	-
5	9	0.145	0.592
1	-	0.158	0.570
1	-	-	-
5	10	0.158	0.570
1	-	-	-
6	11	0.159	0.570
1	-	-	-
6	12	0.165	0.584
1	-	-	-
6	13	0.168	0.617
1	-	-	-
6	14	0.170	0.608
1	-	-	-
6	15	0.177	0.614
1	-	-	-
6	16	0.178	0.636
1	-	-	-
6	17	0.185	0.639
1	-	-	-
2	-	0.183	0.667
4	18	-	-
1	-	-	-
6	19	0.183	0.667
1	-	-	-
6	20	0.183	0.667
1	-	-	-
6	21	0.198	0.700
1	-	-	-
6	22	0.200	0.700
7	23	0.200	0.700
7	24	0.206	0.728
7	25	0.208	0.721
7	26	0.203	0.739

Table 5.5: Recirculated digestate characteristics of the experimental campaign A.

Time (d)	**Progressive time** ($week$)	**TS content** ($g_{TS}\ g^{-1}$)	**VS content on TS base** ($g_{VS}\ g_{TS}^{-1}$)
1	-	-	-
6	1	0.189	0.708
7	2	0.190	0.769
7	3	-	-
1	-	-	-
1	-	0.190	0.737
5	4	-	-
3	-	-	-
1	-	0.190	0.737
3	5	-	-
3	-	0.190	0.684
1	-	-	-
3	6	0.190	0.684
3	-	0.190	0.684
1	-	-	-
3	7	0.190	0.684
1	-	-	-
6	8	0.148	0.603
1	-	-	-
1	-	0.197	0.663
5	9	-	-

Table 5.6: Recirculated digestate characteristics of the experimental campaign B.

Variable	Units	Initial conditions
$X_{H_2O,0}$	$g\ l^{-1}$	842.74
$X_{I,0}$	$g\ l^{-1}$	68.97
$X_{BVS,0}$	$g_{VS}\ l^{-1}$	6.70
$X_{NBVS,0}$	$g_{VS}\ l^{-1}$	79.46
$X_{ac,0}$	$g_{VS}\ l^{-1}$	2.13
$S_{ac,0}$	$g_{COD}\ l^{-1}$	0.00
$S_{ch4,0}$	$g_{COD}\ l^{-1}$	0.00
$G_{ch4,0}$	$g_{COD}\ l^{-1}$	0.00

Table 5.7: Initial conditions used in the start-up phase of the experimental campaign A.

the ADM1 value ($kLa = 200.0\ d^{-1}$) to take into account mass transfer limitations due to the high-solids content [83, 1, 78]. The diffusion coefficient was set equal to $D = 1.0 \times 10^{-7}\ m^2\ s^{-1}$ according to [24]. Lastly, the value of the fraction of dead microbial biomass becoming new bio-degradable substrate f was set equal to 0.2.

Parameter	Definition	Unit	Value	Reference
k_{dec}	First order decay rate of the biomass	d^{-1}	0.02	[10]
Y_{ac}	Yield of biomass on substrate	-	0.05	[10]
$K_{s,ac}$	Half saturation constant	$g_{COD}\ l^{-1}$	0.15	[10]
kLa	Gas-liquid transfer coefficient	d^{-1}	2.0	This study
K_H	Henry's law coefficient	$Mbar^{-1}$	0.0011	[10]

Table 5.8: Kinetic parameters used in model simulations.

The experimental input substrate characteristics, feeding conditions and output results of the campaign A were used to calibrate the model parameters while the data of the campaign B were used for the validation procedure. The calibration was performed by defining different range of variation of the selected parameters, plotting the output of interest curves and choosing the values of parameters that optimize the following functions [60]:

$$RMSE\left(\mathbf{p}\right) = \sqrt{\frac{\sum_{i=1}^{N}\left(y_i\left(\mathbf{p}\right) - y_i'\right)^2}{N}} \tag{5.20}$$

$$NRMSE\left(\mathbf{p}\right) = \frac{RMSE\left(\mathbf{p}\right)}{\bar{y'}} \tag{5.21}$$

$$ME\left(\mathbf{p}\right) = 1 - \frac{\sum_{i=1}^{N}\left(y_i\left(\mathbf{p}\right) - y_i'\right)^2}{\sum_{i=1}^{N}\left(y_i' - \bar{y'}\right)^2} \tag{5.22}$$

$$IoA\left(\mathbf{p}\right) = 1 - \frac{\sum_{i=1}^{N}\left(y_i\left(\mathbf{p}\right) - y_i'\right)^2}{\sum_{i=1}^{N}\left(\left|y_i\left(\mathbf{p}\right) - \bar{y'}\right| + \left|y_i' - \bar{y'}\right|\right)^2} \tag{5.23}$$

where:

- $y_i\left(\mathbf{p}\right)$ are the predicted values of the chosen output while y_i' and $\bar{y'}$ are its the observed and the average of the observed values;
- $\mathbf{p} = \left[k_{BVS}, k_{ac}\right] \in \Omega$ is the vector of the parameters being calibrated, where $\Omega \subset \mathbb{R}^2$ is the set of variation of the 2 parameters;
- N is the number of observed values;
- $RMSE\left(\mathbf{p}\right)$ and $NRMSE\left(\mathbf{p}\right)$ are the Root Mean Square Error and its normalized form;
- $ME\left(\mathbf{p}\right)$ is the Modeling Efficiency coefficient;
- $IoA\left(\mathbf{p}\right)$ is the index of agreement.

The optimization problem requires the functions $RMSE\left(\mathbf{p}\right)$ and $NRMSE\left(\mathbf{p}\right)$ to be minimized while $ME\left(\mathbf{p}\right)$ and $IoA\left(\mathbf{p}\right)$ functions have to be maximized ($ME\left(\mathbf{p}\right) \in \left[0,1\right]$, $IoA\left(\mathbf{p}\right) \in \left[0,1\right]$) [69, 99, 109, 119, 138].

The methane production was chosen as output of interest and the function *fmincon* of the optimization toolbox of the software `MATLAB` was used to minimize the function $1/ME\left(\mathbf{p}\right)$. The ranges of variation of model parameters to be calibrated were chosen considering as upper bounds the corresponding values of the disintegration constant and the Monod maximum specific uptake rate of the acetic acid reported in the ADM1 in mesophilic conditions. The reason for this is that the ADM1 considers anaerobic digestion in wet conditions which are more favourable with respect to dry ones. Obviously, the lower bounds of the range of variation of model parameters were derived from the fact that these parameters cannot be negative. Once evaluated model parameters values minimizing the function $1/ME\left(\mathbf{p}\right)$, the quality of the calibration was verified by evaluating the values of the other calibration performance indicators.

The calibrated values of model parameters were then used for model validation. The agreement between the simulated and the experimental methane production was verified by using the data of the experimental campaign B and was evaluated through the values of the functions described by equations (5.20) to (5.23) calculated by fixing the vector $\mathbf{p}$ as resulting from the calibration procedure.

		Index of Performances			
Type of parameters analysis	**Campaign**	**ME**	**IoA**	**RMSE**	**NRMSE**
		(-)	(-)	(l)	(-)
Calibration	A	0.995	0.999	84.0	0.058
Validation	B	0.967	0.993	71.7	0.170

Table 5.9: Performance indicators of the calibration and validation procedures.

5.4 Results and discussion

The calibration procedure allowed to assess the values of the parameters k_{BVS} and k_{ac} that determined the best fit between experimental and simulated cumulative methane production curves. The resulting values of $k_{BVS} = 0.2010\ d^{-1}$ and $k_{ac} = 8.0\ d^{-1}$ minimize the function $1/ME\,(\mathbf{p})$. The good quality of the calibration is reported graphically in the Figures 5.2 and 5.3 and through the values of the indexes of performance described in equations (5.20) to (5.23) and reported in Table 5.9. Particularly, Figure 5.2a shows the experimental and simulated methane productions related to the campaign A while Figure 5.2b display the line of perfect fit and the position of the points having as coordinates the experimental and simulated data of the campaign A (fit line). The accordance between experimental and simulated methane productions observed in the Figure 5.2a is confirmed by the small shift visible between the fit line and the line of perfect fit (Figure 5.2b). Furthermore, in Figure 5.3a are reported the experimental and simulated daily methane productions referred to the campaign A and Figure 5.3b shows the weekly simulated and experimental methane yields. The weekly methane yields have been evaluated as the ratio between the volume of methane produced in each week and the corresponding quantity of VS in grams added into the reactor and it gives information about the reactor conversion efficiency of VS fed into the reactor in methane. The experimental daily production trend is adequately followed by the simulated one. Moreover, except for an overestimation in the first weeks, the simulated weekly methane yields curve indicates that the modelled reactor performance accurately emulates what happened experimentally. Concerning the performance indicators of Table 5.9, the values close to 1 of ME and IoA, the value of 84.0 l of RMSE and a small value of the NRMSE in the calibration case, suggest that the minimization of the function $1/ME\,(\mathbf{p})$ lead to a good parameter estimation. Figure 5.4a shows the simulated concentration profile of the soluble acetic acid S_{ac} while in Figure 5.4b is reported the concentration profile of the microbial biomass involved in the consumption of the acetic acid X_{ac}. In such figures can be observed the spatialization of the variables along the reactor. A little accumulation of the acetic acid in the first half of the reactor indicates that methanogenesis is limiting at the beginning of the reactor and for this reason the microbial species are mainly distributed in the middle and in the second part of the reactor.

The calibrated values of $k_{BVS} = 0.2010\ d^{-1}$ and $k_{ac} = 8.0\ d^{-1}$ were validated using the measurements of the methane production of the experimental campaign B as validation database. The results of the

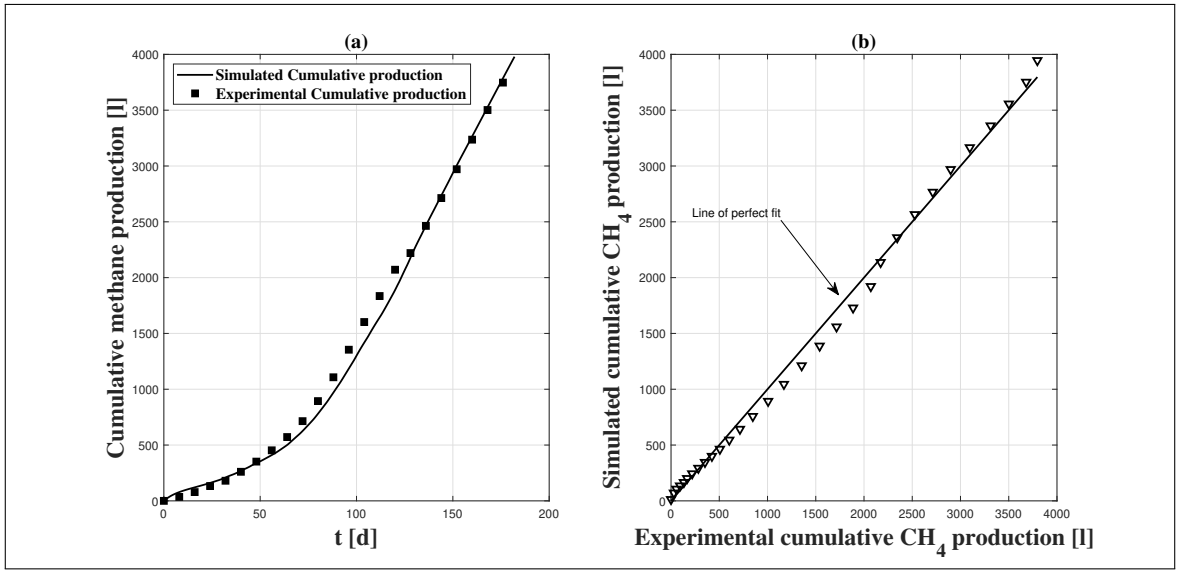

Figure 5.2: Campaign A: experimental and simulated cumulative methane productions (a) and comparison between the fit line and the line of perfect fit (b).

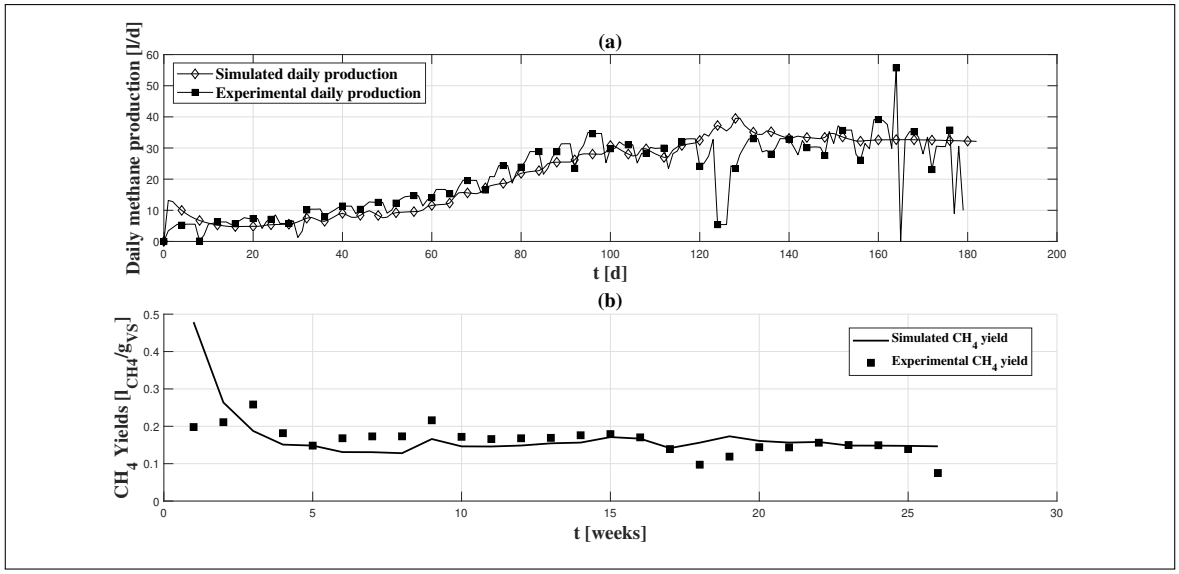

Figure 5.3: Campaign A: experimental and simulated daily methane productions (a) and experimental and simulated methane weekly yields (b).

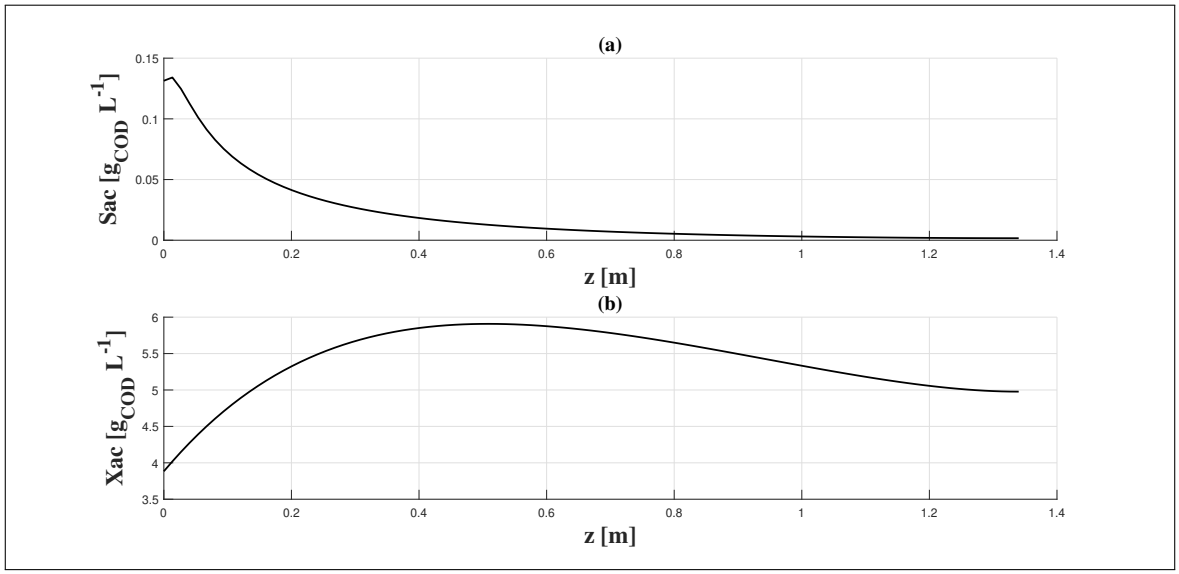

Figure 5.4: Campaign A: Profiles of the simulated soluble acetic acid (a) and microbial biomass (b) concentrations.

validation are reported in Table 5.9 and graphically showed in the Figures 5.5 and 5.6. It can be noticed that the values of all the performance indexes of Table 5.9 referred to the validation case are satisfying: both ME index and the IoA are close to one and despite the higher value with respect to the calibration case of the $NRMSE$, it is still a small value and it can be affirmed that the validation succeeded. The simulated and experimental cumulative methane productions of the campaign B are reported in Figure 5.5a while Figure 5.5b shows the comparison between the fit line and the line of perfect fit in this second case. The simulated methane production curve underestimates the experimental one during the first 4 weeks. During the subsequent period the experimental methane production is perfectly reproduced by the model, as indicated also by the very small shift between the points of the fit line with respect to the points of the line of perfect fit. The underestimation in the initial phase is due to the uncertainty on the reactor dynamics during the period of inactivity. Moreover, Figure 5.6a and 5.6b show the simulated and experimental daily methane production and weekly methane yields curves referred to the experimental campaign B and both figures suggest that the chosen values of the unknown parameters are fully validated, with a few experimental points not fitted by the simulation results. Also in this case, the differences between experimental and simulated results are mainly developed during the initial phase of the experimental campaign B, affected by a great uncertainty due to the suspension of the experimental activities. The calibrated and then validated value of $k_{ac} = 8.0\ d^{-1}$, identical to the value reported in [10] in mesophilic conditions, suggests that, according to the experimental results where no accumulation of acids was observed, the consumption of acetic acid had no limitations in dry conditions with respect to the same process in wet conditions.

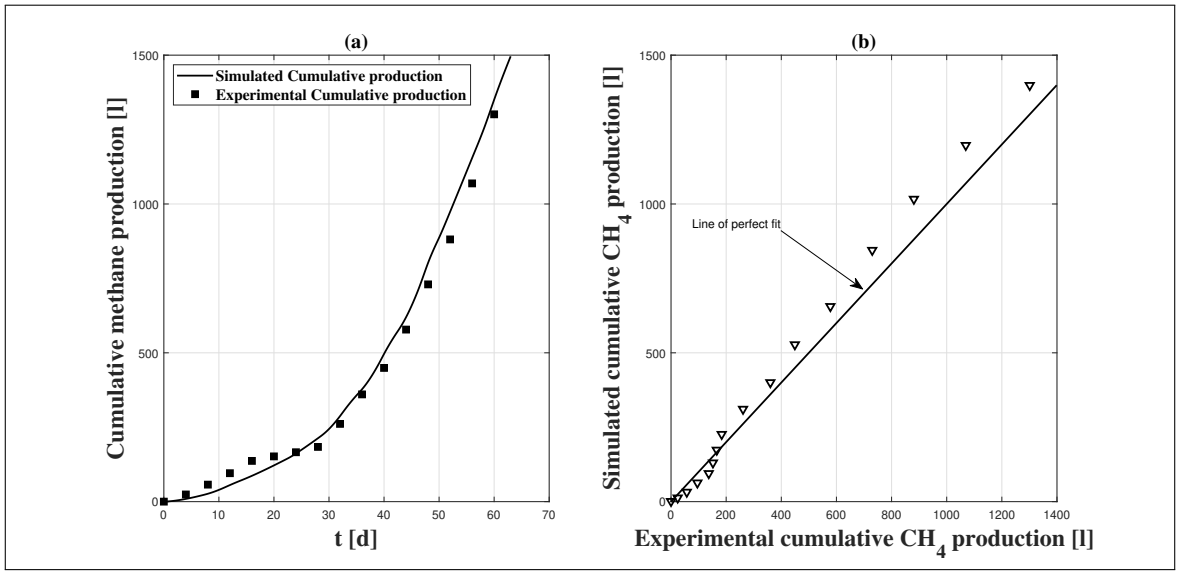

Figure 5.5: Campaign B: experimental and simulated cumulative methane productions (a) and comparison between the fit line and the line of perfect fit (b).

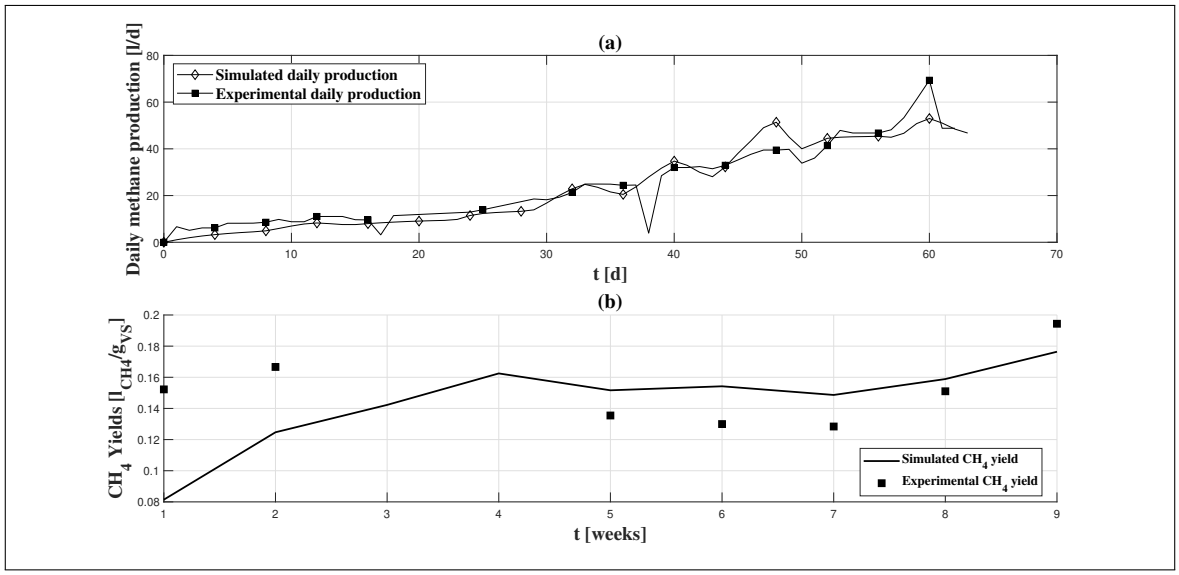

Figure 5.6: Campaign B: experimental and simulated daily methane productions (a) and experimental and simulated methane weekly yields (b).

5.5 Conclusions

This study focuses on the calibration and validation of the parameters of a model of dry anaerobic digestion in plug-flow reactors. Based on the results of a previous study focused on the screening of model parameters, the kinetic constant of the process of conversion of the bio-degradable fraction of volatile solids in acetic acid k_{BVS} and the Monod maximum specific uptake rate for the acetic acid k_{ac} are selected for

model calibration and validation. The methane production measurements of two experimental campaigns of dry anaerobic digestion in an horizontal plug-flow reactor of cattle manure at total solids content of 30% and 25%, were used as database of the calibration and validation procedures, whose quality was detected through four methods of performance evaluation. The model calibration results showed the potential of the model in predicting experimental results. This potential was confirmed by the validation success, suggesting that the model is a powerful instrument to describe processes of this type and that can be used as a tool to design and manage plants performing dry anaerobic digestion.

Chapter 6

General discussion and recommendations

The main objective of this research was to develop a mathematical model capable to describe the dynamics of dry anaerobic digestion processes in plug-flow reactors. The lack of scientific literature on the topic negatively affects the development of mathematical tools capable to support and improve control systems for this kind of process. The main difficulties in modeling dry anaerobic digestion processes in plug-flow reactors is due to the kind of phenomenon that, depending on both space and time as physical dimensions, requires the definition, implementation and analysis of non-linear PDEs. Moreover, the uncertainty linked to some aspects such as turbulence, variation of mass, density and porosity along the reactor and dispersion phenomena need a deeper analysis to be correctly incorporated.

The kinetic processes involved in anaerobic digestion systems have been widely studied experimentally [84, 98, 28] and a significant amount of mathematical models have been proposed over the years to describe the anaerobic digestion process in completely mixed environments [80, 38]. The most representative model of this class is the ADM1, which consists of a system of non-linear ODEs that condenses the main bio-physico-chemical processes occurring in anaerobic digestion environments. However, ADM1 lacks of a thoughtful implementation of many physico-chemical processes and does not consider the disintegration process as affected by the particle size distribution which actually plays a crucial role in the definition of substrate availability and methane production for the anaerobic digestion of complex particulate compounds. With this aim, Chapter 2 summarizes the main proposed approaches found in literature to extend the ADM1 and essentially focuses on the mathematical modeling of the disintegration process through a modified surface-based kinetic. A local sensitivity analysis was performed to investigate the most influencing parameters of the model. Considering the produced methane or the volatile fatty acids concentrations as quantity of interest, the parameters showed different weight on the output values. Despite this, for both methane and volatile fatty acids concentrations, the disintegration kinetic constant presented the highest sensitivity among disintegration/hydrolysis related parameters and Monod specific uptake rates, confirming the role of the disintegration process in determining the methane production rate for the digestion of complex particulate compounds. The model was successfully calibrated and validated with ad-hoc anaerobic digestion experiments carried out using potato waste as organic substrate. The calibration was operated on the disintegration constant and also on some key kinetic parameters of the ADM1, to take in account the fact that the simulated process involved potato waste as main substrate, contrary to the original ADM1 where activated sludge is usually considered as main substrate. The model properly predicted the cumulative methane production and volatile fatty acids concentration profiles achieved during lab-scale experiments. Finally, validation results showed the ability of the modified surface-based model to adequately describe real processes where a wide range of particle size characterizes the substrate fed to anaerobic digestion reactors. In Chapter 3 continuum mechanics principles were applied to derive the equations of a mathematical model for the dry anaerobic digestion process of solid waste in plug-flow reactors. The model is based on a system of convection-diffusion-reaction equations in one-dimensional case and is capable to predict substances concentrations along the reactor. Moreover, the model describes the variation of the system velocity with time and space, accounting for the mass variation along the reactor due to degrading

processes that convert solid components in gaseous ones. The equation governing the convective velocity is derived by considering the hypothesis that the density of the treated waste matrix within the reactor is constant over time and the sum of the volume fractions of the bio-components constituting the waste matrix is constrained to unity. The obtained velocity variation law depends on the bio-components kinetics and allows to balance the consumption of the volatile solids in order to keep constant the mass of the system along the reactor, which is the main consequence of the two model hypothesis. The system of PDEs was integrated numerically and numerical simulations were performed to show model consistency with experimental evidence and highlight that such mathematical tool could be used to manage, size and optimize the operation of real plants. Indeed, simulation results showed that the model is useful to investigate the effect of operating and physical parameters on process performance in terms of organic compounds removal efficiency and methane production. Moreover, concentration trends of the intermediate products can be monitored and this could help in detecting if the process develops correctly.

The new model derived in Chapter 3 depends on a set of parameters of different nature and Chapter 4 focused on the global sensitivity analysis and uncertainty quantification for the cited model. This study was aimed to understand the overall effect of uncertainty of input parameters on the methane production. The Morris screening test and the quantitative sensitivity analysis with Sobol' indices showed, with a remarkable accordance, that the kinetic parameters linked to the consumption of the bio-degradable volatile solids and acetic acid mainly affects the model output. The quantity of interest are less sensitive to the values assumed by the physical parameters describing the gas-transfer and diffusion phenomena. Methane is rapidly released in the gas-phase and, except for very small values of the gas-transfer coefficient neglecting the methane release, great variations of this parameter have no effect on the final output value. Moreover, the sensitivity of the diffusion coefficient in a 1-D model of this type, where the diffusion is not linked to kinetic processes, seemed relatively little with respect to the sensitivity of kinetic parameters. Lastly, the other kinetic parameter describing the microbial biomass decay showed a small relevance in determining the value of the model output and this suggested that their effective assessment becomes less important during model calibration procedures.

Subsequently, in Chapter 5 the identified most influencing parameters of the model presented in Chapter 3 and discussed in Chaper 4 were calibrated and validated based on the experimental results of two campaigns of dry anaerobic digestion in a horizontal plug-flow reactor. The reactor was fed with cattle manure considering a total solids content of 30% and 25% for the two campaigns. The calibration and validation results were screened through four different indexes, that is the coefficient of the Modelling Efficiency (ME) method, the Index of Agreement (IoA), the Root Mean Square Error (RMSE) and its normalized form (NRMSE). The model calibration allowed to assess the value of the kinetic constant describing the conversion of bio-degradable compounds in acetic acid. The calibrated maximum specific uptake rate of acetic acid resulted the same as ADM1 suggesting that the consumption of acetic acid had no limitations in dry conditions with respect to the same process in wet conditions. The half-saturation constant and the yield of biomass on substrate, after physico-chemical considerations have been set as in the ADM1. Also

the remaining kinetic parameters values come from ADM1, except for the gas-liquid transfer coefficient, which was decreased with respect to its original ADM1 value to account for mass transfer limitations due to the high-solids content. Furthermore, the value of the adopted operating parameters such as reactor length, substrate inlet velocity, hydraulic retention time and organic loading rate reflected the experimental conditions. Moreover, the diffusion coefficient value was selected from the literature. The values of the indexes obtained through the validation procedure, suggest that the model is effectively able to reproduce fundamental phenomena occurring during a dry anaerobic digestion process in plug-flow reactors and can represent a powerful tool to design and manage plants performing dry anaerobic digestion.

A quantitative analysis of model equations through numerical simulations has been performed to verify model consistency with experimental evidence. Future research activities may be devoted to the qualitative analysis, including the study of existence and uniqueness of solutions, positivity properties and linear and nonlinear stability. However, the developed model is meant to be an important starting point for the modeling of such a complex process. Further improvements may be incorporated to enhance model capability. For instance, the kinetic model may be extended to the complete ADM1 framework. This will allow to predict all species dynamics involved in an anaerobic digestion process, such as pH and volatile fatty acids concentration profiles along the reactor and their acid-base equilibria within the semi-solid medium. Moreover, the composition of the biogas could be better characterized with the aim to determine the exact energetic power generated through the digestion process. Additionally, the differential equation describing the methane concentration within the reactor head-space may be modified by introducing a loss term that reproduces a certain gas tapping from the head-space of the reactor which is closer to the real operating conditions of such systems. Another improvement of the model could come from considering a variable density of the treated matrix along the reactor. Lastly, the diffusion could be considered affecting kinetic processes and the model extension to 2D and 3D domains could help to analyse the effect of other phenomena occurring along the directions different from the system movement direction on the anaerobic digestion process performance.

Bibliography

[1] Amel Abbassi-Guendouz, Doris Brockmann, Eric Trably, Claire Dumas, Jean-Philippe Delgenès, Jean-Philippe Steyer, and Renaud Escudié. Total solids content drives high solid anaerobic digestion via mass transfer limitation. *Bioresource technology*, 111:55–61, 2012.

[2] T Al Seadi, D Ruiz, H Prassl, M Kottner, T Finsterwaldes, S Volke, and R Janssers. Handbook of biogas. *University of Southern Denmark, Esbjerg*, 2008.

[3] JF Andrews. Kinetic models of biological waste treatment processes. In *Biotechnol. Bioengng. Symp*, volume 2, pages 5–33, 1971.

[4] John F Andrews. Dynamic model of the anaerobic digestion process. *Journal of the Sanitary Engineering Division*, 95(1):95–116, 1969.

[5] John F Andrews and Stephen P Graef. Dynamic modeling and simulation of the anaerobic digestion process. ACS Publications, 1970.

[6] Irini Angelidaki, Lars Ellegaard, and Birgitte K Ahring. A comprehensive model of anaerobic bioconversion of complex substrates to biogas. *Biotechnology and bioengineering*, 63(3):363–372, 1999.

[7] APHA/AWWA/WEF. *Standard methods for the examination of water and wastewater*, volume 20th ed. United Book Press, Inc., Baltimore, Maryland (USA), 1998.

[8] Ernesto L Barrera, Henri Spanjers, Kimberly Solon, Youri Amerlinck, Ingmar Nopens, and Jo Dewulf. Modeling the anaerobic digestion of cane-molasses vinasse: extension of the anaerobic digestion model no. 1 (adm1) with sulfate reduction for a very high strength and sulfate rich wastewater. *Water research*, 71:42–54, 2015.

[9] Damien J Batstone. Modelling and control in anaerobic digestion: achievements and challenges. 2013.

[10] Damien J Batstone, J Keller, Irini Angelidaki, SV Kalyuzhnyi, SG Pavlostathis, A Rozzi, WTM Sanders, H Siegrist, and VA Vavilin. The iwa anaerobic digestion model no 1 (adm1). *Water Science and technology*, 45(10):65–73, 2002.

[11] Damien J Batstone, Daniel Puyol, Xavier Flores-Alsina, and Jorge Rodríguez. Mathematical modelling of anaerobic digestion processes: applications and future needs. *Reviews in Environmental Science and Bio/Technology*, 14(4):595–613, 2015.

[12] DJ Batstone, S Tait, and D Starrenburg. Estimation of hydrolysis parameters in full-scale anerobic digesters. *Biotechnology and bioengineering*, 102(5):1513–1520, 2009.

[13] Michael Baudin, Khalid Boumhaout, Thibault Delage, Bertrand Iooss, and Jean-Marc Martinez. Numerical stability of sobol'indices estimation formula. In *Proceedings of the 8th International Conference on Sensitivity Analysis of Model Output (SAMO 2016). Le Tampon, Réunion Island, France*, 2016.

[14] Michaël Baudin, Anne Dutfoy, Bertrand Iooss, and Anne-Laure Popelin. Open turns: An industrial software for uncertainty quantification in simulation. *arXiv preprint arXiv:1501.05242*, 2015.

[15] Hassen Benbelkacem, Julien Bollon, Rémy Bayard, Renaud Escudié, and Pierre Buffière. Towards optimization of the total solid content in high-solid (dry) municipal solid waste digestion. *Chemical Engineering Journal*, 273:261–267, 2015.

[16] Hassen Benbelkacem, Diana Garcia-Bernet, Julien Bollon, Denis Loisel, Rémy Bayard, Jean-Philippe Steyer, Rémy Gourdon, Pierre Buffière, and Renaud Escudié. Liquid mixing and solid segregation in high-solid anaerobic digesters. *Bioresource technology*, 147:387–394, 2013.

[17] Lorenzo Benedetti, Damien J Batstone, Bernard De Baets, Ingmar Nopens, and Peter A Vanrolleghem. Global sensitivity analysis of biochemical, design and operational parameters of the benchmark simulation model no. 2. 2008.

[18] Olivier Bernard, Zakaria Hadj-Sadok, Denis Dochain, Antoine Genovesi, and Jean-Philippe Steyer. Dynamical model development and parameter identification for an anaerobic wastewater treatment process. *Biotechnology and bioengineering*, 75(4):424–438, 2001.

[19] Kenneth B Bischoff. A note on boundary conditions for flow reactors. *Chemical Engineering Science*, 16(1-2):131–133, 1961.

[20] Géraud Blatman and Bruno Sudret. Efficient computation of global sensitivity indices using sparse polynomial chaos expansions. *Reliability Engineering & System Safety*, 95(11):1216–1229, 2010.

[21] F. Blumensaat and J. Keller. Modelling of two-stage anaerobic digestion using the iwa anaerobic digestion model no. 1 (adm1). *Water Research*, 39(1):171 – 183, 2005.

[22] D Bolzonella, P Pavan, S Mace, and F Cecchi. Dry anaerobic digestion of differently sorted organic municipal solid waste: a full-scale experience. *Water Science and Technology*, 53(8):23–32, 2006.

[23] David Bolzonella, L Innocenti, P Pavan, P Traverso, and F Cecchi. Semi-dry thermophilic anaerobic digestion of the organic fraction of municipal solid waste: focusing on the start-up phase. *Bioresource technology*, 86(2):123–129, 2003.

[24] S Brito-Espino, A Ramos-Martín, SO Pérez-Báez, and C Mendieta-Pino. Application of a mathematical model to predict simultaneous reactions in anaerobic plug-flow reactors as a primary treatment for constructed wetlands. *Science of The Total Environment*, 713:136244, 2020.

[25] Francesca Campolongo and Andrea Saltelli. Sensitivity analysis of an environmental model: an application of different analysis methods. *Reliability Engineering & System Safety*, 57(1):49–69, 1997.

[26] Yucheng Cao and Artur Pawłowski. Sewage sludge-to-energy approaches based on anaerobic digestion and pyrolysis: Brief overview and energy efficiency assessment. *Renewable and Sustainable Energy Reviews*, 16(3):1657–1665, 2012.

[27] J Cariboni, D Gatelli, R Liska, and A Saltelli. The role of sensitivity analysis in ecological modelling. *Ecological modelling*, 203(1-2):167–182, 2007.

[28] My Carlsson, Anders Lagerkvist, and Fernando Morgan-Sagastume. The effects of substrate pretreatment on anaerobic digestion systems: a review. *Waste management*, 32(9):1634–1650, 2012.

[29] F Carrera-Chapela, A Donoso-Bravo, D Jeison, I Díaz, JA Gonzalez, and G Ruiz-Filippi. Development, identification and validation of a mathematical model of anaerobic digestion of sewage sludge focusing on h2s formation and transfer. *Biochemical engineering journal*, 112:13–19, 2016.

[30] KJ Chae, AM Jang, SK Yim, and In S Kim. The effects of digestion temperature and temperature shock on the biogas yields from the mesophilic anaerobic digestion of swine manure. *Bioresource technology*, 99(1):1–6, 2008.

[31] Xiaojuan Chen, Zhihua Chen, Xun Wang, Chan Huo, Zhiquan Hu, Bo Xiao, and Mian Hu. Application of adm1 for modeling of biogas production from anaerobic digestion of hydrilla verticillata. *Bioresource technology*, 211:101–107, 2016.

[32] Alessandro Chiumenti, Francesco da Borso, and Sonia Limina. Dry anaerobic digestion of cow manure and agricultural products in a full-scale plant: Efficiency and comparison with wet fermentation. *Waste Management*, 71:704–710, 2018.

[33] Bernardino D'Acunto. *Computational Partial Differential Equations for Engineering Sciences*. Nova Science Publishers, 2012.

[34] PV Danckwerts. Continuous flow systems distribution of residence times chemical engineering science genie chimique vol. 2. 1953.

[35] L De Bere. Anaerobic digestion of solid waste: state-of-the-art. *Water science and technology*, 41(3):283–290, 2000.

[36] Wolf-Dieter Deckwer and Enno A Mählmann. Boundary conditions of liquid phase reactors with axial dispersion. *The Chemical Engineering Journal*, 11(1):19–25, 1976.

[37] José A Delgado and AE Rodrigues. Analysis of the boundary conditions for the simulation of the pressure equalization step in PSA cycles. *Chemical Engineering Science*, 63(18):4452–4463, 2008.

[38] Andres Donoso-Bravo, Johan Mailier, Cristina Martin, Jorge Rodríguez, Cesar Arturo Aceves-Lara, and Alain Vande Wouwer. Model selection, identification and validation in anaerobic digestion: a review. *Water research*, 45(17):5347–5364, 2011.

[39] Andrés Donoso-Bravo, Constanza Sadino-Riquelme, Daniel Gómez, Camilo Segura, Emky Valdebenito, and Felipe Hansen. Modelling of an anaerobic plug-flow reactor. process analysis and evaluation approaches with non-ideal mixing considerations. *Bioresource technology*, 260:95–104, 2018.

[40] John A Eastman and John F Ferguson. Solubilization of particulate organic carbon during the acid phase of anaerobic digestion. *Journal (Water Pollution Control Federation)*, pages 352–366, 1981.

[41] G. Esposito, L. Frunzo, Liotta F., A. Panico, and F. Pirozzi. Bio-methane potential tests to measure the biogas production from the digestion and co-digestion of complex organic substrates. *Open Environ. Engine J.*, (5):1–8, 2012.

[42] G. Esposito, L. Frunzo, A. Giordano, Liotta F., A. Panico, and F. Pirozzi. Anaerobic codigestion of organic wastes. *Rev. Environ. Sci. Biotechnol.*, (11):325–341, 2012.

[43] G Esposito, L Frunzo, A Panico, and F Pirozzi. Model calibration and validation for ofmsw and sewage sludge co-digestion reactors. *Waste Management*, 31(12):2527–2535, 2011.

[44] G Esposito, L Frunzo, Ad' Panico, and G d'Antonio. Mathematical modelling of disintegration-limited co-digestion of ofmsw and sewage sludge. *Water Science and Technology*, 58(7):1513–1519, 2008.

[45] C Fall and JL Loaiza-Navía. Design of a tracer test experience and dynamic calibration of the hydraulic model for a full-scale wastewater treatment plant by use of aquasim. *Water Environment Research*, 79(8):893–900, 2007.

[46] Zahra Fatolahi, Golnaz Arab, and Vahid Razaviarani. Calibration of the anaerobic digestion model no. 1 for anaerobic digestion of organic fraction of municipal solid waste under mesophilic condition. *Biomass and Bioenergy*, 139:105661, 2020.

[47] Øyvind Fiksen, Michael J Follows, and Dag L Aksnes. Trait-based models of nutrient uptake in microbes extend the michaelis-menten framework. *Limnology and oceanography*, 58(1):193–202, 2013.

[48] Jameson Filer, Huihuang H Ding, and Sheng Chang. Biochemical methane potential (bmp) assay method for anaerobic digestion research. *Water*, 11(5):921, 2019.

[49] S Fiore, B Ruffino, G Campo, C Roati, and MC Zanetti. Scale-up evaluation of the anaerobic digestion of food-processing industrial wastes. *Renewable Energy*, 96:949–959, 2016.

[50] L Frunzo, Fernando G Fermoso, V Luongo, MR Mattei, and G Esposito. Adm1-based mechanistic model for the role of trace elements in anaerobic digestion processes. *Journal of environmental management*, 241:587–602, 2019.

[51] Santiago García-Gen, Philippe Sousbie, Ganesh Rangaraj, Juan M Lema, Jorge Rodríguez, Jean-Philippe Steyer, and Michel Torrijos. Kinetic modelling of anaerobic hydrolysis of solid wastes, including disintegration processes. *Waste management*, 35:96–104, 2015.

[52] Luana Cardoso Grangeiro, Sâmilla Gabriella Coêlho de Almeida, Bruna Sampaio de Mello, Lucas Tadeu Fuess, Arnaldo Sarti, and Kelly J Dussán. New trends in biogas production and utilization. In *Sustainable Bioenergy*, pages 199–223. Elsevier, 2019.

[53] Gamze Güngör-Demirci and Göksel N Demirer. Effect of initial cod concentration, nutrient addition, temperature and microbial acclimation on anaerobic treatability of broiler and cattle manure. *Bioresource technology*, 93(2):109–117, 2004.

[54] Hinrich Hartmann and Birgitte K Ahring. Anaerobic digestion of the organic fraction of municipal solid waste: influence of co-digestion with manure. *Water research*, 39(8):1543–1552, 2005.

[55] JJ Heijnen and JP Van Dijken. In search of a thermodynamic description of biomass yields for the chemotrophic growth of microorganisms. *Biotechnology and Bioengineering*, 39(8):833–858, 1992.

[56] DT Hill and CL Barth. A dynamic model for simulation of animal waste digestion. *Journal (Water Pollution Control Federation)*, pages 2129–2143, 1977.

[57] L Hinken, M Huber, D Weichgrebe, and K-H Rosenwinkel. Modified adm1 for modelling an uasb reactor laboratory plant treating starch wastewater and synthetic substrate load tests. *Water research*, 64:82–93, 2014.

[58] Jens Bo Holm-Nielsen, Teodorita Al Seadi, and Piotr Oleskowicz-Popiel. The future of anaerobic digestion and biogas utilization. *Bioresource technology*, 100(22):5478–5484, 2009.

[59] Hugh M Hulburt. Chemical processes in continuous-flow systems. *Industrial & Engineering Chemistry*, 36(11):1012–1017, 1944.

[60] PHM Janssen and PSC Heuberger. Calibration of process-oriented models. *Ecological Modelling*, 83(1-2):55–66, 1995.

[61] Ajay Kumar Jha, Jianzheng Li, Loring Nies, and Liguo Zhang. Research advances in dry anaerobic digestion process of solid organic wastes. *African Journal of Biotechnology*, 10(65):14242–14253, 2011.

[62] O.P. Karthikeyan and C. Visvanathan.

[63] M Kayhanian. Ammonia inhibition in high-solids biogasification: an overview and practical solutions. *Environmental technology*, 20(4):355–365, 1999.

[64] Konrad Koch. Calculating the degree of degradation of the volatile solids in continuously operated bioreactors. *Biomass and Bioenergy*, 74:79–83, 2015.

[65] Richa Kothari, AK Pandey, S Kumar, VV Tyagi, and SK Tyagi. Different aspects of dry anaerobic digestion for bio-energy: An overview. *Renewable and Sustainable Energy Reviews*, 39:174–195, 2014.

[66] G Lastella, C Testa, G Cornacchia, M Notornicola, F Voltasio, and Vinod Kumar Sharma. Anaerobic digestion of semi-solid organic waste: biogas production and its purification. *Energy conversion and management*, 43(1):63–75, 2002.

[67] Alonzo W Lawrence. Application of process kinetics to design of anaerobic processes. ACS Publications, 1971.

[68] Ronan Le Hyaric, Hassen Benbelkacem, Julien Bollon, Rémy Bayard, Renaud Escudié, and Pierre Buffière. Influence of moisture content on the specific methanogenic activity of dry mesophilic municipal solid waste digestate. *Journal of Chemical Technology & Biotechnology*, 87(7):1032–1035, 2012.

[69] David R Legates and Gregory J McCabe Jr. Evaluating the use of "goodness-of-fit" measures in hydrologic and hydroclimatic model validation. *Water resources research*, 35(1):233–241, 1999.

[70] Y. Li, S.Y. Park, and J Zhu. Solid-state anaerobic digestion for methane production from organic waste. *Renew. Sust. Energ. Rev.*, (15):821–826, 2011.

[71] Yebo Li, Stephen Y Park, and Jiying Zhu. Solid-state anaerobic digestion for methane production from organic waste. *Renewable and sustainable energy reviews*, 15(1):821–826, 2011.

[72] Yue Li, Yinguang Chen, and Jiang Wu. Enhancement of methane production in anaerobic digestion process: A review. *Applied energy*, 240:120–137, 2019.

[73] Yueh-Fen Li, Po-Hsu Chen, and Zhongtang Yu. Spatial and temporal variations of microbial community in a mixed plug-flow loop reactor fed with dairy manure. *Microbial biotechnology*, 7(4):332–346, 2014.

[74] Yun Li, Hang Liu, Guoxue Li, Wenhai Luo, and Ying Sun. Manure digestate storage under different conditions: chemical characteristics and contaminant residuals. *Science of the Total Environment*, 639:19–25, 2018.

[75] Yen-Hui Lin and Chih-Lung Wu. Sensitivity analysis of phenol degradation with sulfate reduction under anaerobic conditions. *Environmental Modeling & Assessment*, 16(2):213–225, 2011.

[76] Flavia Liotta, Patrice Chatellier, Giovanni Esposito, Massimiliano Fabbricino, Eric D Van Hullebusch, and Piet NL Lens. Hydrodynamic mathematical modelling of aerobic plug flow and nonideal flow reactors: a critical and historical review. *Critical Reviews in Environmental Science and Technology*, 44(23):2642–2673, 2014.

[77] Geert Lissens, Philippe Vandevivere, L De Baere, EM Biey, and Willy Verstraete. Solid waste digestors: process performance and practice for municipal solid waste digestion. *Water science and technology*, 44(8):91–102, 2001.

[78] Can Liu, Huan Li, Yuyao Zhang, and Qingwu Chen. Characterization of methanogenic activity during high-solids anaerobic digestion of sewage sludge. *Biochemical Engineering Journal*, 109:96–100, 2016.

[79] L Luning, EHM Van Zundert, and AJF Brinkmann. Comparison of dry and wet digestion for solid waste. *Water science and technology*, 48(4):15–20, 2003.

[80] G Lyberatos and IV Skiadas. Modelling of anaerobic digestion–a review. *Global Nest Int J*, 1(2):63–76, 1999.

[81] Michael Madsen, Jens Bo Holm-Nielsen, and Kim H Esbensen. Monitoring of anaerobic digestion processes: A review perspective. *Renewable and sustainable energy reviews*, 15(6):3141–3155, 2011.

[82] Bikash Chandra Maharaj, Maria Rosaria Mattei, Luigi Frunzo, Eric D van Hullebusch, and Giovanni Esposito. Adm1 based mathematical model of trace element complexation in anaerobic digestion processes. *Bioresource technology*, 276:253–259, 2019.

[83] Karthik R Manchala, Yewei Sun, Dian Zhang, and Zhi-Wu Wang. Anaerobic digestion modelling. In *Advances in Bioenergy*, volume 2, pages 69–141. Elsevier, 2017.

[84] Chunlan Mao, Yongzhong Feng, Xiaojiao Wang, and Guangxin Ren. Review on research achievements of biogas from anaerobic digestion. *Renewable and sustainable energy reviews*, 45:540–555, 2015.

[85] Amandine Marrel, Bertrand Iooss, Beatrice Laurent, and Olivier Roustant. Calculations of sobol indices for the gaussian process metamodel. *Reliability Engineering & System Safety*, 94(3):742–751, 2009.

[86] VMG Molla and RG Padilla. Description of the matlab functions sens_sys and sens_ind. *Universidad Politécnica de Valencia, Spain*, 2002.

[87] D Montecchio, A Gallipoli, A Gianico, G Mininni, P Pagliaccia, and CM Braguglia. Biomethane potential of food waste: modeling the effects of mild thermal pretreatment and digestion temperature. *Environmental technology*, 38(11):1452–1464, 2017.

[88] Max D Morris. Factorial sampling plans for preliminary computational experiments. *Technometrics*, 33(2):161–174, 1991.

[89] Yilmaz Muslu. Numerical approach to plug-flow activated sludge reactor kinetics. *Computers in Biology and Medicine*, 30(4):207–223, 2000.

[90] Norio Nagao, Nobuyuki Tajima, Minako Kawai, Chiaki Niwa, Norio Kurosawa, Tatsushi Matsuyama, Fatimah Md Yusoff, and Tatsuki Toda. Maximum organic loading rate for the single-stage wet anaerobic digestion of food waste. *Bioresource Technology*, 118:210–218, 2012.

[91] Leo ML Nollet. *Handbook of Food Analysis: Residues and other food component analysis*, volume 138. CRC Press, 2004.

[92] NA Noykova and M Gyllenberg. Sensitivity analysis and parameter estimation in a model of anaerobic waste water treatment processes with substrate inhibition. *Bioprocess Engineering*, 23(4):343–349, 2000.

[93] Antonio Panico, Ernesto Salzano, Luigi Frunzo, and Francesco Pirozzi. Innovative parameters to control the efficiency of anaerobic digestion process. *CHEMICAL ENGINEERING*, 43, 2015.

[94] Vicente Pastor-Poquet, Stefano Papirio, Jean-Philippe Steyer, Eric Trably, Renaud Escudié, and Giovanni Esposito. High-solids anaerobic digestion model for homogenized reactors. *Water research*, 142:501–511, 2018.

[95] Regina J Patinvoh, Adib Kalantar Mehrjerdi, Ilona Sárvári Horváth, and Mohammad J Taherzadeh. Dry fermentation of manure with straw in continuous plug flow reactor: Reactor development and process stability at different loading rates. *Bioresource technology*, 224:197–205, 2017.

[96] JRA Pearson. A note on the Danckwerts boundary conditions for continuous flow reactors. *Chemical Engineering Science*, 10(4):281–284, 1959.

[97] Sagor Kumar Pramanik, Fatihah Binti Suja, Shahrom Md Zain, and Biplob Kumar Pramanik. The anaerobic digestion process of biogas production from food waste: Prospects and constraints. *Bioresource Technology Reports*, 8:100310, 2019.

[98] Rajinikanth Rajagopal, Daniel I Massé, and Gursharan Singh. A critical review on inhibition of anaerobic digestion process by excess ammonia. *Bioresource technology*, 143:632–641, 2013.

[99] Leonardo Ramirez-Lopez, Karsten Schmidt, Thorsten Behrens, Bas van Wesemael, Jose AM Demattê, and Thomas Scholten. Sampling optimal calibration sets in soil infrared spectroscopy. *Geoderma*, 226:140–150, 2014.

[100] C.E. Rasmussen and C Williams. *Gaussian processes for machine learning*. MIT Press, 2006.

[101] Jens Christian Refsgaard and B Storm. Construction, calibration and validation of hydrological models. In *Distributed hydrological modelling*, pages 41–54. Springer, 1990.

[102] Ruben Reif, Francisco Omil, and Juan M Lema. Removal of pharmaceuticals by membrane bioreactor (mbr) technology. In *Comprehensive Analytical Chemistry*, volume 62, pages 287–317. Elsevier, 2013.

[103] EU Remigi and Christopher Andrew Buckley. *Co-digestion of High-strength/toxic Organic Effluents in Anaerobic Digesters at Wastewater Treatment Works*. Water Research Commission Pretoria, South Africa, 2006.

[104] P.T. Roy, N. El Moçayd, S. Ricci, J. Jouhad, N. Goutal, M. De Lozzo, and M.C. Rochoux. Comparison of polynomial chaos and gaussian process surrogates for uncertainty quantification and correlation estimation of spatially distributed open-channel steady flows. *Stochastic Environmental Research and Risk Assessment*, 32(6):1723 – 1741, 2018.

[105] Andrea Saltelli, Ksenia Aleksankina, William Becker, Pamela Fennell, Federico Ferretti, Niels Holst, Sushan Li, and Qiongli Wu. Why so many published sensitivity analyses are false: A systematic review of sensitivity analysis practices. *Environmental modelling & software*, 114:29–39, 2019.

[106] Andrea Saltelli, Marco Ratto, Terry Andres, Francesca Campolongo, Jessica Cariboni, Debora Gatelli, Michaela Saisana, and Stefano Tarantola. *Global sensitivity analysis: the primer*. John Wiley & Sons, 2008.

[107] Cecilia Sambusiti, F Monlau, Elena Ficara, A Musatti, M Rollini, Abdellatif Barakat, and Francesca Malpei. Comparison of various post-treatments for recovering methane from agricultural digestate. *Fuel Processing Technology*, 137:359–365, 2015.

[108] WTM Sanders, M Geerink, G Zeeman, and G Lettinga. Anaerobic hydrolysis kinetics of particulate substrates. *Water Science and Technology*, 41(3):17–24, 2000.

[109] Abraham Savitzky and Marcel JE Golay. Smoothing and differentiation of data by simplified least squares procedures. *Analytical chemistry*, 36(8):1627–1639, 1964.

[110] Gürkan Sin, Dirk JW De Pauw, Stefan Weijers, and Peter A Vanrolleghem. An efficient approach to automate the manual trial and error calibration of activated sludge models. *Biotechnology and bioengineering*, 100(3):516–528, 2008.

[111] Ram Bux Singh. *Bio-gas Plant: Generating Methane from Organic Wastes & Designs with Specifications*. Gobar Gas Research Station, 1975.

[112] Ilya M Sobol. Sensitivity analysis for non-linear mathematical models. *Mathematical modelling and computational experiment*, 1:407–414, 1993.

[113] Kimberly Solon, Xavier Flores-Alsina, Krist V Gernaey, and Ulf Jeppsson. Effects of influent fractionation, kinetics, stoichiometry and mass transfer on ch4, h2 and co2 production for (plant-wide) modeling of anaerobic digesters. *Water Science and Technology*, 71(6):870–877, 2015.

[114] P Sosnowski, A Wieczorek, and S Ledakowicz. Anaerobic co-digestion of sewage sludge and organic fraction of municipal solid wastes. *Advances in Environmental Research*, 7(3):609–616, 2003.

[115] Theo SO Souza, Andrea Carvajal, Andres Donoso-Bravo, Mar Peña, and Fernando Fdz-Polanco. Adm1 calibration using bmp tests for modeling the effect of autohydrolysis pretreatment on the performance of continuous sludge digesters. *Water research*, 47(9):3244–3254, 2013.

[116] Vadake R Srinivasan and John J Sansalone. Plug flow anaerobic digester, January 6 2004. US Patent 6,673,243.

[117] B Tartakovsky, SJ Mu, Y Zeng, SJ Lou, SR Guiot, and P Wu. Anaerobic digestion model no. 1-based distributed parameter model of an anaerobic reactor: Ii. model validation. *Bioresource technology*, 99(9):3676–3684, 2008.

[118] N Tippayawong and P Thanompongchart. Biogas quality upgrade by simultaneous removal of co2 and h2s in a packed column reactor. *Energy*, 35(12):4531–4535, 2010.

[119] Clément Trellu, Yoan Pechaud, Nihal Oturan, Emmanuel Mousset, David Huguenot, Eric D Van Hullebusch, Giovanni Esposito, and Mehmet A Oturan. Comparative study on the removal of humic acids from drinking water by anodic oxidation and electro-fenton processes: mineralization efficiency and modelling. *Applied Catalysis B: Environmental*, 194:32–41, 2016.

[120] A. Trucchia, V. Egorova, G. Pagnini, and M.C. Rochoux. On the merits of sparse surrogates for global sensitivity analysis of multi-scale nonlinear problems: application to turbulence and fire-spotting model in wildland fire simulators. *Communications in Nonlinear Science and Numerical Simulation*, 2019.

[121] A. Trucchia, M.R. Mattei, V. Luongo, L. Frunzo, and M.C. Rochoux. Surrogate-based uncertainty and sensitivity analysis for bacterial invasion in multi-species biofilm modeling. *Communications in Nonlinear Science and Numerical Simulation*, 73:403 – 424, 2019.

[122] AR Van Cauwenberghe. Further note on Dankwert's boundary conditions for flow reactors. *Chemical Engineering Science*, 21(2):203–205, 1966.

[123] Jules B Van Lier, Nidal Mahmoud, and Grietje Zeeman. Anaerobic wastewater treatment, 2008.

[124] P. Vandevivere. New and broader applications of anaerobic digestion. *Critical Rev. Env. Sci. and Technol.*, (29):151–173, 1999.

[125] VA Vavilin, LY Lokshina, X Flotats, and Irini Angelidaki. Anaerobic digestion of solid material: Multidimensional modeling of continuous-flow reactor with non-uniform influent concentration distributions. *Biotechnology and bioengineering*, 97(2):354–366, 2007.

[126] VA Vavilin, VB Vasiliev, AV Ponomarev, and SV Rytow. Simulation model 'methane'as a tool for effective biogas production during anaerobic conversion of complex organic matter. *Bioresource technology*, 48(1):1–8, 1994.

[127] Vasily A Vavilin, Sergey V Rytov, Ljudmila Ya Lokshina, Spyros G Pavlostathis, and Morton A Barlaz. Distributed model of solid waste anaerobic digestion: effects of leachate recirculation and ph adjustment. *Biotechnology and Bioengineering*, 81(1):66–73, 2003.

[128] C Veluchamy and Ajay S Kalamdhad. A mass diffusion model on the effect of moisture content for solid-state anaerobic digestion. *Journal of cleaner production*, 162:371–379, 2017.

[129] Xiaojiao Wang, Gaihe Yang, Fang Li, Yongzhong Feng, Guangxin Ren, and Xinhui Han. Evaluation of two statistical methods for optimizing the feeding composition in anaerobic co-digestion: Mixture design and central composite design. *Bioresource technology*, 131:172–178, 2013.

[130] Andrew Whiting and Adisa Azapagic. Life cycle environmental impacts of generating electricity and heat from biogas produced by anaerobic digestion. *Energy*, 70:181–193, 2014.

[131] E Wicke. Physical processes in chemical reactor engineering. *Advances in Chemistry Series*, (148):75–97, 1975.

[132] Binxin Wu. Integration of mixing, heat transfer, and biochemical reaction kinetics in anaerobic methane fermentation. *Biotechnology and bioengineering*, 109(11):2864–2874, 2012.

[133] Sihuang Xie, Faisal I Hai, Xinmin Zhan, Wenshan Guo, Hao H Ngo, William E Price, and Long D Nghiem. Anaerobic co-digestion: A critical review of mathematical modelling for performance optimization. *Bioresource Technology*, 222:498–512, 2016.

[134] D. Xiu and G.E. Karniadakis. The wiener–askey polynomial chaos for stochastic differential equations. *SIAM Journal on Scientific Computing*, 24(2):619–644, 2002.

[135] Chonggang Xu, Yuanman Hu, Yu Chang, Yan Jiang, Xiuzhen Li, Renchang Bu, and Hongshi He. Sensitivity analysis in ecological modeling. *Ying yong sheng tai xue bao= The Journal of Applied Ecology*, 15(6):1056–1062, 2004.

[136] Fuqing Xu, Yebo Li, and Zhi-Wu Wang. Mathematical modeling of solid-state anaerobic digestion. *Progress in Energy and Combustion Science*, 51:49–66, 2015.

[137] Fuqing Xu, Zhi-Wu Wang, Li Tang, and Yebo Li. A mass diffusion-based interpretation of the effect of total solids content on solid-state anaerobic digestion of cellulosic biomass. *Bioresource technology*, 167:178–185, 2014.

[138] Junzeng Xu, Xiaoyin Liu, Shihong Yang, Zhiming Qi, and Yijiang Wang. Modeling rice evapotranspiration under water-saving irrigation by calibrating canopy resistance model parameters in the penman-monteith equation. *Agricultural Water Management*, 182:55–66, 2017.

[139] Liang Yu, Pierre Christian Wensel, Jingwei Ma, and Shulin Chen. Mathematical modeling in anaerobic digestion (ad). *J Bioremed Biodeg S*, 4(2), 2013.

[140] Zhike Zi. Sensitivity analysis approaches applied to systems biology models. *IET systems biology*, 5(6):336–346, 2011.

[141] Ayrat M Ziganshin, Thomas Schmidt, Frank Scholwin, Olga N Il'inskaya, Hauke Harms, and Sabine Kleinsteuber. Bacteria and archaea involved in anaerobic digestion of distillers grains with solubles. *Applied microbiology and biotechnology*, 89(6):2039–2052, 2011.

[142] Ž Zonta, MM Alves, X Flotats, and J Palatsi. Modelling inhibitory effects of long chain fatty acids in the anaerobic digestion process. *Water research*, 47(3):1369–1380, 2013.